Use of a unique reporter cassette to examine 5′ to 3′ resection at a site specific DNA double–strand break during meiosis

Anna Bishop–Bailey

A thesis submitted for the degree of Doctor of Philosophy

February 2006

University of Sheffield

Department of Molecular Biology and Biotechnology

Summary

Meiotic recombination in *Saccharomyces cerevisiae* is initiated by the formation of DNA double strand breaks (DSBs), which are created by Spo11 protein. Recombination preferentially occurs between homologous chromosomes, in order to establish interhomologue connections. These connections serve as a platform for genetic recombination and to promote accurate homologue disjunction at the first meiotic division (MI). Specific mechanisms are in place to ensure that meiotic DSB repair is directed towards interchromosomal repair, and genes thought to be involved in these mechanisms were examined in a DSB assay, where interchromosomal repair was precluded. Genes involved in the formation and processing of Spo11-DSBs were also examined. In meiosis, the regulation of resectioning is critical to repair outcome, and this assay was designed to measure two different lengths of resection tract.

In a *mek1* mutant, there was an increase in the generation of longer resection tracts, suggesting that Mek1 protein may exert its influence over repair template choice by negatively regulating DSB resectioning. An *sae2* mutant was found to generate fewer shorter resection tracts, and was delayed for DSB repair. This suggested that Sae2 protein may have an early role in resectioning, by influencing repair template choice. Mutants of the MRX complex were all compromised for DSB repair, while an *exo1* mutant failed to generate long resection tracts only.

Finally, from work on a *dmc1* mutant, the prospect of protein sequestration at sites of excess single stranded DNA was proposed.

Acknowledgements

Many many thanks: To Alastair, first and foremost. I really appreciate all of the time and effort you have made for me. I couldn't have written the thesis without your constant advice and guidance. Thanks also for always lending a sympathetic ear!

To the members of the Goldman and Sudbery groups, past and present. I would particularly like to acknowledge Matt Neale and Helene, who both helped me enormously when I was a mere callow youth.

To the lovely Janet, the essential piece of the lab jigsaw. Thank you so much for all of the assistance you have given me, I will really miss the laughs that we had!

To my Sheffield friends, Kay, Helene, Helen, Claire, Emma, Kate, Ali and Michelle, not least for feeding, watering me, and for giving me a bed. Thanks for all of the good times, here's to many more!

To Max, Lisa and the kids, for always providing me with a welcome distraction when required!

Finally to my Mum, thank you so much for your unstinting support. I hope it was worth it! (By the way, you were right; it does feel like I've run a marathon!)

The road is long, with many a winding turn

-Bob Russell/Bobby Scott

Abbreviations

Ade	adenine
Ade+	adenine prototrophic
amp	ampicillin
amp^{R}	ampicillin resistance
A. nidulans	*Aspergillus nidulans*
BSA	bovine serum albumin
C. elegans	*Caenorhabditis elegans*
°C	degrees celsius
CFU	colony forming unit
ChIP	chromatin immunoprecipitation
Chr. Coord	chromosomal coordinates
CTAB	hexadecyltrimethylammonium bromide
C-terminal	carboxy-terminal
D. melanogaster	*Drosophila melanogaster*
dAG	diploid strain number
DAPI	4′,6′–diamidino–2–phenylindoline
dH_20	deionised water
DNA	deoxyribonucleic acid
dNTP	deoxynucleotide triphosphate
DSB	double strand break
ds	double stranded
E. coli	*Escherichia coli*

EDTA	ethylene-diaminetetraacetic acid
FISH	fluorescence *in situ* hybridisation
5-FOA	5-fluoroorotic acid
G418	G418 Disulphate
h(*MRE11*)	human (*MRE11)* gene
hAG	haploid strain number
HO	homothallic
hph^R	hygromycin resistance gene
HR	homologous recombination
hr	hour
IR	ionising radiation
K-Ac	potassium acetate
kb	kilobases
lin.	linearised
l	litre
µg	microgram
µl	microlitre
M	molar
mM	millimolar
mg	milligram
min	minute
ml	millilitre
MI/II	first/second meiotic division

MMS	methyl methanesulphonate
MRX	Mre11/Rad50/Xrs2 complex
NHEJ	non-homologous end joining
OD_X	optical density$_{wavelength}$
ORF	open reading frame
pAG	plasmid strain number
PCR	polymerase chain reaction
rpm	revolutions per minute
RT	room temperature
S. cerevisiae	*Saccharomyces cerevisiae*
S. pombe	*Schizosaccharomyces pombe*
Sc	synthetic complete (medium)
SC	synaptonemal complex
SAP	shrimp alkaline phosphatase
sec	seconds
ss	single stranded
SSA	single strand annealing
2TY	2x tryptone, yeast extract
Unpub.	unpublished
Ura	uracil
UV	ultraviolet
UP-H_20	ultra pure water
VDE	*VMA1*–derived endonuclease

v/v	volume by volume
w/o	without
w/w	weight by weight
WT	wildtype

PAGE NUMBERS CUT OFF

IN

ORIGINAL

Chapter 1

Introduction

1.1 *Saccharomyces cerevisiae*

Saccharomyces cerevisiae (budding yeast) is a model organism for studying cellular processes in higher eukaryotes. *S. cerevisiae* has several qualities making it well suited for molecular genetic experimentation. Most importantly, it represents a simplified version of higher eukaryotes, it is unicellular, the genome is fully sequenced, annotated and readily manipulated, it is easy to culture and yields large numbers of progeny.

S. cerevisiae is particularly suited to experiments examining the meiotic cell cycle as specific strains have the ability to undergo rapid and synchronous sporulation (Kane and Roth, 1974).

1.2 The Meiotic Cell Cycle

The eukaryotic nucleus divides in one of two ways, by meiosis or mitosis. While mitosis represents asexual cell division, the process of meiosis facilitates sexual reproduction, (comprehensively reviewed in (Zickler and Kleckner, 1998)). Meiosis enables two important functions in the eukaryotic cell, a haploid stage in the lifecycle and the generation of genetic recombinant progeny. Two nuclear divisions occur in meiosis, the first reduces chromosome number, and the second is an equational division of the genetic material. As meiosis is an essential process for sexual reproduction, it is logical that the genes regulating the process show considerable conservation throughout eukaryotes. Although the key characteristics of meiosis have been studied and understood for the last

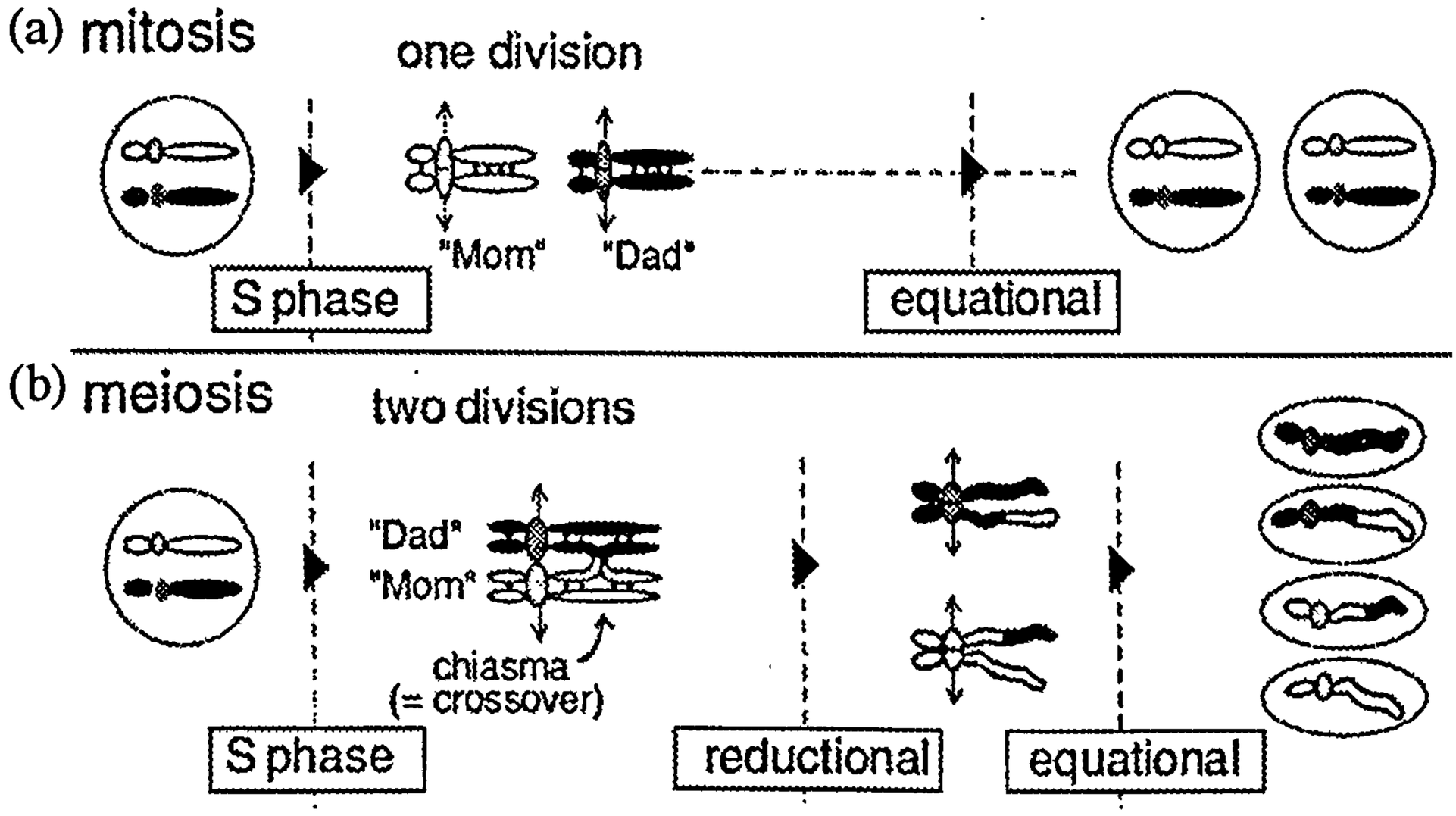

Figure 1.2*i*: Chromosome Segregation in Mitosis and Meiosis: Prior to the one mitotic and two meiotic nuclear division(s), the chromosomes are replicated (S-phase) to create identical sister chromatids. (a) During mitosis, sister chromatids are intimately associated, through sister chromatid cohesion to ensure bipolar orientation on the metaphase plate. Spindle fibres from opposite poles become attached to the sister kinetochores, and via poleward forces, the chromosomes become appropriately orientated. At anaphase, loss of sister chromatid cohesion along the chromatid arms, (then at the centromeric regions), permits sister chromatid disjunction to opposite poles (equational segregation). (b) Prior to the first meiotic division, homologous chromosomes become aligned and recombine, creating interhomologue connections termed chiasmata (prophase I). Pairs of connected homologues (bivalents) undergo bipolar orientation on the MI spindle (analogous to sister chromatids in mitosis). At anaphase I, loss of sister chromatid cohesion along the chromosomal arm regions permits the homologue kinetochores to move to opposite poles, while maintenance of sister chromatid cohesion at the centromeric regions ensures that the segregation is reductional. For the second meiotic division, sister chromatids become aligned, again via spindle fibre attachment at the sister kinetochores. Loss of sister chromatid cohesion in the centromeric regions marks anaphase II, permitting the disjunction of recombinant sister chromatids (equational segregation). (Figure taken from Zickler and Kleckner, 1998).

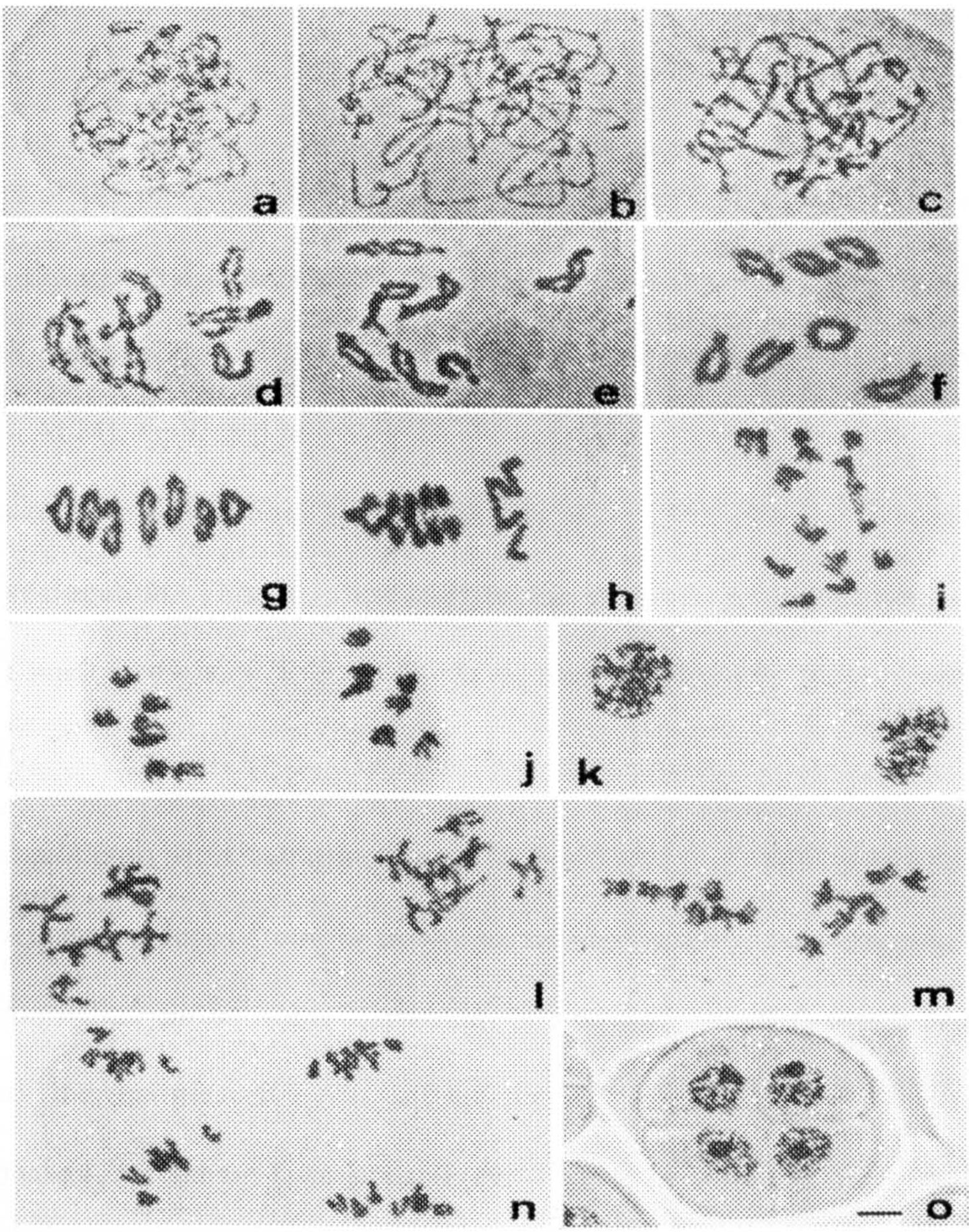

Figure 1.2*ii*: Meiotic divisions I and II in the rye *Secale cereale* microsporocytes: (A-F) prophase I, (A) early zygotene; chromosomal condensation and early pairing. (B-D) early to late pachytene; continued chromosomal condensation and homologue pairing, followed by synapsis. (E) diplotene; progressive loss of sister chromatid cohesion. (F) diakinesis; homologous chromosomes are distinguishable, connected by chiasmata. (G, H) metaphase I; homologous chromosomes align on the MI spindle. (I, J) anaphase I; reductional segregation of homologues (K) telophase I. (L) prophase II. (M) metaphase II; sister chromatids align along the MII spindle. (N) anaphase II; equational segregation of sister chromatids. (O) Four haploid pollen cells. (Bar = 5μ). (Figure taken from Zickler and Kleckner 1998)

PAGE NUMBERING AS ORIGINAL

the last 30 years that have provided an insight into the molecular and ultrastructural aspects of meiosis (John, 1990).

The function of the meiotic cell cycle is to generate genetically diverse offspring with exactly half the parental chromosome complement. This occurs by one round of DNA replication (S-phase), followed by two rounds of nuclear division (MI/MII) (Figure 1.2*i* and Figure 1.2*ii*). At MI, replicated homologous chromosomes (maternal and paternal) move to opposite poles, in a reductional segregation. At MII, sister chromatids disjoin, in an equational segregation. This is in contrast to the mitotic cell cycle, where only one (equational) nuclear division follows S-phase, thus maintaining chromosome number (Figure 1.2*i*).

At the first meiotic division, centromere number is reduced from diploid to haploid, while the genetic content reduces from 4x to 2x. In order to achieve this, meiotic cells must undergo homologous chromosome alignment, pairing and synapsis, which occur during prophase I of the meiotic cell cycle. MI consists of four cytologically distinguishable stages: prophase I, metaphase I, anaphase I and telophase I (Figure 1.2*iii*). Near identical stages are found in all organisms.

1.2.1 Prophase I

Prior to prophase I, premeiotic cells exist in a G1/G0 state, characterised by nuclear expansion. Premeiotic S-phase follows, which is a period of DNA replication. Specific connections form between sister chromatids (sister chromatid cohesion, Section 1.3.1), and

PAGE NUMBERING AS ORIGINAL

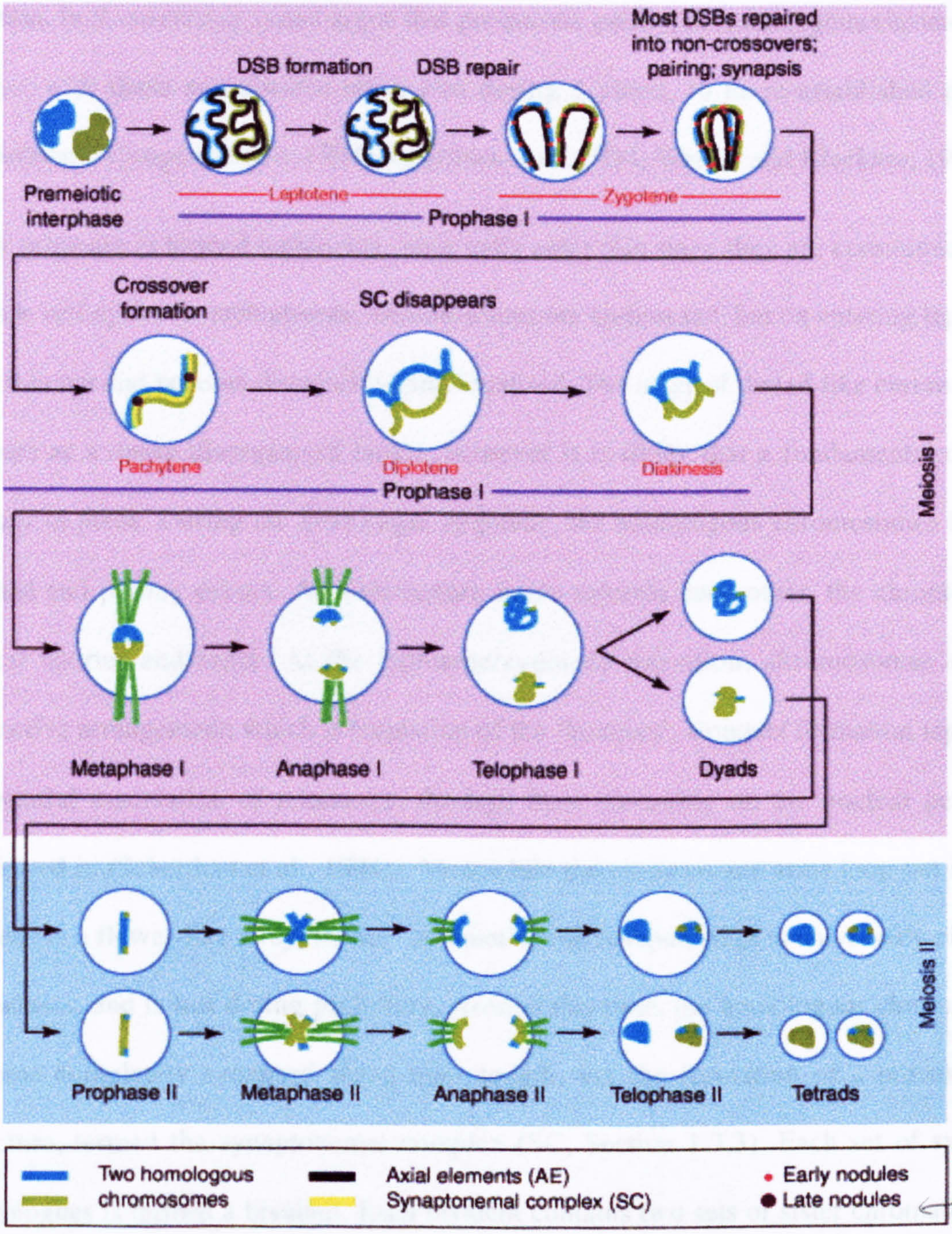

Figure 1.2*iii*: Stages in Meiosis The top two panels show the extended meiotic prophase I, major events include DSB formation and repair, crossover formation, homologous chromosome pairing and synapsis. Chromosomal interactions between prophase homologous chromosomes result in the formation of paired homologues (bivalents) and the reciprocal exchange of sister chromatid arms, from crossing-over. Homologous chromosomes disjoin at anaphase I, and sister chromatids in anaphase II, (analogous to mitotic division). Virtually identical stages are found in all organisms studied (Figure from Pawlowski and Cande, 2005).

S-phase is distinguishable by the presence of diffuse chromatin. Mitotic and meiotic S-phases are largely analogous, with the exception that meiotic S-phase is of much longer duration. In *S. cerevisiae*, some argue that premeiotic pairing of homologous chromosomes occurs, with these associations being lost during S-phase, to be re-established prior to chromosome synapsis (Klein, 1994; Scherthan et al., 1994; Weiner and Kleckner, 1994).

Early prophase is termed leptonema, once cells enter this stage they are committed to the meiotic cell cycle. At preleptotene, chromosomes are compacted, but on entering leptotene, they thin out and become discernibly individualised. The array of thread-like chromosomes appears as a dense disorganised tangle, however it is likely that a fundamental order is already in place. During the next stage, zygotene, the homologous chromosomes become aligned and pairing occurs. As homologues move towards each other, the chromosomes appear shorter and fatter. At the leptotene/zygotene transition, chromosomes adopt a distinctive arrangement, which is formation of the 'bouquet'. Bouquet formation represents the spatial association of telomeres, through their clustering on the nuclear periphery (reviewed in (Scherthan et al., 1994)). Meanwhile the chromosome arms loop out into the nucleus in a flower-like array, (hence 'bouquet'). The bouquet stage is universally observed in meioses, and is lost during pachytene. Around this time, the homologous chromosomes become completely synapsed along their length, via the formation of a proteinaceous structure, termed the synaptonemal complex (SC, Section 1.3.3). Each set of synapsed homologues is termed a bivalent. Each bivalent contains two sets of sister chromatids, one pair originating from each parental chromosome.

The tight associations between homologues cause pachytene chromosomes to appear at their most short and thick. In the next stage, diplotene, the SC is dissembled and individual homologues become distinguishable again. When the chromosomes move apart, chiasmata can be visualised at the points where the homologues remain connected. The final stages of prophase are diakenesis and prometaphase, when in readiness for chromosomal segregation at MI, the homologues undergo shortening and compaction.

1.3 Meiosis in Detail

It is during prophase I that the most striking modifications to chromosome organisation in the meiotic nucleus occur. Gross conformational changes include chromosome condensation, pairing, and synapsis. Recombination alters chromosomal conformation at both a nucleotide level, in the generation of gene conversions, and also at a structural level, in the formation of chiasmata.

1.3.1 Sister Chromatid Cohesion

Sister chromatid cohesion is established during S-phase, where premeiotic DNA replication produces sister chromatids that are tightly bound. In mitosis, cohesion between sister chromatids prevents their premature disjunction during attachment to the mitotic spindle. The cohesin proteins Smc1, Smc3, Scc1 and Scc3 make up a multisubunit complex that is required for cohesion between mitotic sister chromatids, while in meiosis Scc1 is substituted for the meiosis-specific homologue, Rec8 (Klein et al., 1999). Sister chromatid cohesion occurs along the length of the chromatids, excluding the sites of chiasmata, and is present until anaphase I. During the first meiotic division, sister chromatids must remain

tightly bound, to ensure disjunction of homologues and not sisters. In order to resolve chiasmata, cohesion between sister chromatids is lost only in regions distal to the crossover, that is, along the chromosome arms. The cohesin complex is maintained at the centromeric region through to anaphase II, thus preventing premature sister chromatid disjunction. Moreover, by tying the sisters together until the second meiotic division, promotes their correct orientation on the meiotic spindle, and accurate disjunction at MII (reviewed in (Nasmyth et al., 2000)).

1.3.2 Homologous Chromosome Pairing

Homologous chromosome pairing requires homologues to overcome spatial separation within the nucleus, in order to become associated. Once in close proximity, the homologues are able to compare sequence homologies (reviewed recently in (Pawlowski and Cande, 2005)). Fluorescence *in situ* hybridisation (FISH) of *S. cerevisiae* has been used to demonstrate multiple pairing sites along chromosome lengths (Scherthan et al., 1994; Weiner and Kleckner, 1994). Although the mechanism of homologue pairing is not widely understood, there appears to exist a strong connection with meiotic recombination. Pairing of homologous chromosomes in prophase seemingly occurs independently of chromosome condensation and SC formation. However, the correlation between pairing sites and future recombination events supports the proposal that these early pairing sites later become recombination initiation sites. (Scherthan et al., 1994; Weiner and Kleckner, 1994).

1.3.3 Synaptonemal Complex

While pairing is based on homology recognition for homologue interaction, synapsis is the process of cementing that association by creation of the synaptonemal complex (SC). The SC is a tripartite proteinaeous zip-like structure, which establishes and maintains the close association between homologous chromosomes along their entire length during meiotic prophase (reviewed in (Heyting, 1996). The SC is thought to influence the number and distribution of crossovers, plus convert these crossovers into stable chiasmata, thus ensuring accurate disjunction of homologues at MI (reviewed in (Roeder and Bailis, 2000).

Sister chromatids of each meiotic prophase chromosome develop a single proteinaceous axis, termed the axial element (AE). Through meiotic prophase, the AEs of homologous chromosomes become connected along their length by multiple transverse filaments, forming the SC. Between the axial connections, which are now termed lateral elements (LE), a third longitudinal structure, the central element (CE), forms ('the zip'). Hence, the tripartite structure of the SC comprises of two lateral and a single central element. The tripartite SC structure is universally conserved among organisms, although differences exist at an ultrastructural level. Interestingly, meiotic cells of S*chizosaccharomyces pombe* and *Aspergillus nidulans* do not possess a detectable SC, although LEs are present in *S. pombe,* similar to those contained within the SC.

In *S. cerevisiae* there are three meiosis-specific components of the SC, Red1, Hop1 and Zip1. While the protein products of *HOP1* and *RED1* are localised to the AEs, the protein product of *ZIP1* is required for the formation of the CE.

The interplay between chromosome synapsis and recombination appears to differ, depending on the organism being studied. In *S. cerevisiae*, mutants blocked for SC formation, still create Spo11-double strand breaks (DSBs, Section 1.5), while in *spo11* mutants, where meiotic DSBs are prevented, SC formation is also blocked. This suggests that in yeast, Spo11-DSBs are not only initiated before synapsis, but they are also required for the formation of the SC. Therefore, synapsis is not required for the initiation of recombination. This is in accord with studies of the timing of recombination and synapsis in *S. cerevisiae*, where it was reported that meiotic DSBs were created in early prophase, prior to the appearance of the SC (Padmore et al., 1991). Furthermore, in the organisms previously mentioned, that don't create SC (that is, *A. nidulans* and *S. pombe*), recombination still occurs.

Conversely, in *Drosophila melanogaster* and *Caenorhabditis elegans*, it is homologue pairing that initiates synapsis, only then are Spo11-DSBs formed.

Events subsequent to the initiation of recombination also appear to influence the onset of synapsis in *S. cerevisiae*. Mutants that create wildtype (WT) levels of Spo11-DSBs, but are blocked from generating recombination intermediates, accumulate unresected breaks, and form only partial SC (Alani et al., 1990; McKee and Kleckner, 1997; Prinz et al., 1997). Meanwhile, mutants that accumulate Spo11-DSBs with long 3′ single-stranded (ss)DNA tails, assemble almost wildtype levels of SC, but synapsis is delayed (Bishop et al., 1992; Rockmill et al., 1995).

1.4 Recombination

DSB repair is classified into two major categories, homologous recombination (HR) and nonhomologous or illegitimate recombination. HR is characterised by broken DNA strands base pairing with a homologous partner. While HR typically requires many hundreds of bases of homology, nonhomologous repair ligates DNA termini that display microhomology, that is, a very limited number of homologous bases pairs. These repair pathways are conserved between *S. cerevisiae* and higher eukaryotes, although their relative contributions depend on the organism, cell type and stage of the cell cycle (Pastink et al., 2001). HR is the predominant DSB repair method in *S. cerevisiae*, while it is nonhomologous repair in mammalian cells.

Meiotic recombination is initiated during zygotene, when homologous chromosomes become aligned and paired. Interhomologue recombination normally results in a gene conversion, which involves the transfer of genetic material from one nonsister chromatid to another. Gene conversion events are associated with crossovers at a frequency of approximately 50% (Fogel and Hurst, 1967; Jinks-Robertson and Petes, 1986; Orr-Weaver and Szostak, 1985). Reciprocal gene conversion events are required for chiasmata formation and the accurate disjunction of homologous chromosomes at MI.

1.4.1 Double Strand Break Repair Model

DSB repair by homologous recombination can occur by a number of different mechanisms (reviewed in (van den Bosch et al., 2002)). A universal feature of homologous

PAGE NUMBERING AS ORIGINAL

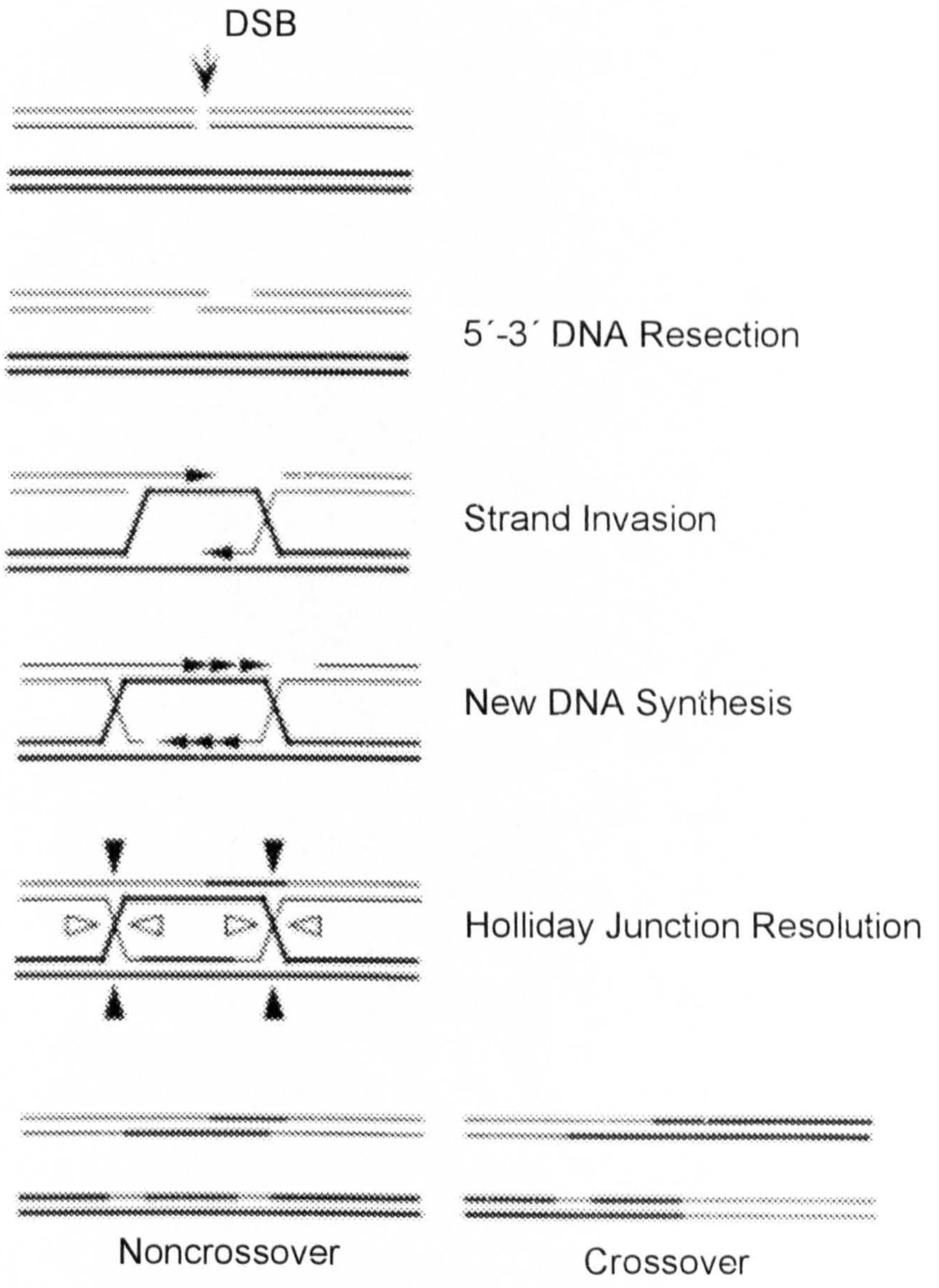

Figure 1.4.1 Szostak DSB Repair Model: DSB formation is followed by 5'-3' resectioning of the DNA termini. The resulting 3' ssDNA tails are highly recombinogenic and can invade a homologous template, to initiate novel DNA synthesis. A double Holliday-Junction forms and is resolved via the alternative cleavage of crossed (open arrowhead) or noncrossed (closed arrowhead) strands. (Figure taken from Paques and Haber, 1999)

recombination is the generation of 3′-ssDNA tails. The canonical model for DSB repair was described by Szostak *et al*, (1983), whereby the linear 3′ ssDNA tails which are highly recombinogenic, invade an intact homologous DNA duplex generating the characteristic four-stranded branch structure, termed a Holliday junction (HJ) (Figure 1.4.1). The 3′ ends of the invading DNA strands serve as primers for the initiation of novel DNA synthesis. Two HJs form a joint molecule, which can be visualised on a two-dimensional gel (Schwacha and Kleckner, 1997) (Schwacha and Kleckner, 1994). Strand invasion is catalysed by the DNA strand exchange proteins, Dmc1 and Rad51 ((Kadyk and Hartwell, 1992; Symington, 2002) (Bishop et al., 1992). Creation of the double HJ permits the generation of recombination crossover products, via the alternative resolution of this joint molecule. If both of the HJs are cleaved equally, that is both sets of noncrossed or crossed strands, the gene conversion is not associated with crossing over. If there is cleavage of noncrossed strands from one HJ, and of crossed strands from the other, this causes the crossover of flanking markers. Novel DNA synthesis generates heteroduplex sequence, which needs to be fixed. Mismatch repair proteins target these regions of heteroduplex and re-establish DNA strand homology.

The Szostak model for DSB repair predicts that novel DNA is generated in both donor and recipient. However it has been widely reported that heteroduplex DNA is only observable in the recipient molecule, while donor DNA appears to remain unaltered (Fan et al., 1995; Gilbertson and Stahl, 1996; Goyon and Lichten, 1993). Furthermore, if the formation of crossovers and noncrossovers derive from the resolution of HJs, both repair products would be expected to appear concurrently. However, it has been demonstrated that noncrossovers appear with similar timing to joint molecule resolution, while there is a lag of

approximately 30 minutes until crossovers are formed (Allers and Lichten, 2001). Thus, noncrossovers may be formed through a different pathway, one that is independent of joint molecule formation. This has lead to the development of a modified version of the gene conversion model, called synthesis-dependant strand annealing (Figure 1.4.2).

1.4.2 Synthesis-Dependant Strand Annealing

This DSB repair model predicts that the two DNA termini act independently of each other in the homology search, and that stable heteroduplex intermediates between the 3′-ssDNA tails and the template regions do not form (Figure 1.4.2). Thus, after strand invasion, the HJ does not enlarge but instead migrates into the gap created. Following DNA synthesis, the newly synthesised strands are displaced and anneal to the 5′ ends of the DSB. Synthesis-dependant strand annealing has been suggested to be involved in mating-type switching in *S. cerevisiae* and more recently in meiotic gene conversion (Allers and Lichten, 2001).

1.4.3 Single Strand Annealing

Another homologous recombination repair pathway is single strand annealing (SSA), which is very efficient when a DSB occurs between two flanking homologous regions (Figure 1.4.3). SSA was first studied in *Xenopus laevis* oocytes, and is by some considered to be a subpathway of homologous recombination.

Following DSB formation (Figure 1.4.3a), the SSA pathway requires the 5′-3′ resectioning of DNA to extend as far as the homologous sequences, in order to uncover them (Figure 1.4.3b). These complementary regions are used to align the broken DNA strands, before

PAGE NUMBERING AS ORIGINAL

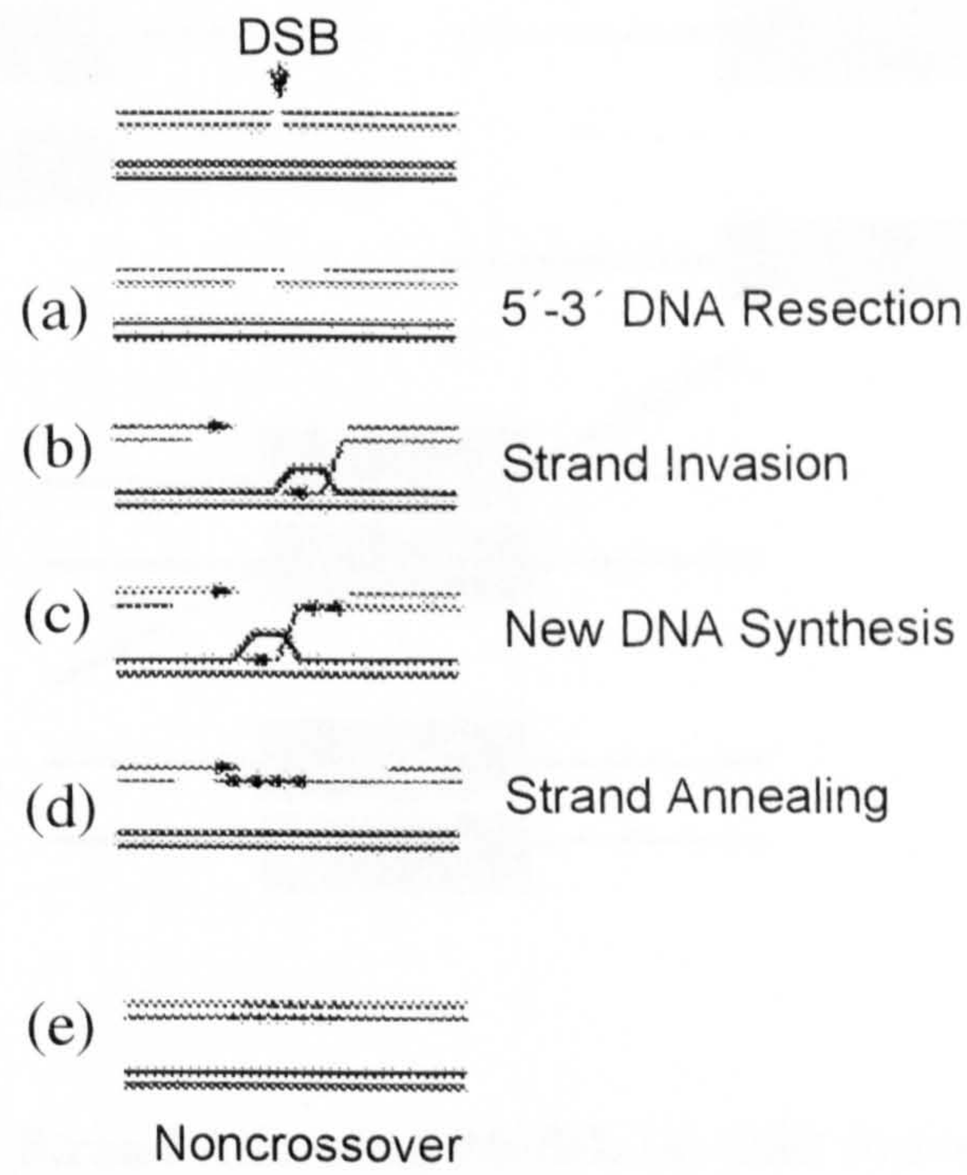

Figure 1.4.2 Synthesis-Dependent Strand Annealing Model: (a) Following 5´-3´ DNA resectioning, (b) one DNA terminal end invades the donor and (c) novel DNA synthesis occurs. The newly synthesised strand is displaced until it meets the other end, (d) which is then used as a primer for the replicated second strand. (e) The repaired DNA represents a noncrossover. (Figure taken from Haber, 2000)

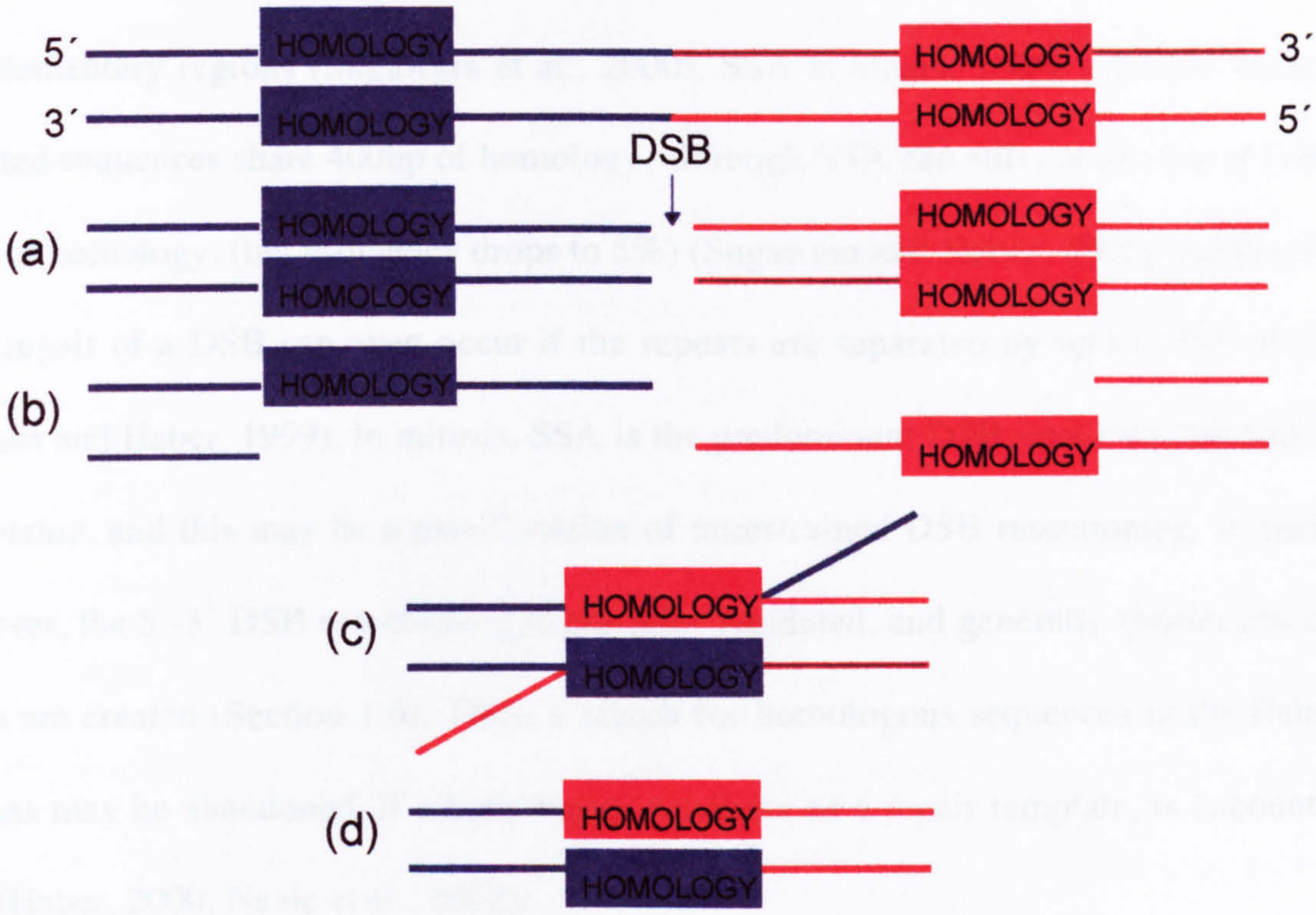

Figure 1.4.3 Single Strand Annealing Model: (a) DSB formation and (b) 5´-3´ DNA resectioning exposes the complementary regions, (c) which become annealed. (d) Removal of nonhomologous 3´ tails by nucleotide excision repair proteins, Rad1 and Rad10, followed by strand ligation completes the SSA process

they anneal and become ligated (Figure 1.4.3c and Figure 1.4.3d). SSA requires the nucleotide excision repair proteins Rad1 and Rad10, to remove the nonhomologous 3´ ssDNA tails. A single copy of the homologous sequence remains, termed deletion product.

The efficiency of SSA is dependent on the length and sequence identity of the flanking complementary regions (Sugawara et al., 2000). SSA is almost 100% efficient when the repeated sequences share 400bp of homology, although SSA can still occur with as little as 60bp of homology, (but efficiency drops to 5%) (Sugawara and Haber, 1992). Furthermore, SSA repair of a DSB can even occur if the repeats are separated by up to 15kb of DNA (Paques and Haber, 1999). In mitosis, SSA is the predominant DSB repair mechanism in *S. cerevisiae*, and this may be a manifestation of unrestrained DSB resectioning. In meiosis however, the 5´-3´ DSB resectioning is carefully regulated, and generally shorter resection tracts are created (Section 1.6). Thus, a search for homologous sequences in the flanking regions may be abandoned, if a homologue, available as a repair template, is encountered first (Haber, 2000; Neale et al., 2002).

1.5 DSB Formation Initiates Meiotic Recombination

All meiotic recombination pathways are initiated by the induction of meiosis-specific DSBs, and these breaks were first observed in genomic regions that recombine at high frequencies (Nicolas et al., 1989). Evidence to support the proposal that DSBs are the catalyst for meiotic recombination, include the observed increase in recombination frequency when DSBs are introduced into wildtype cells (Kolodkin et al., 1986; Malkova et

al., 1996), and the correlation shown between DSB formation and recombination kinetics (Cao et al., 1990; Goyon and Lichten, 1993; Padmore et al., 1991).

Meiotic DSBs are not sequence-specific, but have a high prevalence in potential transcription promotor regions (Baudat and Nicolas, 1997; Wu and Lichten, 1994). One theory is that chromatin structure may determine the sites of meiosis-specific DSBs. Alterations to chromatin structure lead to corresponding changes in the occurrence of DSBs, and DSB hotspots demonstrate hypersensitivity to deoxyribonuclease I, in both meiotic and mitotic cells (Wu and Lichten, 1994). These results indicate that chromatin remodelling prior to meiosis may be important for determining break sites. Meiotic DSB formation has an absolute requirement for the protein products of at least 11 genes, *MEI4*, *MER1*, *MER2*, *REC102*, *REC104*, *REC114*, *MRE2* and *SPO11*, which are all meiosis-specific, plus *MRE11*, *RAD50* and *XRS2* (MRX) (comprehensively reviewed in (Krogh and Symington, 2004)). Null mutations of any of these genes abolish both DSB formation and meiotic recombination.

The catalyst of meiotic DSBs was first discovered in cells carrying a *rad50S* mutation, where unresected breaks were found to accumulate with a covalently linked protein at the 5′ strand termini (Keeney and Kleckner, 1995; Liu et al., 1995). A short time afterwards the protein was identified as Spo11 (Keeney et al., 1997).

PAGE NUMBERING AS ORIGINAL

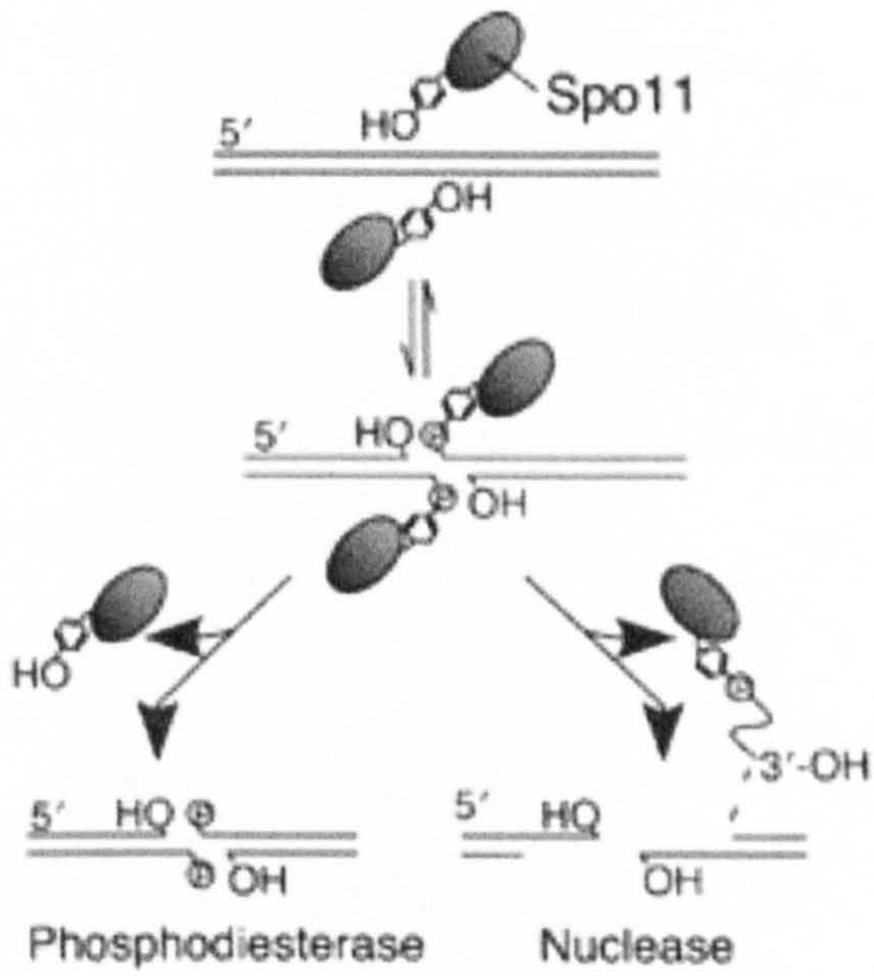

Figure 1.5: Alternative Mechanisms for Spo11 Protein Release. Spo11 protein creates meiotic DSBs via a reversible transesterase reaction. Covalently-bound Spo11 attacks the DNA backbone via a tyrosine side chain, generating a phosphodiester linkage between the 5′ terminus and Spo11 protein. Previously, Spo11 protein was thought to be released from the break site by either direct hydrolysis of the protein-DNA linkage via a phosphodiesterase, or single-stranded endonuclealytic cleavage. It has recently been confirmed that Spo11 protein-release is via nuclease action, attached to an oligonucleotide with a free 3′ -hydroxyl group. (Figure taken from Neale *et al* 2005).

Spo11 protein creates meiotic DSBs via a reversible transesterase reaction, analogous to those catalysed by DNA topoisomerases. Indeed, Spo11 protein contains several motifs that are common to Type II topoisomerases (Bergerat et al., 1997). Covalently-bound Spo11 attacks the DNA backbone via a tyrosine side chain, generating a phosphodiester linkage between the 5′ terminus and Spo11 protein. A major step forward has been made recently in the elucidation of Spo11 protein-release from the sites of DSB formation (Neale et al., 2005). Spo11 is released from the break site, attached to an oligonucleotide with a free 3′ -hydroxyl group, via endonucleolytic cleavage (Figure 1.5). Two distinct Spo11-oligonucleotide complexes were identified, differing in nucleotide length. Tantalisingly, this may be the result of strand cleavage at different intervals flanking the DSB site, raising the possibility of asymmetrical DSB processing (Neale et al., 2005).

Studies in *S. cerevisiae* of a null and catalytic mutation of *SPO11*, *(spo11-Y135F*, substitution of active tyrosine), demonstrated a defect in homologue pairing and SC formation (Loidl et al., 1994; Neale et al., 2002; Weiner and Kleckner, 1994). Furthermore, Spo11 protein has been shown to influence DSB resectioning (Neale et al., 2002).

1.5.1 The Components of DSB Repair

A universal feature of meiotic recombination is that after Spo11 protein removal, DSBs undergo a process of 5′-3′ resectioning, generating 3′-ssDNA tails. The resection machinery comprises the MRX complex, Sae2, and maybe other, as yet unknown proteins. Null mutations of *MRE11*, *RAD50* and *XRS2* prevent the formation of Spo11-DSBs

altogether, while a null mutation of SAE2, causes unresected breaks to accumulate (Alani et al., 1990; McKee and Kleckner, 1997; Prinz et al., 1997).

Sae2 protein was first isolated and characterised in a screen for mutants blocked at intermediate stages of meiotic prophase, it is required for the removal of Spo11 protein from meiotic DSB sites. (McKee and Kleckner, 1997; Prinz et al., 1997). Loss of Sae2 protein function causes Spo11 to remain covalently bound to meiotic DSBs, effectively blocking the DNA termini from the resectioning machinery. Sae2 protein functions jointly with the MRX complex during meiotic DSB processing and in the DNA damage response in mitosis.

The protein products of the *MRE11*, *RAD50* and *XRS2* genes form a stable complex, which appears to have separate and specific roles in meiosis and mitosis (Cao et al., 1990; Ivanov et al., 1992; Johzuka and Ogawa, 1995). Unique amongst the genes involved in meiotic DSB formation and processing in *S. cerevisiae*, the MRX complex is involved in certain metabolic events, including telomere maintenance, the cell cycle response to DNA damage (with Tel1, an ATM homologue), intraS-phase checkpoint, alongside more explicable roles in mitotic DSB repair, homologous recombination and NHEJ (reviewed in (Haber, 1998)). Two Mre11 molecules bridge together two Rad50 molecules, with one Xrs2 molecule (Hopfner et al., 2002; Johzuka and Ogawa, 1995; Usui et al., 1998). *MRE11* and *RAD50* encode evolutionarily conserved multi-domained proteins homologous to *E. coli* SbcC and SbcD proteins, respectively. SbcC and SbcD interact physically, and possess double-stranded (ds)-exonuclease activity and single-stranded (ss)- endonuclease *in vivo* (Paull and

Gellert, 1998). The homology shared between the proteins added weight to the proposal that the MRX complex formed the resectioning machinery that was required in meiotic DSB processing (Sharples and Leach, 1995).

The MRX complex possesses DNA binding, end recognition and nuclease activities, and as a physical complex, it stabilises sister chromatid and homologous chromosome interactions, thus fulfilling a structural role in homologous recombination (Bressan et al., 1999). Null mutations of *MRE11*, *RAD50* and *XRS2* fail to create Spo11-DSBs, thus meiotic recombination cannot be initiated, and meiotic lethality ensues.

Through various studies, including the discovery of a number of separation of function mutations, the many roles of the MRX complex have been delineated, with a primary function being described in the 5′-3′ resectioning of DSBs. For example, a *rad50S* mutant was found to create Spo11-DSBs, but these breaks accumulate unresected, analogous to the *sae2* phenotype (Alani et al., 1990). It was observed that HO-DSBs at the *MAT* locus experience delayed, and reduced levels of 5′-3′ resectioning in MRX null mutants (Ivanov et al., 1994; Llorente and Symington, 2004; Tsubouchi and Ogawa, 1998), while nuclease-defective alleles, *mre11-H125N* and *mre11-D56N*, convey sensitivity to IR and methyl methanesulfonate (MMS), but to a less severe degree than a null MRE11 mutation (Moreau et al., 1999).

Given the amount of evidence that has accumulated, the exact role of the MRX complex in Spo11-DSB processing remains unclear, due to a significant anomaly. The 3′-5′ polarity of the exonuclease activity displayed by the MRX complex *in vitro*, is opposite to that observed in meiotic DSB resectioning (Furuse et al., 1998; Trujillo et a!., 1998; Usui et al.,

1998). However, the polarity of the endonuclease activity of MRX is in the appropriate direction. An attractive prospect therefore, is that the ssDNA endonuclease activity of MRX, in concert with a helicase, degrades the 5′ ssDNA termini at Spo11-DSB sites (Moreau et al., 1999). Alternatively, the MRX complex may have a more indirect role in DSB resectioning, by recruiting other 5′-3′ polarised exonucleases to the sites of Spo11-DSBs.

Exo1 (exonuclease I) protein was first isolated in *S. pombe* cells induced to undergo meiosis (Szankasi and Smith, 1992). Subsequently, the transcription of Exo1 protein was found to be meiotically induced in *S. cerevisiae*, suggesting a role for Exo1 in meiotic DNA metabolism (Tsubouchi and Ogawa, 2000). Exo1 protein has the apposite polarity for 5′-3′ DSB resectioning, and in high-copy number *EXO1* suppresses the MMS sensitivity of *mre11*, *rad50* and *xrs2* strains (Lewis et al., 2002; Tsubouchi and Ogawa, 2000). A null *exo1* mutation increases MMS sensitivity in *mre11* and *rad50* mutants, while *mre11 exo1* double mutants are more delayed for HO-DSB resectioning than the single *mre11* mutant. Despite this seemingly compelling evidence , because Spo11-DSBs are still created and processed in an *exo1* mutant, the Exo1 protein discounts itself as the primary activity of the DSB resectioning machinery.

Interestingly, another potential role for Exo1 protein has been described in meiosis, that of promoting crossing over, to ensure accurate homologue disjunction at MI (Khazanehdari and Borts, 2000; Kirkpatrick et al., 2000). Strains mutant for *EXO1* display reduced levels of crossing over, causing a reduction in spore viability, which is associated with homologous chromosome nondisjunction (reviewed in (Tran et al., 2004)).

1.5.2 The MRX Complex and Genome Stability

While Mre11 and Rad50 are highly conserved proteins, the Xrs2 sequence has diverged more rapidly, with Xrs2 substituted for human (h)Nbs1 protein in the mammalian complex (Petrini, 1999; Tauchi et al., 2002). The metabolic defects observed in yeast null MRX mutants are also observed in mammalian cells. Chromosomal instability syndromes are caused by mutations in the mammalian MRX complex; Nijmegan breakage syndrome is caused by truncations in hNBS1, and Ataxia-telangiectasia-like disorder is caused by hypomorphic mutations of hMRE11 (Stewart et al., 1999; Varon et al., 1998). Cells derived from sufferers of these disorders are characterised by common DNA damage response defects, that is hypersensitivity to ionising radiation and defective checkpoint responses. Thus both of these disorders cause genome instability, predisposing affected individuals to cancer (D'Amours and Jackson, 2002) (Petrini, 1999).

1.6 Regulation of DSB Resectioning

The 5′-3′ DSB resectioning step, common to all homologous recombination pathways requires stringent control. The degree to which DNA is resected during DSB processing is critical to repair outcome. The generation of longer resection tracts can lead to the exposure of intramolecular flanking homologies, causing DSB repair to be directed along an intrachromosomal repair route, for example nonhomologous end joining (NHEJ) or SSA (SSA, Section 1.4.3). This may be advantageous to the cell, especially if a homologous chromosome is not available as a repair template. However intrachromosomal recombination does not fulfil the essential requirements of meiosis, that is, the generation

of interhomologue crossovers. The risk of loss of heterozygosity, which would be increased in these deleterious repair processes, further highlights how critical the process of regulating DSB resectioning is.

1.7 Repair Template Choice

Mitotic recombination, which is required for DNA repair caused by replication problems or by exogenous factors (such as ionising radiation or genotoxins), is mediated by using sister chromatids as repair templates, by the RecA homologue Rad51 (Kadyk and Hartwell, 1992; Symington, 2002). However in meiosis, cells must respond to the programmed action of meiotic DSBs differently, by mediating DSB repair between nonsister chromatids. Thus, the preferential direction of DSB repair in meiosis is towards the homologous chromosome, which also requires the meiosis-specific RecA homologue, Dmc1 protein (Bishop et al., 1992; Schwacha and Kleckner, 1997). The bias shown by the meiotic cell is purposeful; permitting crossover formation exclusively between homologous chromosomes, not only maintains their tight association until reductional segregation, but also allows for the reciprocal exchange of genetic material between homologues.

Still under investigation is whether the interhomologue bias displayed by meiotic cells is a manifestation of active promotion of interhomologue recombination, or active suppression of intersister recombination. Alternatively, a combination of both processes may be at work.

Dmc1 protein has a pivotal role in establishing and facilitating meiotic interhomolog exchange, along with Red1, Mek1, Rad51, Rad55 and Rad57 (Schwacha and Kleckner,

1997; Wan et al., 2004). The loss of strand exchange function causes *dmc1* cells to accumulate Spo11-DSBs, with the broken DNA termini undergoing additional 5′ to 3′ resectioning (Bishop et al., 1992). However, whether Dmc1 protein is a component that provides specificity for nonsister strand exchange is doubtful. It has been demonstrated that overexpression of Rad51 protein largely suppresses the recombination defect of a *dmc1* mutant (Tsubouchi and Roeder, 2003). While in other organisms that undergo Spo11-DSB mediated meiotic recombination, such as *C. elegans* and *D. melanogaster*, no Dmc1 orthologue exists at all (Villeneuve and Hillers, 2001).

As meiotic DNA strand exchange preferentially occurs between homologous chromosomes, even in the absence of Dmc1 protein, the possibility of a block to intersister repair appears to be a feasible alternative to explain the observed repair bias. Recently, a separate mechanism for ensuring that crossovers occur between homologues only, has been described (Wan et al., 2004). This involves three meiosis-specific chromosomal core proteins, Mek1, Red1 and Hop1. Activation of Mek1 kinase, (which coincides with the formation of Spo11-DSBs), is thought to mediate inhibition of the proteins required for repair between sister chromatids, such as Rad54 (Wan et al., 2004). Thus, during Spo11-DSB processing, Mek1 protein effectively creates a barrier to intersister repair, thus pushing repair towards the homologous chromosome (Wan et al., 2004). Further work on the Mek1 protein complex has demonstrated that it is Hop1 activation of Mek1 protein, through dimerisation, that enables Mek1 to target proteins involved in intersister repair (Niu et al., 2005).

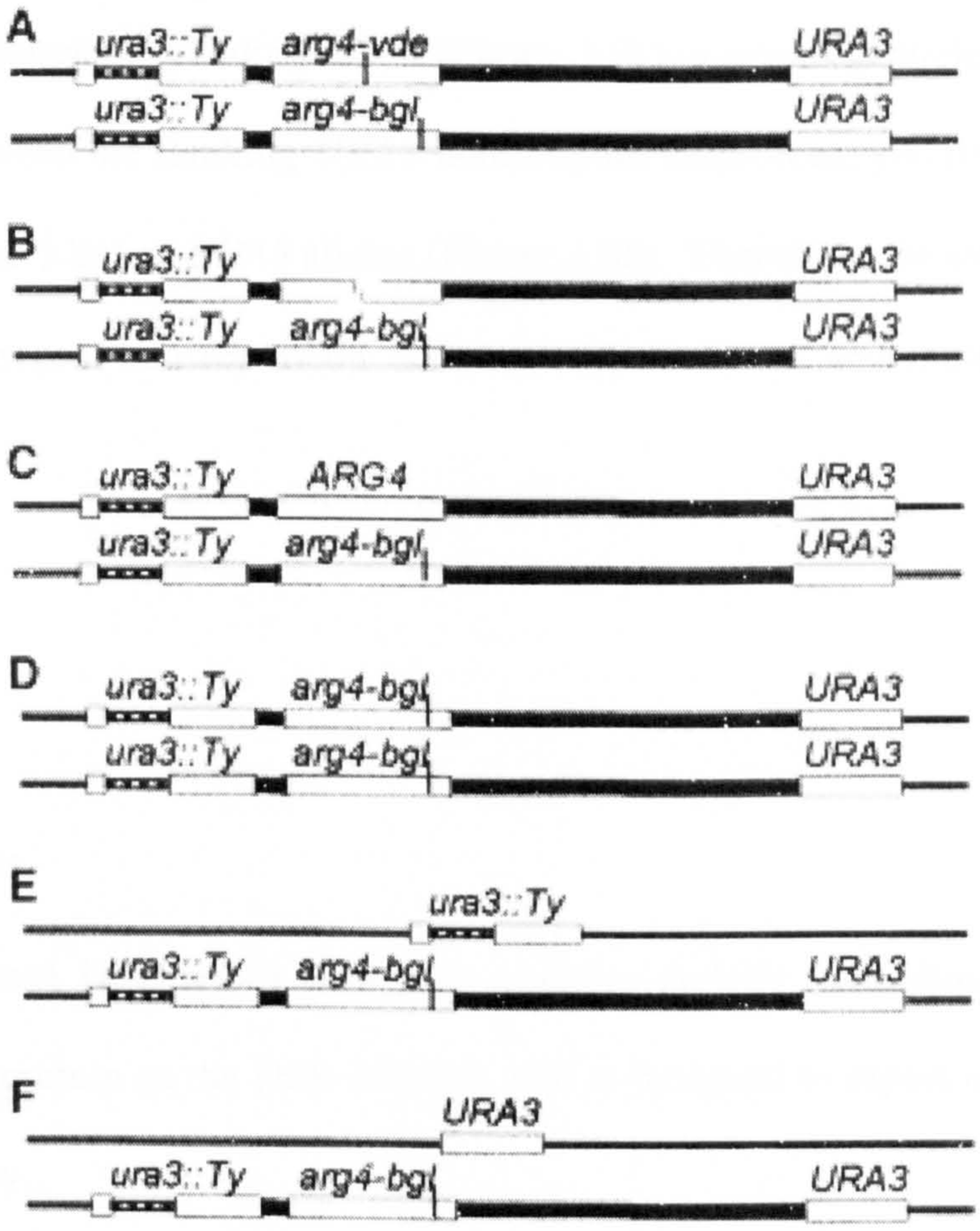

Figure 1.8: Original VDE-DSB Reporter Assay. (a) Parental cassette DNA containing the VDE-DSB site, with *URA3* flanking homologies and a donor *arg4-bgl* allele on the homologue. (C–F) Different products of DSB repair at the *arg4-VDE* locus: (C) gene conversion to *ARG4*, (D) gene conversion to *arg4-bgl*, (E) repair using flanking repeated sequences leading to *ura3::Ty* deletion product, and (F) repair using flanking repeated sequences leading to *URA3* deletion product. (Figure taken from Neale *et al* 2002).

1.8 Origins of the Assay in this Study

Repair of a meiosis-specific DSB has been previously studied in a different reporter assay (Neale et al., 2002). In that assay, a DSB created by VDE endonuclease was flanked by WT and mutant *URA3* alleles (Figure 1.8a). Following formation of the VDE-DSB (Figure 1.8b), four repair outcomes were possible: a gene conversion event using the *arg4-bgl* allele as repair template, yielding *ARG4* (Figure 1.8c) or *arg4-bgl* aileles (Figure 1.8d), or a SSA event between the flanking *URA3* homologous sequences, yielding deletion products *ura3::Ty* (Figure 1.8e) or *URA3* alleles (Figure 1.8f). Therefore, the assay was designed to distinguish between, and report on both interchromosomal and intrachromosomal DSB repair.

1.9 Initial Aims

To create a novel DSB repair assay for studying meiotic recombination; that does not require Spo11 protein as the DSB catalyst, and is designed to report on intrachromosomal DSB repair only.

Characterise a number of mutants for DSB repair and DNA resection tract length.

Screen for novel mutants that affect regulation of DSB resectioning.

Chapter 2

Materials and Methods

Table 2.1 *Escherichia coli* Strains

Name	Genotype	Source
DH5α	*supE44 ΔlacU169(ϕ80 lacZΔM15) hsdR17 recA1 endA1 gyrA96 thi–1 relA1*	Laboratory Resource

Table 2.2 Plasmids

Name	Description	Source
pAG72	*kanMX4* cassette in pBS423	M. Lichten
pAG73	*XRS2* expression vector driven by *HOP1* promoter, *hph*MX4 cassette	PMJ704, V. Borde
pAG126	*natMX4* cassette in pFA6	(Goldstein and McCusker, 1999)
pAG157	*hphMX4* cassette in pFA6	(Goldstein and McCusker, 1999)
pAG304	*xrs2-11* fragment in TA vector (Invitrogen) (hAG 1161, primers xrs2-11F/R, Table 2.4)	This Study
pAG406	Precursor cassette, containing Δ*ade2 ura3Δ arg4-nsp URA3* (clockwise orientation)	PMJ113_115Δ*ura3*, M. Ramachandran and A. Goldman, (Unpub.)
pAG407	pAG405 with *arg4-VDE* insert at *Bam*HI site (*BamHI* fragment from pAG404), making Δ*ade2 ura3Δ arg4-VDE URA3* (anticlockwise orientation)	PMJ113_115Δ*ura3*+*URA3*Rev, This Study
pAG408	pAG406 with *arg4-VDE* insert at *Bam*HI site (*BamHI* fragment from pAG404), making Δ*ade2 ura3Δ arg4-VDE URA3* (clockwise orientation)	PMJ113_115Δ*ura3*+*URA3*, This Study

2.3 *Saccharomyces cerevisiae* Strains

Table 2.3.1 Haploid Strains

All haploid strains are derivatives of SKI (Kane and Roth, 1974), unless stated otherwise. All haploid strains are *ura3 lys2 ho::LYS2*, unless stated otherwise. Only mutant alleles shown.

Name	Genotype	Source
hAG2	*MAT***a** *trp1::hisG*	S55, M. Lichten
hAG3	*MAT***a** *trp1::hisG*	S56, M. Lichten
hAG55	*MAT***a** *ura2 (URA3)*	S317, M. Lichten

hAG56	*MATα ura2 (URA3)*	S318, M. Lichten
hAG287	*MATα arg4-nsp,bgl leu2-K sae2::kanMX*	S1195, V. Borde
hAG320	*MATα arg4-nsp dmc1Δ::ARG4*	DKB195, D. Bishop
hAG416	*MATα ade2Δ(EcoRV-StuI) arg4-nsp,bgl leu2-R nuc1Δ::LEU2 TFP1::VDE*	(Neale et al., 2002)
hAG417	*MAT***a** *ade2Δ(EcoRV-StuI) arg4-nsp,bgl leu2-R nuc1Δ::LEU2 TFP1::VDE*	(Neale et al., 2002)
hAG418	*MATα ade2Δ(EcoRV-StuI) arg4-nsp,bgl leu2-R nuc1Δ::LEU2*	M.J.N and A.S.H.G (Unpub.).
hAG419	*MATα ade2Δ(EcoRV-StuI) arg4-nsp,bgl leu2-R nuc1Δ::LEU2 spo11(Y135F)-HA3His6::kanMX*	(Neale et al., 2002)
hAG678	*MAT***a** *arg4-bgl leu2::hisG his4B::LEU2 trp1 mre11-58s*	S1359, H. Ogawa
hAG684	hAG3 transformed with pAG408	This Study
hAG690	*MATα cyh2-z rad50Δ::hisG*	ORT4603, V. Borde
hAG692	*MATα arg4-nsp,bgl leu2-K xrs2Δ::kanMX*	ORT4620, V. Borde
hAG693	*MATα arg4-nsp,bgl leu2 mre11Δ::kanMX*	ORT4700, V. Borde
hAG695	hAG2 transformed with pAG407	This Study
hAG1161 (W303)	*MAT***a***-inc ADH4cs::HIS2 ade1 his2 leu2 trp1 ura3 xrs2-11::KANMX*	KSC1621,(Nakada et al., 2003)

Table 2.3.2 Diploid Strains

All diploid strains are SK1, *MAT***a**/α and homozygous for *ura3 lys2 ho::LYS2*, unless stated otherwise. Only mutant alleles shown.

Name	Genotype	Source
dAG630	*ade2::URA3 -(arg4-VDE, ura3) trp1::hisG ARG4* *Δade2(EcoRV-StuI) TRP1 arg4-nsp,bgl* *LEU2 TFP1* *leu2-R nuc1Δ::LEU2 TFP1::VDE*	This Study
dAG646	*ade2::URA3 -(arg4-VDE, ura3) trp1::hisG ARG4* *Δade2(EcoRV-StuI) TRP1 arg4-nsp,bgl* *LEU2* *leu2-R nuc1Δ::LEU2*	This Study
dAG649	*ade2::URA3[1] -(arg4-VDE, ura3) trp1::hisG ARG4* *Δade2(EcoRV-StuI) TRP1 arg4-nsp,bgl* *LEU2 TFP1* *leu2-R nuc1Δ::LEU2 TFP1::VDE*	This Study
dAG720	*ade2::URA3 -(arg4-VDE, ura3) trp1::hisG ARG4* *Δade2(EcoRV-StuI) TRP1 arg4-nsp,bgl* *LEU2 TFP1::VDE* *leu2-R nuc1Δ::LEU2 TFP1::VDE*	This Study
dAG732	*ade2::URA3 -(arg4-VDE, ura3) trp1::hisG leu2* *Δade2(EcoRV-StuI) TRP1 leu2 nuc1::LEU2* *ARG4 TFP1 mek1Δ::LEU2*	This Study

ade2::URA3[1] denotes opposite orientation of *URA3* in Inverted Cassette strain, dAG649

	arg4-nsp TFP1::VDE mek1Δ::LEU2	
dAG759	*ade2::URA3-(arg4-VDE, ura3) leu2-R* *Δade2(EcoRV-StuI) leu2-R nucΔ1::LEU2* *arg4-nsp,bgl TFP1 spo11(Y135F)-HA3His6::kanMX* *arg4-nsp,bgl TFP1::VDE spo11(Y135F)-HA3His6::kanMX*	This Study
dAG946	*ade2::URA3-(arg4-VDE, ura3) trp1::hisG ARG4* *Δade2(EcoRV-StuI) TRP1 arg4-nsp,bgl* *LEU2 TPFI xrs2::kanMX* *leu2-R TFP1::VDE xrs2::kanMX*	This Study
dAG951	*ade2::URA3-(arg4-VDE, ura3) ARG4 LEU2* *Δade2(EcoRV-StuI) arg4-nsp,bgl leu2::hisG* *TFP1 rad50Δ:hisG* *TFP1::VDE rad50Δ:hisG*	This Study
dAG975	*ade2::URA3-(arg4-VDE, ura3) trp1::hisG arg4-bgl* *Δade2(EcoRV-StuI) TRP1 arg4-bgl* *LEU2 TFP1 mre11-58s* *his4::LEU2 TFP1::VDE mre11-58s*	This Study
dAG1000	*ade2::URA3-(arg4-VDE, ura3) leu2-K ARG4* *Δade2(EcoRV-StuI) leu2-R arg4-nsp,bgl* *TFP1 NDT80 xrs2::kanMX* *TFP1::VDE ndt80::NATMX xrs2::kanMX*	This Study
dAG1010	*ade2::URA3-(arg4-VDE, ura3) LEU2 arg4-nsp,bgl* *Δade2(EcoRV-StuI) leu2-R arg4-nsp,bgl* *TFP1 mre11Δ::kanMX* *TFP1::VDE mre11Δ::kanMX*	This Study
dAG1093	*ade2::URA3-(arg4-VDE, ura3)) LEU2 ARG4* *Δade2(EcoRV-StuI) leu2-K arg4-nsp,bgl* *TFP1 ndt80::NATMX xrs2::kanMX* *TFP1::VDE ndt80::NATMX xrs2::kanMX*	This Study
dAG1200	*ade2::URA3-(arg4-VDE, ura3) LEU2* *Δade2(EcoRV-StuI) leu2-R nuc1Δ::LEU2* *ARG4 TFP1 sae2::kanMX* *arg4-nsp,bgl TFP1::VDE sae2::kanMX*	This Study
dAG1215	*ade2::URA3 -(arg4-VDE, ura3) trp1::hisG leu2* *Δade2(EcoRV-StuI) TRP1 leu2 nuc1::LEU2* *arg4-nsp,bgl TFP1 mek1Δ::LEU2 sae2::KanMX* *arg4-nsp TFP1::VDE mek1Δ::LEU2 sae2::KanMX*	This Study
dAG1236	*ade2::URA3-(arg4-VDE, ura3) LEU2 ARG4 HIS4* *Δade2(EcoRV-StuI) leu2-R arg4-bgl his4B* *TFP1 rad54Δ* *TFP1::VDE rad54Δ*	This Study
dAG1265	*ade2::URA3-(arg4-VDE, ura3) LEU2 arg4-nsp TFP1* *Δade2(EcoRV-StuI) leu2-R arg4-nsp TFP1::VDE* *dmc1Δ::ARG4* *dmc1Δ::ARG4*	This Study
dAG1271	*ade2::URA3-(arg4-VDE, ura3) LEU2* *Δade2(EcoRV-StuI) leu2-R nuc1Δ::LEU2* *ARG4 trp1::hisG TFP1 xrs2-11::kanMX* *arg4-nsp,bgl TRP1 TFP1::VDE xrs2-11::kanMX*	This Study
dAG1284	*ade2::URA3-(arg4-VDE, ura3) leu2-R arg4-nsp* *Δade2(EcoRV-StuI) leu2-R nuc1Δ::LEU2 arg4-nsp* *TFP1 dmc1Δ::ARG4 spo11(Y135F)-HA3His6::kanMX*	This Study

	TFP1::VDE dmc1Δ::ARG4 spo11(Y135F)-HA3His6::kanMX	
dAG1300	*HO TRP1 leu2 VMA1-201 exo1Δ::kanMX* *ho::hisG trp1 leu2 LEU2::VMA1::URA3 exo1Δ::kanMX*	YOC3121 (Fukuda et al., 2003)
dAG1305	*ade2::URA3-(arg4-VDE, ura3) trp1::hisG LEU2 ARG4* *Δade2(EcoRV-StuI) TRP1 leu2-R arg4-nsp,bgl* *TFP1 exo1Δ::kanMX* *TFP1::VDE exo1Δ::kanMX*	This Study

2.4 PCR Primers

Synthesised by MWG-Biotech, with high–purity salt free purification

Name	DNA Sequence	Description
MN03	GGTACAATCACTTGGATTGCTCC	*TFP1* locus
MN04	AAGCTTCTCTGGCTGCAACCGGC	*TFP1* locus
xrs2-11F	TGAGGGACAGTCATAGCGG	*XRS2* locus
xrs2-11R	AGAGGCTACGTTGTTCTGGC	*XRS2* locus
XRS2-F	AACGTGGGTACAGACGGG	*XRS2* locus
XRS2-R	CAAGAGTTGCCAAAGACGGG	*XRS2* locus
drugpromotor	CCTTGACAGTCTTGACGTGC	*TEF* promoter
drugterminator	CAGATGCGAAGTTAAGTGCG	*TEF* terminator
Leftconstruct_F	GCCCAATGTGTCCATCTGAC	*ADE2* locus, (upstream)
Leftconstruct_R	GCCTGTTTGCTGCCTCAAC	*ADE2* locus, (upstream)
AB01	CTTGTTGCATGGCTACGAACCG	5′ *ADE2* locus
AB02	CCCAATGCGTCTCCCTTGTC	5′ *URA3* locus
AB03	TAGGCGTATCACGAGGCCC	pBR322 specific
AB04	ATCCTCGGTTCTGCATTGAGCC	*ADE2* locus, (downstream)
seqP1_F	CCCTGAGCTGCGCACGTCAAG	*XRS2* ORF
seqP2_F	CGGATCTGAAACACAGTAGC	*XRS2* ORF
seqP3_F	GGCTGAATAATATCAGAGTG	*XRS2* ORF
seqP4_F	CCCAACATTGCAGAGGCAG	*XRS2* ORF
seqP5_F	CGCACGCATTTGTTGAAGC	*XRS2* ORF
seqP6_F	GGGCACAGAAGAAAACGAAG	*XRS2* ORF

2.5 Growth Media and Stock Solutions

All media and stock solutions were made in dH_20 and autoclaved at 15lbs/in^2 for 15min at 121°C, or filter sterilised through 0.45μm filters. UP-H_20 used in DNA reactions, was distilled water passed through a Millipore system and autoclaved to make it ultra pure. Reagents were mainly from the companies Sigma-Aldrich, Difco and BDH. Percentage concentrations given throughout the study are w/v for solid and v/v for liquid chemicals.

2.5.1 Media

2TY:

1.1% tryptone, 1% yeast extract, 0.5% sodium chloride, 1.5% agar (solid media) pH7.4. For selection of DH5α strains that contained a plasmid conveying drug resistance, antibiotic was added to autoclaved cooled 2TY:

amp^R: 50μg/ml ampicillin, (Sigma-Aldrich)

hph^R: 100μg/ml hygromycin B (Sigma-Aldrich)

nat^R: 50μg/ml nourseothricin (Werner BioAgents)

YEAPD:

1% yeast extract, 2% peptone, 2% D-glucose, 2% agar (solid media), 40μg/ml adenine. Yeast strains containing MX drug resistance genes were selected for on YEAPD medium plus antibiotic, (added to autoclaved, cooled YEAPD):

*kan*MX: 200µg/ml G418 (Melford)

*hph*MX: 300µg/ml hygromycin B (Sigma-Aldrich)

*nat*MX: 100µg/ml nourseothricin (Werner BioAgents)

Minimal:

2% D-glucose, 0.68% yeast nitrogen base (w/o amino acids), 2% agar.

Synthetic complete (Sc):

Made up as minimal media plus 0.85g/l of complete master mix and 1μl/ml of 2M NaOH (liquid Sc, no agar). Complete master mix contained 0.8g adenine, 0.8g arginine, 4.0g aspartic acid, 0.8g histidine, 2.4g leucine, 1.2g lysine, 0.8g methionine, 2.0g phenylalanine, 8.0g threonine, 0.8g tryptophan, 1.2g tyrosine and 0.8g uracil. Dropout master mix was as Complete, minus the amino acid(s) used for selection.

5-FOA:

2x stock made in 500ml dH_20: 1.4% yeast nitrogen base w/o amino acids, 4% agar, 4% D-glucose, 100μg/ml uracil, plus appropriate supplemental amino acids.

1g 5-fluoorotic acid dissolved in 500ml dH_20, filter sterilised, and then added with thorough mixing to autoclaved cooled 2x stock.

PSP2 (pre-sporulation medium):

0.67% yeast nitrogen base w/o amino acids, 0.1% yeast extract, 1% potassium acetate, 1.02% potassium hydrogen phthalate, 40μg/ml adenine.

K-Ac (sporulation medium):

Liquid media: 1% potassium acetate (J.T.Baker), supplemented with 10μg/ml adenine, plus appropriate amino acid supplements at 10μg/ml to complement the auxotrophies of the yeast strain. Solid media: 2% potassium acetate, 2% agar, 0.1% yeast extract, 0.05% D-glucose, 10μg/ml adenine.

2.5.2 Solutions

10xTE:

100mM Tris base, 10mM EDTA, pH7.5

10xTNE:

100mM Tris.HCl, 2M NaCl, 10mM EDTA, pH7.4

50xTAE:

2M Tris base, 100mM EDTA, 0.95M acetic acid

20xSSPE:

3.6M NaCl, 200mM NaH_2PO_4, 20mM EDTA, pH7.4

Plasmid TENS:

1M NaOH, 10% SDS, 10xTE

Genomic TENS:

2% Triton-X-100, 1% SDS, 100mM NaCl, 10mM Tris.HCl pH8.0, 1mM EDTA

6x Loading Dye:

0.25% Bromophenol-blue, 20% sucrose

Heavy Loading Dye (southern gels):

0.25% Bromophenol blue, 0.25% xylene cynanol, 20% ficol

Proteinase K Solution:

10mM Tris.HCl pH7.5, 20mM $CaCl_2$, 50% glycerol, filter sterilised before addition of 20mg/ml Proteinase K

RNase Solution:

10mg/ml RnaseA, 10mM Tris.HCl pH7.5, 22.5mM NaCl. Incubated at 100°C for 15 mins, cooled slowly.

Spheroplasting Solution (±20% glycerol):

1M sorbitol, 50mM KPO_4, pH7.5, 10mM EDTA, pH7.5, (20% glycerol)

CTAB Extraction solution:

3% CTAB, 0.1M Tris-HCl pH7.5, 25mM EDTA, 2M NaCl, 2%PVP_{40}

CTAB Dilution solution:

1% CTAB, 50mM Tris-HCl pH7.5, 10mM EDTA pH8.0

Sodium Phosphate Buffer, pH7.5 (plasmid rescue):

100mM Na_2HPO_4, 100mM NaH_2PO_4.2H2O

Hydroxylamine solution (plasmid mutagenesis):

1M hydroxylamine, 50mM sodium pyrophosphate pH7, 100mM sodium chloride, 2mM EDTA

Prehybridisation solution:

2x SSPE, 1% SDS, 0.5% non-fat dry milk, 5μg/ml boiled salmon sperm DNA

Hybridisation solution:

2x SSPE, 1% SDS, 0.5% non-fat dry milk, 5% dextran sulphate (Sigma-Aldrich)

Washing buffers (southern hybridisation):

First wash: 2% SSPE, 1% SDS, Second wash: 0.5% SSPE, 1% SDS, Third wash: 0.1% SSPE, 1% SDS

2.6 *Escherichia coli* Techniques

2.6.1 *E. coli* Growth Conditions

All plasmids were maintained in *E. coli* DH5α cells, which were chemically competent for transformation. Fresh colonies were obtained by streaking out cells from glycerol stocks onto solid 2TY plus 30μg/ml ampicillin, to maintain selection of the amp^R-containing plasmids, and then incubated at 37°C overnight.

2.6.2 Preservation and Storage of DH5α Cells

Transformed *E. coli* cells were stored in 50% sterile glycerol at –80°C. Fresh colonies were inoculated into 5ml of 2TY plus 50μg/ml ampicillin media and incubated at 37°C overnight. The cultures were spun at 3000g for 5min and the pellets resuspended in 1ml glycerol. The resuspensions were aliquoted into duplicate sterile glass screw-capped vials, and stored at –80°C.

2.6.3 Transformation of DH5α Cells

The chemically competent DH5α cells were transformed with plasmid DNA using a heat-shock method. 50μl of cells were mixed with a small amount of transforming plasmid DNA and incubated on ice for 15min. The cell reactions were heat shocked at 42°C for 90sec and then 450μl of 2TY media was added and the cells incubated at 37°C for 1hr with agitation (no selection). Cells were plated out onto solid 2TY media plus antibiotic for plasmid selection, (typically ampicillin or hygromycin B) and incubated overnight at 37°C.

2.7 *Saccharomyces cerevisiae* Techniques

2.7.1 *S. cerevisiae* Growth Conditions

All *S. cerevisiae* strains were of the SK1 background. Diploid SK1 cells are universally used in meiotic studies due to their ability to sporulate rapidly (Kane and Roth, 1974). Consequently, all diploid (and haploid) cells were struck out fresh from glycerol stock for each experiment, onto solid media and incubated at 30°C for 48hr.

2.7.2 Preservation and Storage of Yeast Clones

To prevent spontaneous sporulation of diploid cells, strains were stored in 50% sterile glycerol at –80°C. Fresh colonies were inoculated into 5ml of YEAPD media and incubated at 30°C overnight. The cultures were centrifuged at 3000g for 2min and the pellets resuspended in 1ml glycerol. The resuspensions were aliquoted into duplicate sterile glass screw-capped vials, and stored at –80°C.

2.7.3 Haploid Cell Mating

Diploidisation occurs when two haploid cells of opposite mating type (*MAT***a**/α) undergo cell fusion. Fresh single colonies of equal size and opposite mating type were mixed together, in a small patch on solid YEAPD medium. After an overnight incubation at 30°C, a small amount of cells (consisting of a mixture of parental haploids and diploids) was restreaked onto YEAPD. After 48hr incubation at 30°C, single colonies were tested for diploidisation.

2.7.4 Diploid Testing

After mating, single colonies were tested for their ability to mate with tester haploid strains, hAG55 and hAG56 (*ura2*), exploiting the fact that diploid cells are sterile, thus unable to mate. All strains used in this study were *URA2*, so if mating occurred, there would be complementation of the nutritional mutation in hAG55 or hAG56. Each potential diploid was mated with both tester strains, and incubated at 30°C overnight. The matings were replica plated to solid minimal media and following an overnight incubation at 30°C, the presence or absence of growth was assessed. Growth on minimal medium indicated complementation of the *ura2* mutation; therefore the parental colony was a haploid. A lack of growth indicated that complementation had not occurred with either mating type, so the parental colony must have been diploid. Diploidisation could be further confirmed by testing for the ability to sporulate.

2.7.5 Sporulation on Solid Medium

To induce asynchronous meioses in diploid cells, single fresh colonies were patched onto YEAPD plates and incubated overnight at 30°C. The patches were replica-plated onto solid 2% K-Ac medium and incubated at 30°C for 2-3 days. The presence of mature asci (tetrads) in the patch was used to measure the degree of sporulation.

2.7.6 Tetrad Dissection

Following sporulation on solid K-Ac medium, a small amount of tetrads were incubated in 20µl β-glucuronidase (9.45U/µl, Sigma-Aldrich) at 30°C for 20min. β-glucuronidase breaks down the asci that hold spores together, thus allowing tetrads to be broken down into their component spores. 200µl UP-H_20 was added to the cells, vortexed and then 20µl of the suspension plated out onto a level YEAPD plate, ready for spore dissection, using a micro-manipulater (Singer). After tetrad dissection, the spores were incubated at 30°C for 48hr to allow germination and cell growth. To assess spore segregation patterns, the YEAPD plates were replica plated to selective media and incubated overnight at 30°C. Spore mating types were ascertained by replica plating the YEAPD plates with confluent cultures of tester strains, hAG55 and hAG56, incubated overnight at 30°C and replica plated to minimal media. Complementation with hAG55 or hAG56 denoted that spores were *MAT*α or *MAT***a** respectively. (Haploids only selected from four-spore viable tetrads).

2.7.7 Selection of Ura- Colonies

To counter select against Ura+ yeast strains, fresh colonies were patched onto solid YEAPD, incubated overnight at 30°C, and then replica plated onto 5-FOA solid medium. 5-

fluoroorotic acid disrupts the uracil biosynthetic pathway in *S. cerevisiae*, so following a 2-3 day incubation at 30°C, Ura+ cells are screened out.

2.7.8 Chemical Transformation of *S. cerevisiae*

For high efficiency transformation of haploid cells with plasmid DNA or linear DNA fragments, a modified lithium acetate method was used (Gietz et al., 1995). A 5ml YEAPD culture was incubated overnight at 30°C, and the OD_{600} of 40-fold diluted cells measured. Cells were then inoculated into 20ml YEAPD in 250ml conical flasks, to OD_{600} of 0.1 and 0.2. The cultures were incubated at 30°C at 200rpm for 3-5hr, to allow at least two cell divisions. Cell cultures grown to an OD_{600} of 0.6-0.8 were centrifuged at 3000g for 2min and the harvested cells washed in 10ml of UP-H_2O, centrifuged as before, and then resuspended in 1ml of 100mM lithium acetate. The cells were spun at 17,000g for 15sec and the pellets resuspended in 160µl of 100mM lithium acetate. 50µl aliquots of cells were pelleted at 17,000g for 15sec and the supernatant removed. 240µl of 50% PEG was added (to shield the cells from the high concentration of lithium acetate), followed by 36µl 1M lithium acetate, 10µl 10mg/ml (heat) de*Natured* salmon sperm DNA, 1-10µg transforming DNA and UP-H_2O to a total volume of 360µl. The reactions were vortexed vigorously for 1min, and then incubated for two 30min intervals, first at 30°C, then at 42°C to heat shock. The reactions were gently pelleted at 4,000g for 15sec and the supernatant removed. The cells were resuspended in 1ml UP-H_2O and plated out onto appropriate selective solid media and incubated at 30°C (2-3 days). For hph^R selection of episomal *xrs2* transformants, the transformation reactions were plated onto YEAPD media and incubated at 30°C for 48hr, to allow confluent cell growth. The plates were then replica-plated onto YEAPD plus hygromycin B and incubated at 30°C for 48hr.

2.7.9 Electroporation Transformation of *S. cerevisiae*

5ml YEAPD cultures were incubated overnight at 30°C and then pelleted at 3000g for 2min. The pellets were washed three times in 3ml 1.2M ice-cold sorbitol, centrifuged as before, and then resuspended in a minimum volume. 5-10μg of transforming DNA was ethanol precipitated with 5μl heat de*Natured* salmon sperm DNA (10mg/ml), and resuspended in 5μl of 1xTE. 40μl of washed cells was mixed with the DNA and gently pipetted into a Gene Pulser cuvette (BioRad), where the cells were exposed to an electrical pulse. 400μl of ice-cold 1.2M sorbitol was added to the electroporated cells to buffer the cells. The cells were plated out onto selective media containing 1.2M sorbitol, and incubated at 30°C for 72hr. Sizeable colonies were struck out onto selective media and incubated at 30°C for a further 48hr to select for true transformants.

2.7.10 Meiotic Timecourses (Synchronous)

A fresh diploid colony was inoculated into 5ml YEAPD in a 50ml conical flask. The culture was vortexed and then grown in a shaking incubator at 30°C, 300rpm for 24hr. To measure cell density, the OD_{600} of 20-fold diluted cells was taken. Cultures with an OD_{600} of 14-22 were used to inoculate multiple dilutions of the presporulation media, PSP2. Dilutions of between 1/100 and 1/1000 of the YEAPD starter culture were made into 300ml of PSP2 in 2l conical flasks and incubated at 30°C, 300rpm for 24hr. Cell density was measured by taking the OD_{600} of 2-fold diluted cells, and cultures with an OD_{600} of 1.4-1.8 were selected for inoculation into sporulation media. To ensure that the cell cultures were ready to enter synchronous meioses, they were examined under a light microscope to

ensure they contained a large proportion of swollen unbudded cells. The cells were pelleted at 3000g for 2min at 28°C and then rapidly washed in 300ml of 1% liquid K-Ac. The cells were centrifuged as before, and the pellet resuspended in 300ml 1% K-Ac plus 0.001% adenine, 0.001% arginine and 0.001% PPG1000. The cells were then transferred into 3l baffled flasks, and incubated at 30°C, 300rpm for the duration of the time course. The first time point was taken immediately. The cells' passage from presporulation to sporulation was completed in the minimum amount of time, to ensure that the first time point taken truly represented the initiation of meiosis. To this end, all media and flasks were prewarmed to 30°C. Cells samples were taken at hourly time points, up to and including T=8hr.

2.7.11 Processing Meiotic Time Point Cells

At each time point, 25ml of cells were aliquoted into 6ml 50% glycerol (ice-cold) and 300µl 10% sodium azide. The tubes were inverted and left on ice for 15min. Cells were pelleted at 3000g for 2min and then washed in 8ml of spheroplasting solution (plus 20% glycerol) and centrifuged as before. The supernatant was removed and the pellets snap-frozen in a dry ice/ethanol bath, the cells were then stored at –80°C.

2.7.12 DAPI Staining of Cells to Monitor Meiotic Progression

For each meiotic time point, 500µl of cells were fixed in 500µl of 100% ethanol (ice-cold), and stored at –20°C. The cells were centrifuged at 17,000g for 1min and the pellets resuspended in 1ml UP-H_20. 1µl of DAPI (0.5mg/ml) was added and the cells incubated in darkness for 5min for nuclear staining. The cells were pelleted as before, and resuspended

in a small volume of 1xTE. Cell nuclei were visualised using a fluorescence microscope (Leica DMLB Epifluorescence). At least 200 cells per time point were counted and scored for the number of DAPI-staining bodies present.

2.8 Molecular Biology Techniques

2.8.1 Small Scale Plasmid DNA Extraction from *E.coli* (miniprep).

A fresh *E.coli* colony was inoculated into 5ml of 2TY plus ampicillin and incubated overnight at 37°C with agitation. 1.5ml of the culture was pelleted at 17,000g for 1min, most of the supernatant was removed and the pellet resuspended in the residual 50-100µl. 300µl of plasmid TENS was added and the mixture vortexed before the addition of 150µl of sodium acetate (3M, pH5.5). The mixture was again vortexed until a white precipitate of protein and cell debris had formed, it was then centrifuged at 17,000g for 10min and the DNA-containing supernatant retained ready for ethanol precipitation.

2.8.2 Large Scale Plasmid DNA Extraction from *E.coli* (midiprep).

1ml from a 5ml overnight *E.coli* culture was inoculated into 100ml 2TY plus ampicillin and incubated at 37°C overnight. Cells were harvested and processed using a DNA Purification System (Promega), following the manufacturers guidelines. After DNA elution from the kit column, it was centrifuged for 5min at 17,000g to remove any residual column resin. To ensure maximum purity, the DNA was further cleaned by ethanol precipitation.

2.8.3 Ethanol Precipitation

Following small-scale (Section 2.8.1) or large-scale (Section 2.8.2) plasmid DNA extraction, the DNA was reprecipitated by the addition of sodium acetate (10% v/v, 3M pH5.5) and ice-cold ethanol (200% v/v). Miniprep DNA was incubated at –80°C for 20min to encourage precipitation, and then pelleted at 17,000g for 30min (these steps not generally required for midiprep DNA). The supernatant was removed and the DNA washed twice in 1ml of 70% ethanol. Great care was taken to remove all of the ethanol from the DNA, with any residual ethanol removed by bench centrifuge-pulsing down and pipetting off. Miniprep DNA was typically resuspended in 30µl of TE–RNase (10μg/ml Rnase A in 1xTE), and midiprep DNA, in 100µl of 1xTE.

2.8.4 Hydroxylamine Mutagenesis

A modified hydroxylamine method was used for plasmid mutagenesis (Busby et al., 1982). Hydroxylamine causes the conversion of cytosine (C) bases into hydroxylaminocytosine, which base pairs with adenosine, creating GC to AT transition mutations in dsDNA. 20µg target plasmid was added to 1ml fresh hydroxylamine solution, the mixture was vortexed and incubated at 75°C. The degree of mutagenesis was titered by removing 100µl aliquots at several time points (T=0, 10, 20, 60 and 90min) into new tubes, and the reactions rapidly stopped on ice. The hydroxylamine was removed using a PCR purification kit (Qiagen) and the plasmid DNA resuspended in 30µl 1xTE. (Parallel time points taken with no hydroxylamine removal, as a positive control for mutagenesis). 1µl of mutagenised DNA per time point was transformed into *E.coli* (Section 2.6.3), and following incubation, colony counts were performed on the 2TY plus ampicillin plates. The degree of mutagenesis per time point was calculated by scoring null mutations in amp^R, as compared

to T= 0hr (no mutagenesis). Plasmid DNA with a mutagenesis rate of approximately 5% was amplified, by pooling and scraping the selected *E.coli* colonies into 100µl 2TY plus ampicillin, ready for large scale DNA extraction (Section 2.8.2), and transformation into yeast (Section 2.7.9).

2.8.5 Episomal Plasmid Rescue from *S. cerevisiae*

Transformed cells were harvested at 3000g for 1min from 5ml YEAPD plus hygromycin B cultures. The cells were washed in 1ml dH_20, centrifuged at 15,000g for 1min, and then resuspended in 800µl of 50mM sodium phosphate buffer plus 0.9M sorbitol and 0.01% 2-mercaptoethanol. 25µl of 20T zymolyase (10mg/ml) was added to the cells and the reactions incubated at 37°C for 30min with agitation, to allow the cells to become spheroplasted. Incubating the spheroplated cells at 70°C for 20min inactivated the zymolyase, before the addition of 200µl potassium acetate (5M). The cells were rested on ice for 45min, to encourage the separation of cellular debris from plasmid DNA. The precipitate was pelleted at 15,000g for 1min and the plasmid-containing supernatant removed into a fresh tube. 0.55ml of isopropanol was added and the DNA left to precipitate out of the alcohol for 5min at room temperature (RT). The DNA was pelleted at 15,000g for 10min, and the excess salt removed by washing the pellet in 70% ethanol. Following centrifugation, the pellet was air-dried and resuspended in 100µl 1xTE. 10µl of plasmid DNA was used for transformation into *E. coli*, for plasmid amplification.

2.8.6 Yeast Genomic DNA Extraction

A simple and quick technique was used to extract genomic DNA for routine analysis, using sterile glass beads. 1.5ml of an overnight YEAPD culture was centrifuged at 17,000g for 1min. The pelleted cells were resuspended in 200µl genomic TENS and vortexed with sterile glass beads for 1min. 100µl isoamyl:phenol:chloroform (1:24:24) was added, and the cells re-vortexed, before centrifugation at 17,000g for 2min. The DNA-containing aqueous layer was removed into a new tube and 200µl phenol was added to increase the DNA purity. The mixture was vortexed and centrifuged as before, and the top layer removed into a new tube, before DNA extraction via ethanol precipitation.

2.8.7 Yeast Genomic DNA Extraction using CTAB

A modified CTAB method was used to extract high quality genomic DNA from meiotic cells for southern analysis, (Allers and Lichten, 2000). Cell pellets from meiotic time courses were thawed on ice and washed in 1ml spheroplasting solution (ice-cold). The washed pellets were then resuspended in 100µl spheroplasing solution plus 0.5mg/ml 100T zymolyase and 1% βmercaptoethanol, then incubated at 37°C for 6min (tubes inverted once during incubation). 200µl of CTAB extraction solution was added to the spheroplasted cells and the tubes gently vortexed to aid resuspension. 5µl of 20mg/ml Proteinase K and 0.5µl of 10mg/ml Rnase were added and the tubes gently mixed further. The cells were incubated at 37°C for 15min, with a tube inversion and gentle vortexing twice during the reactions. 100µl of chloroform:isoamylalcohol (24:1) was added to the reactions to extract the DNA-CTAB complexes that had formed. The reactions were vigorously vortexed for 20sec, rested for 2min, and re-vortexed. The reactions were spun at 17,000g for 5min to separate

out the aqueous layer containing the DNA-CTAB complexes, which was removed into a fresh tube. An equal volúme (typically 200µl) of CTAB dilution solution was very gently layered on top of the DNA-CTAB solution, and the tubes agitated very slightly to gently disturb the two phases. The tubes were then left for 5min before more gentle agitation to encourage the precipitation of the DNA-CTAB complexes. When a white precipitate began to form, 200µl CTAB dilution solution was again layered on top and the tubes gently agitated to encourage further precipitation. This layering and phase disturbance process was repeated until typically 800µl of CTAB dilution solution had been added, by which time more vigorous agitation was used to maximise the precipitation. The DNA-CTAB complexes were washed twice in 1ml of 0.4M NaCl in 1xTE solution (ice-cold) and then carefully resuspended in 100µl of 1.4M NaCl in 1xTE solution (ice-cold). The DNA was reprecipitated in 200µl 100% ethanol (ice-cold) and then washed twice in 1ml 70% ethanol. All residual ethanol was removed by centrifuge pulsing down and pipetting off. The DNA was then resuspended in 30-50µl 1xTE (ice-cold).

2.8.8 PCR

For routine extensions using purified DNA as template, 50µl PCR reactions consisted of 2x PCR master mix (ABgene), 200nM forward and reverse primers and 100ng yeast genomic DNA. The reactions were mixed on ice, and a typical PCR programme was used (with hot start):

(94°C 30sec) x 1 cycle

(94°C 10sec, x°C 30 sec, 72°C y min) x 30 cycles

(x= primer-specific annealing temperature, y= 1min per 1kb DNA to be amplified).

For long range PCR, Extensor Hi-Fidelity PCR master mix (ABgene) was used and the PCR cycling included modifications for optimal primer annealing and DNA extension (with hot start):

(94°C 2min) x 1 cycle

(94°C 10 sec, x°C 30 sec, 72°C y sec) x 30 cycles

(72°C 7min) x 1 cycle

(x= primer-specific annealing temperature, y= 1min per 1.5kb DNA to be amplified).

2.8.9 Colony PCR

For PCR using crude genomic DNA as template, a small amount of yeast or bacterial colony was spheroplasted in 10µl 20T zymolyase (5mg/ml) for 15min at 37°C. The zymolyase mix was centrifuged at 17,000g for 1min and the spheroplasted cell pellet was incubated at 100°C for 1min to inactivate any nucleases present. The cell pellet was resuspended in UP-H_20 and made up to a 50µl reaction by the addition of 2x PCR master mix (ABgene) and 200nM forward and reverse primers.

2.8.10 Quantification of DNA Concentration

The concentration of DNA solutions was measured using a fluorometer (Hoefer DyNA Quant), with DAPI as the fluorophore. Measurements were taken in a 3ml quartz cuvette, with filter-sterilised 1xTNE buffer plus 1.5µg DAPI. The fluorometer was calibrated for DNA concentration using 100ng/µl *lambda BstEII* (New England Biolabs) as a standard.

Three readings per sample were performed; this along with precision pipetting and adequate mixing of the cuvette was essential to ensure accuracy.

2.8.11 Restriction Enzyme Digestion of DNA

Ethanol purified DNA was digested with restriction enzymes under the conditions specified by the enzyme manufacturer, (typically New England Biolabs, Promega or MBI Fermentas). Digest volumes were made up with UP-H_20, and analytical digests incubated for 1-2hr. Yeast genomic DNA for Southern analysis was digested for 4–5hr, with 1% BSA in the digest volume.

2.8.12 DNA Ligation

DNA ligations were performed with an insert:vector ratio of approximately 3:1 molecules, and linearised plasmids with coordinate ends (e.g. digested with one enzyme) were first treated with SAP (USB) to prevent plasmid religation. Plasmid DNA was incubated with SAP (following manufacturers instructions), at 37°C for 1hr, and the enzyme then inactivated at 65°C for 15min. The plasmid DNA was concentrated via ethanol precipitation and typically 100ng was mixed with insert DNA, 1% T4 ligase buffer and 0.1U T4 ligase enzyme (Promega). Ligation reactions were made up to 10µl with UP-H_20 and incubated at 14°C overnight, before being used for transformation into *E.coli*.

2.8.13 Native DNA Electrophoresis

For routine analysis, DNA (plus 6x loading dye) was fractionated in agarose gels, made up to the appropriate percentage for optimum band separation, (typically 0.7-1.0%). (For

preparative purification, DNA was fractionated in low gelling temperature agarose (Biogene). Gels were run in BioRad tanks for 1-10V/cm in 1xTAE, plus ethidium bromide (10mg/ml, BioRad). For preparative Southern analysis, 1μg of digested DNA per meiotic time point was fractionated in 25cm x 15cm 250ml 0.5% agarose gels, using 16- or 20-well combs. Samples were mixed with heavy loading dye prior to electrophoresis and run at 70V for 17hr to obtain optimal band separation, in 1xTAE plus 10μl ethidium bromide (10mg/ml, BioRad) (buffer circulated).

2.8.14 DNA Purification and Gel Extraction

DNA from PCR and restriction enzyme digests was purified using a PCR purification kit (Qiagen), following the manufacturer's instructions. DNA products could also be separated from contaminating fragments by gel electrophoresis, in low gelling temperature agarose. After optimal band separation, the fragment of interest was excised from the gel, under (minimal) UV guidance for DNA visualisation. DNA was then gel extracted using either a gel extraction kit (Qiagen), following the manufacturer's instructions or phenol chloroform: The DNA-agarose block was melted at 55°C, an equal volume of phenol was added, and the mixture vortexed vigorously for 20sec. The phenol-DNA suspension was allowed to rest for 2min and re-vortexed, then centrifuged at 17,000g, 18°C for 5min. The aqueous layer was removed into a clean tube, and an equal volume of chloroform was added, to remove any residual phenol. The mixture was vortexed for 20sec and centrifuged as before. The aqueous layer was removed into a clean tube, and the DNA extracted via ethanol precipitation.

2.8.15 Southern Blotting

Following gel electrophoresis, stained DNA was visualised with minimal UV exposure, to ensure adequate band separation. The gels were rinsed three times in dH_20 to remove the ethidium bromide and then depurinated in 1l 1/40 HCl for 15min. The HCl was removed by rinsing the gels three times in dH_20 and then soaked in 500ml 0.4M NaOH to de*Nature* the DNA, for a short time. The ssDNA was blotted from the gels onto nylon Zetaprobe membranes (Biorad) via vacuum blotting at 50mbars for 2hr. Throughout blotting, the gel was continually soaked in 0.4M NaOH. Following blotting, the membrane was rinsed three times in 2xSSPE and the blotted DNA UV-crosslinked twice to the membrane to create a permanent transfer.

2.8.16 Generating ^{32}P-labelled DNA Probe

The DNA probe was prepared by a two-step PCR method using genomic DNA as the template for amplification. Products from the first round of PCR were gel purified to enrich for the desired probe fragment, which was then used as the template for the second round of PCR. These secondary PCR products were ethanol precipitated to purify the probe fragment. Labelled DNA probe was made using High Prime Random Labelling (Roche). 40ng purified DNA probe and 0.25ng *lambda BstEII* were incubated at 100°C for 3min to de*Nature* and then 4µl of High Prime was added. 5µl ^{32}P dCTP (ICN) was added and the labelling reaction proceeded at 37°C for 30min. Unincorporated nucleotides were removed from the probe through a spin column (BioRad). Prior to its addition to the hybridisation solution, 300µl of heat de*Natured* salmon sperm was added to the labelled probe and the reaction incubated at 100°C for 2min.

2.8.17 Southern Hybridisation

Cross-linked membranes were prehybridised in glass bottles that had been siliconised to encourage a clean hybridisation (bottles washed with concentrated Forward cleaner, rinsed thoroughly with dH_20, then sequentially coated with 2ml 100% ethanol (removed), 2ml Sigmacote (Sigma-Aldrich) (removed) and 2ml 100% ethanol (removed), then rinsed thoroughly). The hybridisation bottles were prewarmed to 65°C and membranes were incubated in 40ml prehybridisation solution for a minimum of 4hr in a rotation oven. The prehybridisation solution was removed and replaced with hybridisation solution containing ^{32}P-labelled probe the filter was then hybridised at 65°C for at least 18hr. The hybridised filters were sequentially washed in the three washing buffers, with agitation at room temperature for 15min. The filters were lightly patted-dry, to remove excess liquid and then wrapped in Caterwrap. Hybridised bands were visualised via exposure to a Phosphor imaging screen (Kodak), through a protective sheet of screen guard (BioRad).

2.8.18 Scanning Densitometry

A Personal FX phosphorimager (BioRad) was used to scan the density of radiation emitted from the hybridised filter (in complete darkness). Quantification of the emitted signal was assessed using Quantity One software. To quantify the signal in each band, upper and lower boundaries were created, and the signal within each band was calculated automatically, via integration of the area under each peak. (Background hybridisation signal subtracted).

2.8.19 DNA Sequencing

Plasmid DNA recovered from the genetic screen (Chapter 6) was sent to MWG-Biotech for sequencing, following the recommended guidelines for DNA concentration and primer concentration and volume. CodonCode Aligner software was used for analysis of DNA sequences.

2.9 Description of *S. cerevisiae* Strains Used

2.9.1 Strain Nomenclature

All of the experimental diploid strains were homozygous for the defined mutation, for example *xrs2*Δ indicates homozygous *xrs2*Δ*::kan*MX alleles. *TFP1/TFP1* indicates homozygosity at the *TFP1* allele. *TFP1::VDE/TFP1* indicates heterozygosity at the *TFP1* allele.

2.9.2 Inclusion of Strain Information

The haploid strain list (Table 2.3.1) contains only the yeast strains from which specific alleles originate, rather than the manifold intermediate strains used to create the experimental diploids. The diploid strain list (Table 2.3.2) contains all of the experimental diploids used in this study.

2.9.3 General Methods for Creating Yeast Strains of the Desired Genotype

Where a deletion or disruption cassette was available, appropriate haploid strains were directly transformed via the lithium acetate method, to achieve the desired genotype. Where

a mutant allele originated from a non-SK1 strain, (e.g. *xrs2-11*, hAG1161), locus-specific primers were used to amplify the appropriate region via PCR. The PCR product was cloned into a TA vector (Invitrogen) and then transformed into an SK1 strain as before. To create the experimental diploids, intermediate strains were routinely made by mating haploids with appropriate genotypes, followed by sporulation and tetrad dissection. The haploid genotype of spores was determined largely by identifying mutant alleles marked with amino acid biosynthetic genes, or antibiotic resistance genes.

The requisite and non-requisite phenotypes of each mating cross were scored to confirm the expected marker segregation. To ensure haploid ploidy, colonies were selected from four spore viable tetrads only. When alleles disrupted by the same marker were required in a haploid strain, diploids heterozygous for the markers were made and dissected. Only marker+ haploids from 2+:2- segregations were selected, thus ensuring the presence of both alleles in the haploid. When no protrophic or antibiotic resistance markers were available, (e.g. VDE insertion at the *TFP1* locus, creating *TFP1::VDE*), locus-specific primers were used to amplify the appropriate region via PCR. The size of the PCR product, and/or the presence or absence of restriction sites (relative to a reference PCR), was indicative of the genotype.

2.9.4 Methodology for Creating Experimental Diploids for the Repair Assay

Mutant alleles were crossed into an *ade2::arg4-VDE TFP1* haploid strain (hAG684) and a *ade2Δ(EcoRv-StuI) TFP1*::*VDE* haploid strain (hAG416 or hAG417), via matings with the originator mutant allele haploids. These mutant *ade2::arg4-VDE TFP1* and *ade2Δ(EcoRv-StuI) TFP1*::*VDE* haploids were mated to create an experimental diploid, homozygous for

(a)

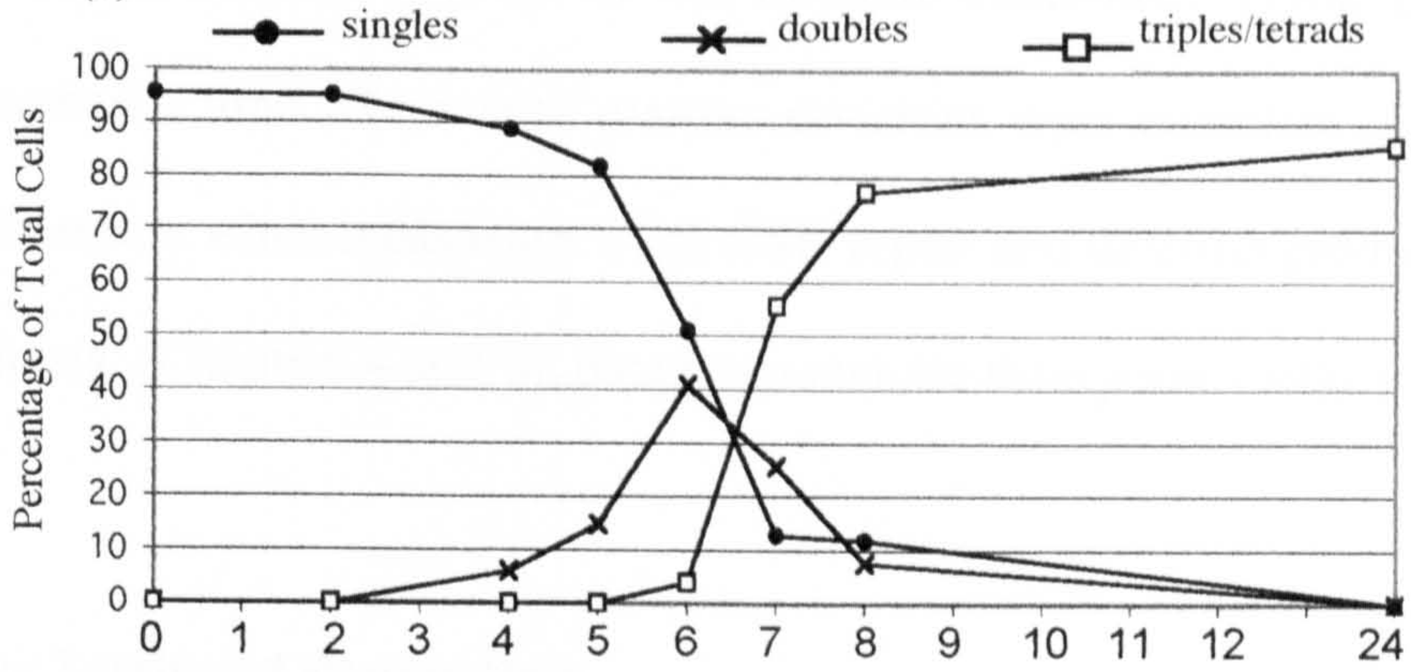

(b)

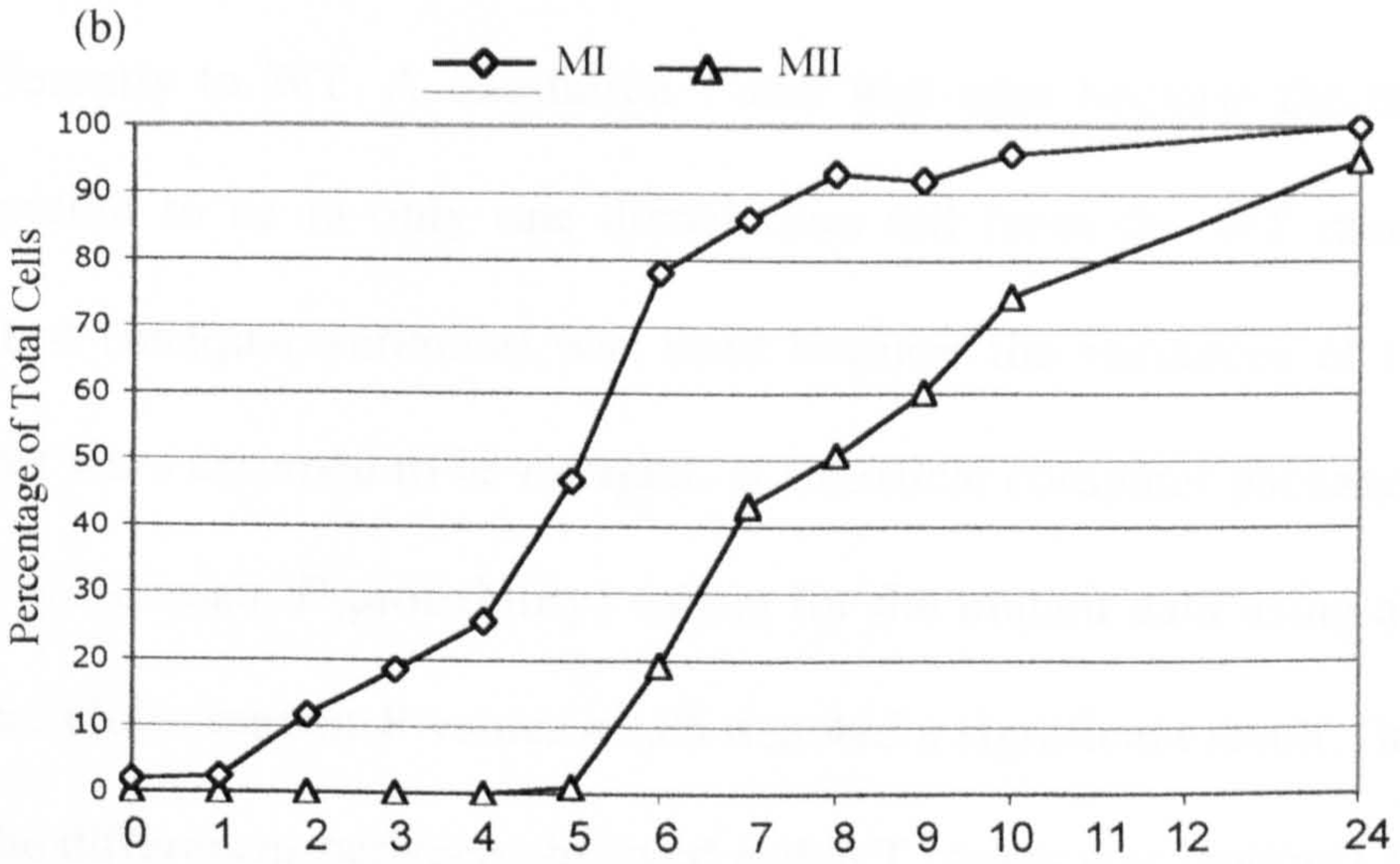

Figure 2.10 Meiotic Cell Cycle Progression in the wildtype strain: (a) Timing of meiosis in the WT strain (dAG630). Cells sampled from synchronous meiotic cultures were stained with DAPI to visualise the nuclei. A minimum of 200 cells were counted, and the percentage of single, double, or triple/tetrad staining bodies was calculated. (b) Progression of meiotic divisions in the WT strain

the chosen mutation. This approach was used to prevent the crossing of *arg4-VDE* and *TFP1*::*VDE* containing strains prior to creation of the final experimental diploid.

2.10 Southern Analysis of Meiotic Cells

For the WT strain (dAG630), and all of the mutants examined, T=8hr post meiotic induction represented a time where both meiotic divisions were complete (MI and MII), (Figure 2.10). Therefore when measuring VDE-DSB repair and deletion product formation via southern analysis, (Chapters 4 and 5), data from meiotic time point T=8hr was used.

2.11 Significance Testing of Repair Data

The Student's T-test (one-tailed, heteroscedastic) was applied to data collected from DNA southern analysis to determine whether any of the mutant strains repaired the VDE-DSB significantly differently to WT. A one-tailed T-test was used because the mutant mean values were expected to be in only one distribution tail from the WT mean value. A heteroscedastic test (unequal variance) was used because the variances of the WT and mutant data ranges were assumed to be unequal. A statistical computer package (Microsoft Excel) was used to calculate *P*(probability) values for the mutant data using a percentage cut-off of 5%. Therefore, mutant *P* values <0.05 denoted a significant result, (less than 5% probability that the differences between observed and WT means was random). Conversely, mutant *P* values >0.05 were judged not to be significantly different from WT, (more than 5% probability that differences in mean values were random).

(Equation for Student's T value given for completion):

PAGE NUMBERING AS ORIGINAL

2.10i Normalisation of Southern Repair Data

For each meiotic timepoint, total VDE-chromatid DNA was calculated as the sum of all of the bands in that lane (excluding the loading control), i.e. parental DNA, VDE-DSB, first deletion product and second deletion product. Quantification of VDE-DSB repair was then expressed as a percentage of total VDE-chromatid DNA (% VDE-chromatid DNA).

$$t = \frac{\bar{x} - \mu}{s / \sqrt{n}}$$

(t = Student's t value, n = number of observations, $\bar{x}$ = mean of observations, s = standard deviation, μ = WT mean).

2.12: Mutant Screening

*xrs2*Δ homozygous diploids (dAG946, *NDT80/NDT80*, and dAG1093, *ndt80/ndt80*) were transformed episomally with hydroxylamine-mutagenised copies of the *XRS2* expression plasmid (pAG73). The heterogenous population of transformants was then screened for adenine prototrophy, using a (qualitative) solid media screen (Section 2.12.1), before being superseded by a quantitative liquid media screen (Section 2.12.2). Prior to screening, plasmid loss was minimised by maintaining episomal transformants in selective media.

2.12.1 Use of *ndt80* Strains

Ndt80 protein is a meiosis-specific transcription factor that is required for exit from pachytene. An *ndt80/ndt80* mutant strain background was used in the genetic screen to retain meiotic inviable mutants.

2.12.2 Solid Media Screen

Single colonies from transformation were patched onto solid YEAPD medium (Figure 2.12.2a), and following 24hr incubation at 30°C, the patches were replica plated onto K-Ac medium to induce meiosis (Figure 2.12.2b). (Pre-meiosis plates retained). Following 48hr

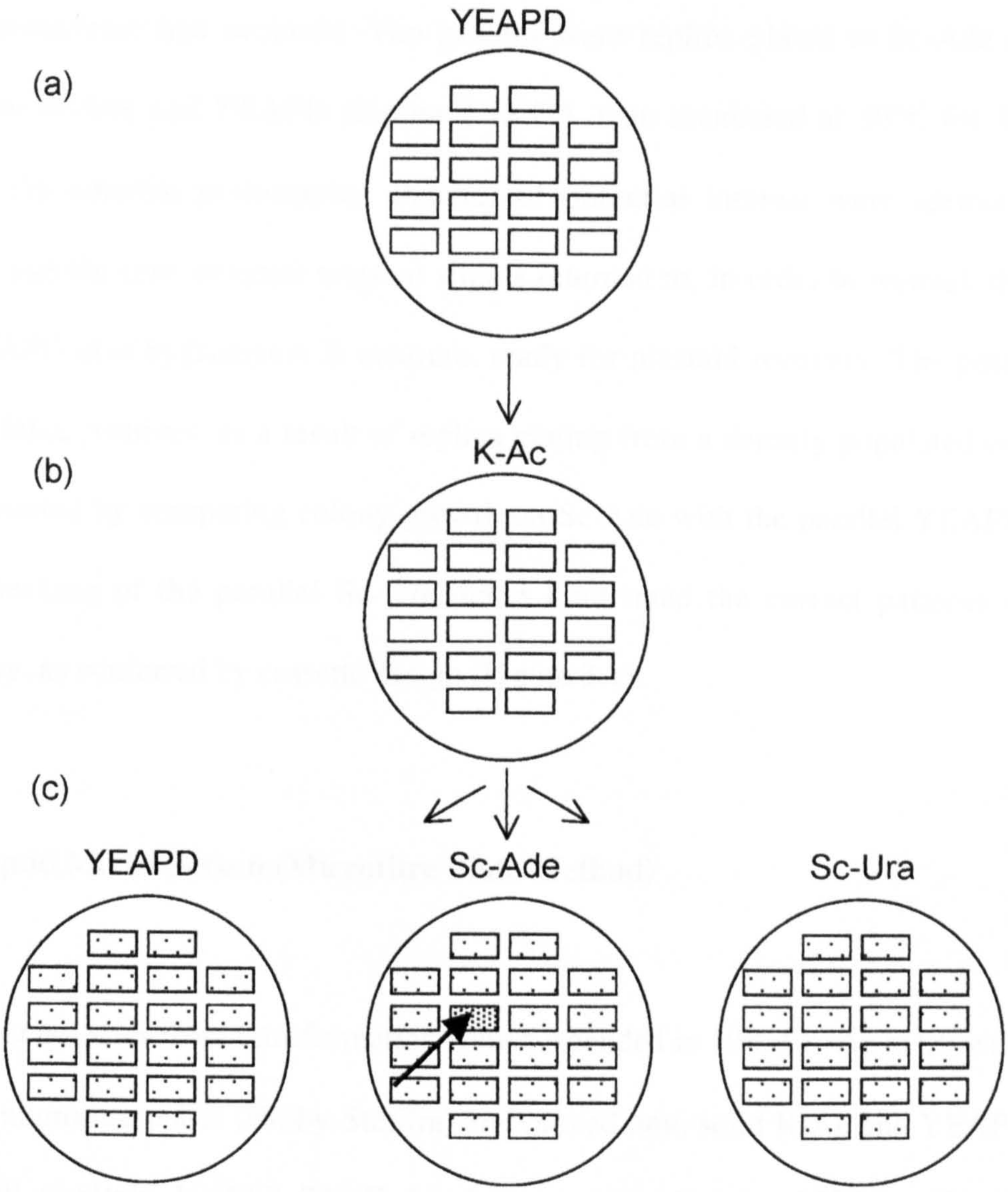

Figure 2.12.2: Solid Media Screen. (a) Single colonies from transformation were patched onto solid YEAPD medium, and after incubation, (b) were replica plated onto K-Ac medium to induce meiosis. After VDE-endonuclease induction, (c) the transformants were replica plated to Sc-Ade, Sc-Ura and YEAPD media. Following incubation, the transformants were screened for adenine prototrophy. (Thick arrow shows example of dense growth of potentially interesting transformant. The original patch (a) returned to for retesting and then plasmid recovery.

incubation, a sample of cells was examined for sporulation, to ensure that expression of VDE-endonuclease had occurred. The patches were replica plated to Sc-Ade medium, along with Sc-Ura and YEAPD (Figure 2.12.2c), then incubated at 30°C for 48hr, and screened for adenine prototrophy. Patches of potential interest were identified (and retested), and the (pre-meiosis) original strains returned to, in order to restreak them onto fresh YEAPD plus hygromycin B medium, ready for plasmid recovery. The potential for selecting false positives, as a result of replica plating from a densely populated cell patch, was discounted by comparing colony growth on Sc-Ade with the parallel YEAPD plates. (Cross checking of the parallel Sc-Ura plates confirmed the correct patterns of uracil auxotrophy, as conferred by cassette design (Figure 3.1).

2.12.3 Liquid Media Screen (Microtitre Plate Method)

Single yeast colonies from transformation were suspended in 100µl K-Ac in 96-well round-bottomed microtitre plates (Bibby-Sterilin) and pinned onto solid K-Ac and YEAPD plates (single well omnitray, NUNC). The K-Ac plates were incubated at 30°C for 48hr to induce meiosis and VDE-endonuclease expression, and a sample of cells checked for sporulation. The transformants were pinned into 50µl UP-H_20, and 10µl of the evenly suspended spores inoculated into 100µl liquid Sc-Ade and YEAPD. The microtitre plates were Parafilm-sealed to prevent evaporation, and incubated with agitation at 30°C. A Multiskan Ascent plate reader was used to measure the cell densities (OD_{595}) of the cultures at different time points during the exponential growth phase, (as determined by growth curves). To correct for higher initial cells innoculums that may create false adenine prototrophy, the cellular growth of transformants in Sc-Ade was normalised to their corresponding growth in

YEAPD, (i.e. OD_{595}Sc-Ade/OD_{595}YEAPD). Transformants with a significantly higher ratio value than the reference strains were picked from the original (pre-meiosis) YEAPD plates, and struck out onto YEAPD plus hygromycin B, in preparation for plasmid recovery.

2.13 Assaying for SSA Repair by Dissection

To determine the repair patterns of the VDE-DSB in the reference and experimental diploid strains, spore dissection was used. Spore colonies were replica plated onto YEAPD, Sc-Ade and -Ura media, and Ade+ and Ura+ recombination frequencies measured per VDE-chromatid, (only two spores per tetrad contained the *arg4-VDE* allele). Spore phenotypes were then examined, to determine the amount of deletion repair products. Three spore phenotypes were observed; i) adenine auxotroph/uracil prototroph, ('parental DNA', VDE-DSB not created, or created and repaired via a nonSSA pathway), ii) adenine auxotroph/ uracil auxotroph, (VDE-DSB repaired via SSA using the proximal *URA3* repeated sequences), iii) adenine prototroph/uracil auxotroph, (VDE-DSB repaired via SSA using the distal *ade2* repeats). Only spores containing the *ade2::arg4-VDE* chromatid had the potential to be Ura+ or Ade+ so by measuring Ade and Ura prototrophy, only cassette-containing spores were assayed.

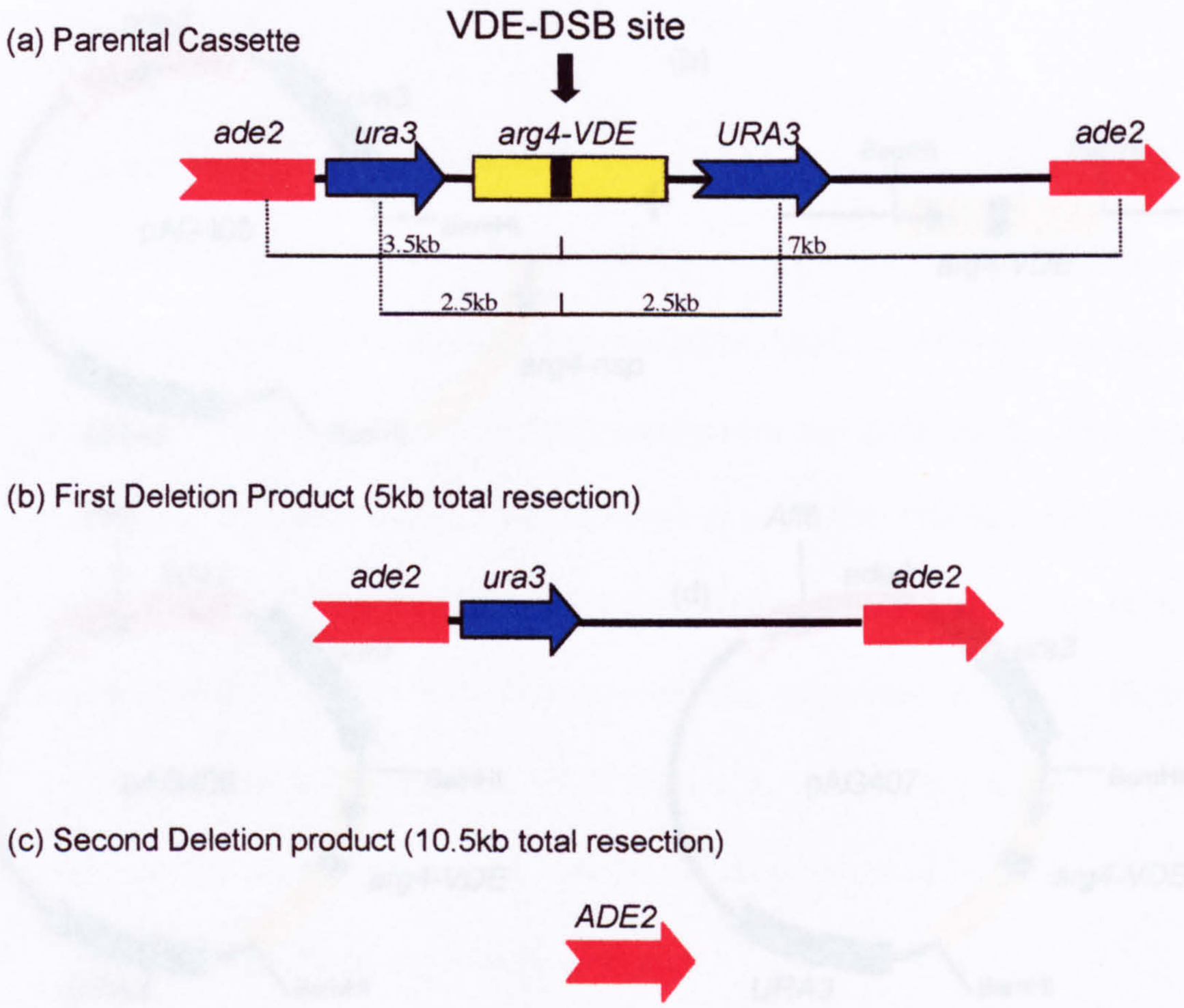

Figure 3.1: Parental *arg4-VDE* Reporter Cassette and Associated Deletion Repair Products (a) Parental cassette DNA, containing the *arg4–VDE* allele (yellow box; black box denotes VDE recognition sequence), flanked proximally by *URA3* and *ura3* direct repeated sequences (blue arrows), and distally by *ade2* direct repeated sequences (red (part)arrows). When VDE-endonuclease cleaves the *arg4-VDE* allele, the VDE-DSB can be repaired via SSA deletion repair by the generation of: (b) Resection tracts of length 2.5kb and 2.5kb (**5kb** total), that uncover the proximal *URA3* repeated sequences, creating first deletion product. (c) Resection tracts of length 7kb and 3.5kb (**10.5kb** total), that uncover the distal *ade2* repeated sequences, creating second deletion product. Following meiosis, diploid experimental strains can be phenotypically screened for (a) Parental DNA (Ura+ Ade-), (b) First deletion product (Ura- Ade-), and (c) Second deletion product (Ura- Ade+).

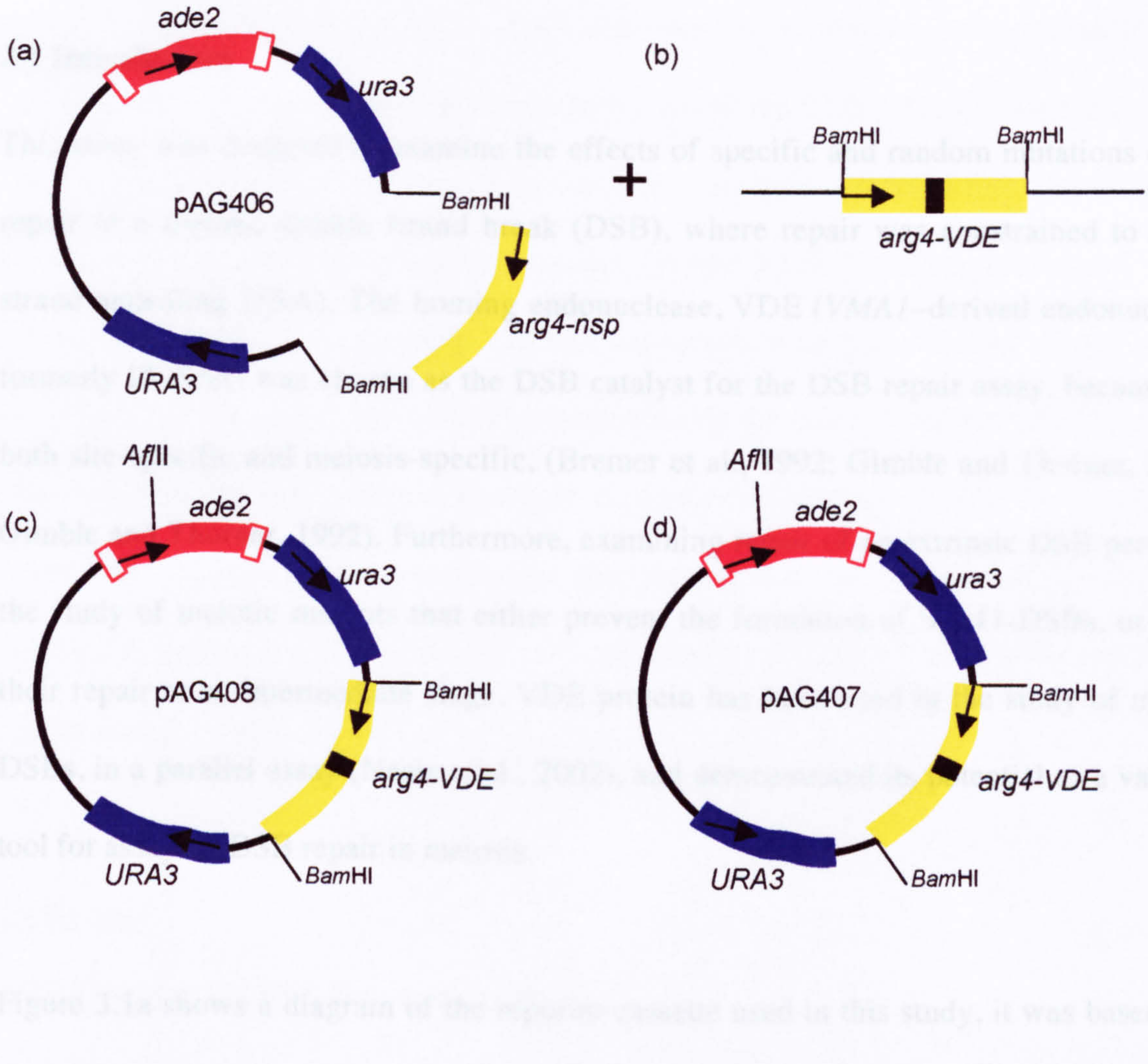

Figure 3.2.1: Construction of *arg4-VDE* Reporter Assay. (a) pAG406, a derivative of pMJ113, {Wu, 1995 #194}, was made available by M. Ramachandran. The *arg4-nsp* allele was liberated from the pBR322-based plasmid via *Bam*HI digestion, to leave a cassette vector containing *URA3* and *ura3* alleles (blue boxes) and a *ade2*Δ allele (red box, see below). (b) The *arg4-VDE* insert (pAG404, *Bam*HI-*Bam*HI) was made available (M. Ramachandran) and (c) ligated into the cassette vector making pAG408. (d) pAG407 was made by ligating the *arg4-VDE* insert (b) into a modified version of pAG406 (made available by M. Ramachandran, not shown), in which the *URA3* allele was in reverse orientation. (Arrows show allele orientation).

Chapter 3

Development of a Repair Assay Reporting on an Extrinsic Meiotic DSB

3.1 Introduction

This study was designed to examine the effects of specific and random mutations on the repair of a meiotic double strand break (DSB), where repair was constrained to single strand annealing (SSA). The homing endonuclease, VDE (*VMA1*–derived endonuclease, formerly PI–*Sce*I) was chosen as the DSB catalyst for the DSB repair assay, because it is both site-specific and meiosis-specific, (Bremer et al., 1992; Gimble and Thorner, 1993;; Gimble and Thorner, 1992). Furthermore, examining repair of an extrinsic DSB permitted the study of meiotic mutants that either prevent the formation of Spo11-DSBs, or block their repair at an intermediate stage. VDE protein has been used in the study of meiotic DSBs, in a parallel assay (Neale et al., 2002), and demonstrated its potential as a valuable tool for assaying DSB repair in meiosis.

Figure 3.1a shows a diagram of the reporter cassette used in this study, it was based on a SSA competition assay. In a previous SSA competition assay, an HO-DSB cut site was flanked by three *ura3* direct repeated sequences, (one repeated sequence on one side of the HO-DSB, and two on the other side) (Sugawara and Haber, 1992). That study demonstrated that deletion repair of a DSB preferentially occurs between the two closest homologous repeats, a fundamental principle of optimal SSA repair. The repair assay used in this study capitalised on the concept of using competing homologous repeated sequences, by studying the repair of a DSB flanked by two sets of direct repeated sequences (Figure 3.1a) The VDE-DSB cut site was flanked proximally by *URA3* and *ura3 (URA3)* homologous sequences, and distally by two *ade2* homologous sequences. The VDE cut site was

contained within a mutant *arg4* allele, *arg4-VDE* (Neale et al., 2002). Hemizygosity in the experimental strains (Figure 3.2.4a), ensured that VDE-DSB repair was directed towards the SSA pathway and two deletion repair outcomes were predicted: Generation of DSB resection tracts of approximately 2.5kb on both sides of the VDE-DSB site were required to uncover the proximal *URA3* repeated homologies. Therefore, a total of **5kb** of resectioning was required to generate first deletion product, (Figure 3.1b). To uncover the distal *ade2Δ* repeated sequences, approximately 7kb of DSB resectioning was required on one side of the VDE-DSB site, and 3.5kb of DSB resectioning on the other. Thus, a total of **10.5kb** of DSB resectioning was required to create second deletion product, (Figure 3.1c). Both genetic and molecular biology techniques were employed to study VDE-DSB repair and to distinguish between first and second deletion product formation, as a measure of DSB resection tract length.

3.2 Results

3.2.1 Creating the SSA Reporter Assay

pAG406, a derivative of pMJ113 (Wu and Lichten, 1995), contained an *arg4-nsp* allele, flanked by *URA3* and *ura3* repeated sequences and *ade2* sequence, was made available for this study (M. Ramachandran) (Figure 3.2.1a). pAG406 was *Bam*HI-digested to liberate the *arg4-nsp* allele and the *arg4-VDE* allelic insert (*Bam*HI-*Bam*HI, pAG404, (M.J.Neale) (Figure 3.2.1b) was ligated in. This created the reporter cassette plasmid, termed pAG408 (Figure 3.2.1c). A modified version of pAG406 was made available (M. Ramachandran, not shown), where the *URA3* allele was inserted in the opposite orientation. The *arg4-VDE* allele was ligated in as before and this plasmid termed pAG407 (Figure 3.2.1d).

3.2.2 Creating *arg4-VDE* Haploid Strains

pAG407 and pAG408 were transformed into DH5α *E.coli* cells and following small-scale plasmid extraction, diagnostic DNA digests were performed to ensure the correct orientation of the allelic elements. Large-scale plasmid extraction was used to amplify plasmid DNA from transformants, which was then linearised by *Afl*II-digestion (Figure 3.2.2a). The linearised plasmids were transformed into Ade+ Ura- yeast strains, disrupting the *ADE2* locus (Chromosome *XV*), via electroporation (Figure 3.2.2b and Figure 3.2.2c). Transformants were selected on Sc-Ura +1M sorbitol medium, and the correct integration of the reporter cassette into the yeast genome was checked via diagnostic PCR. To check the relative positioning of the plasmid on Chromosome *XV*, plasmid-specific primers (AB02 and AB03) were used in conjunction with genome-specific primers (AB01 and AB04), (Figure 3.2.2b and Figure 3.2.2c). Transformants (*ade2::arg4-VDE*) were selected and the strains named hAG684 and hAG695, (transformed with pAG408 and pAG407, respectively).

3.2.3 Measuring Spontaneous Deletion of the *ade2::arg4-VDE* Cassette

To assess spontaneous deletion of the *ade2::arg4-VDE* reporter cassette, the number of Ura- colonies in a mitotic culture of *ade2::arg4-VDE TFP1* haploid cells (hAG684) was measured. Spontaneous cleavage of the *arg4-VDE* allele, or at other locations within the cassette DNA, could cause partial or complete deletion of the cassette DNA from the genome, resulting in uracil auxotrophy. Deletion between the proximal *URA3* repeated sequences, (Figure 3.1b), or between the distal *ade2* repeated sequences (Figure 3.1c), would both cause the loss of the *URA3* allele. Mitotic liquid cultures of hAG684 were plated onto medium containing 5-FOA and YEAPD. The frequency of obtaining Ura-

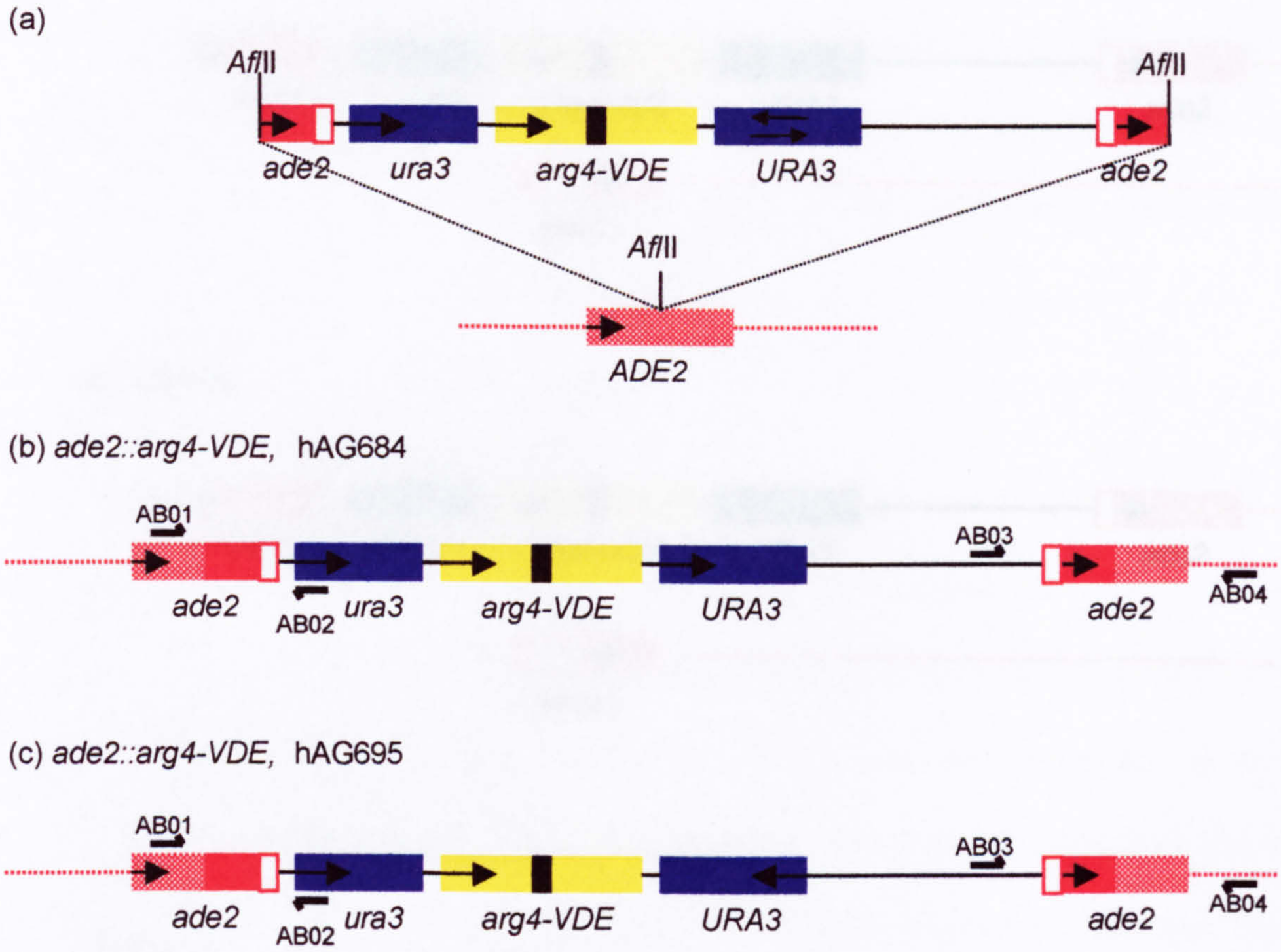

Figure 3.2.2: Creating *arg4-VDE* Haploid Strains. (a) *Afl*II-linearised pAG408 and pAG407 were integrated into hAG2 and hAG3, disrupting the *ADE2* locus (red hatched box) of Chromosome *XV*. This created (b) hAG684 and (c) hAG695. (*ade2* deleted regions indicated by white boxes. Thin black line denotes pBR322-plasmid DNA, red dotted line denotes yeast genomic DNA). (Arrows show allele orientation). Cassette integration was confirmed by PCR using a combination of genome-specific (AB01 and AB04), *ura3* locus-specific (AB02), and pBR322-specific (AB03) primers.

(a) dAG630

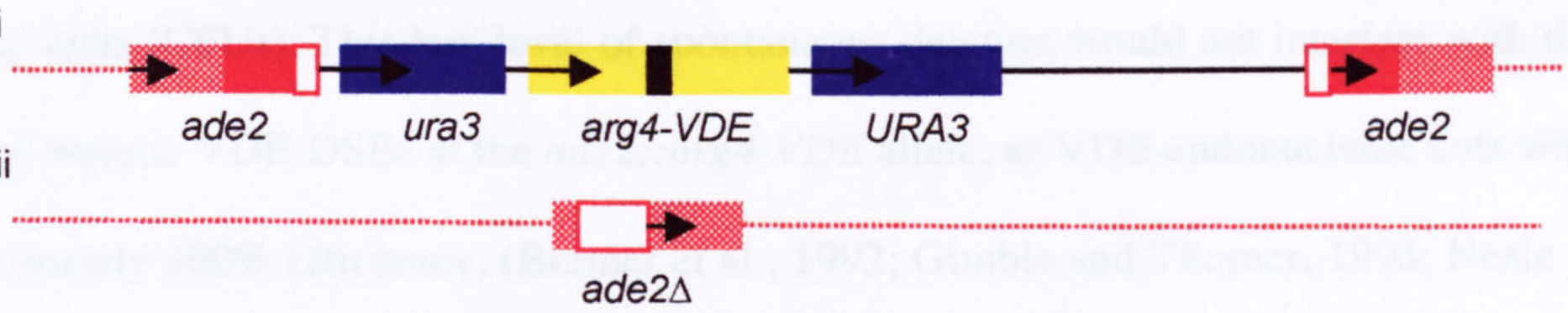

(b) dAG649

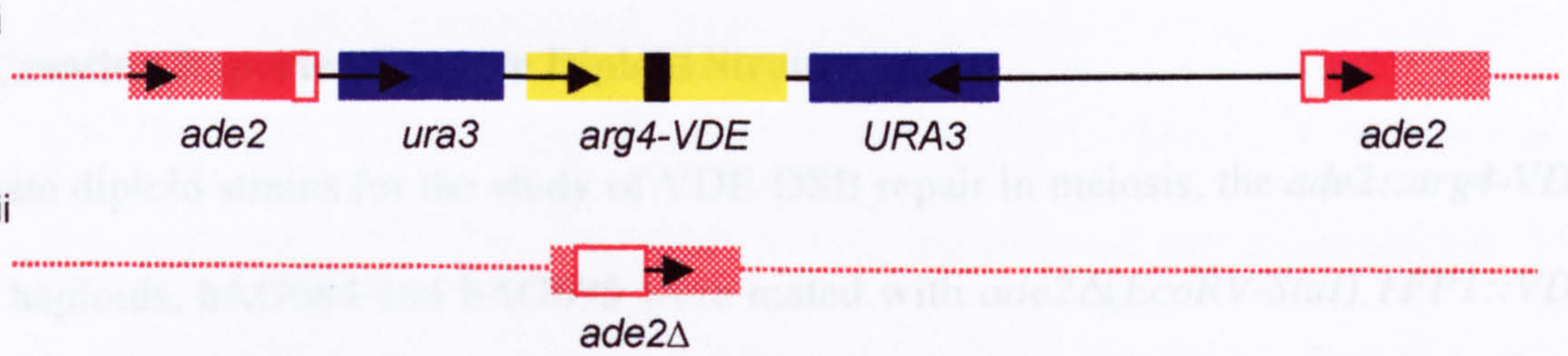

Table (c)

Strain Number	Strain Name	Relevant Genotype
dAG630	WT	*ade2::arg4-VDE/ade2Δ(EcoRV-StuI) TFP1::VDE/TFP1*
dAG649	Inverted-*URA3*	*ade2::arg4-VDE/ade2Δ(EcoRV-StuI) TFP1::VDE/TFP1*
dAG646	*TFP1/TFP1*	*ade2::arg4-VDE/ade2Δ(EcoRV-StuI) TFP1/TFP1*

Figure 3.2.4: Creating Diploid Strains. (a) dAG630 and (b) dAG649, diploid strains heteroallelic at the *ADE2* locus (Chromosome *XV*). (a)i The *ade2::arg4-VDE* chromatid originated from hAG684 and (b)i from hAG695. (a)ii The *ade2*Δ allele chromatid (red hatched box) originated from hAG416 and (b)ii from hAG417, (M.J.Neale). (Thin black line denotes pBR322-plasmid DNA, red dotted line denotes genomic DNA). (a)ii and b)ii The *ade2*Δ allele contained a 645bp *Eco*RV-*Stu*I (+175-819) deletion (A.Goldman), which prevented repair of the *arg4-VDE* allele via interchromosomal repair. (Arrows show allele orientation). Table (c) contains relevant genotype data for the *S. cerevisiae* diploid strains used in Chapter 3. (For complete genotypic information, see Table 2.3.2).

colonies from mitotically growing *ade2::arg4-VDE TFP1* cells was 8.15E-^{4} (±0.4) calculated as the number of uracil auxotrophs relative to the number of viable colony forming units (CFUs). This low level of spontaneous deletion would not interfere with the study of meiotic VDE-DSBs at the *ade2::arg4-VDE* allele, as VDE-endonuclease cuts with approximately 100% efficiency, (Bremer et al., 1992; Gimble and Thorner, 1993; Neale et al., 2002)(.

3.2.4 Creating Reporter Cassette Diploid Strains

To create diploid strains for the study of VDE-DSB repair in meiosis, the *ade2::arg4-VDE TFP1* haploids, hAG684 and hAG695 were mated with *ade2Δ(EcoRV-StuI) TFP1::VDE* haploids, hAG416 and hAG417, respectively (M.J.Neale). This created the diploid strains, dAG630 and dAG649, (Figure 3.2.4a, Figure 3.2.4b and Table 3.2.4c). The use of a deletion allele at the homologous *ADE2* locus (Δ645bp, Figure 3.2.4aii and Figure 3.2.4bii), created hemizygosity and prevented VDE-DSB repair via an interchromosomal exchange, thus forcing repair along the SSA pathway. Strain dAG630, where the *arg4-VDE* allele was flanked by two sets of direct flanking repeated sequences (Figure 3.2.4a), was the primary reference strain in the study, and henceforth is referred to as Wildtype (WT). In dAG649, the proximal *URA* sequences in the reporter cassette were inverted, (Figure 3.2.4b), henceforth, this strain is referred to as Inverted-*URA3*. It was predicted that SSA repair in the Inverted-*URA3* strain would only be possible between the distal *ade2* repeated sequences. The diploid strain, dAG646 was made as a negative control for VDE-cleavage, henceforth referred to as *TFP1/TFP1* strain (Table 3.2.4c). (See Table 2.3.2 for complete genotypic information on dAG630, dAG649 and dAG646.

3.2.5 Measuring Spore Viability

Tetrad dissection was used to assess spore viabilities (See Figure 3.2.5b for example dissection plate of WT spores (dAG630)). Data were collected for all spores, and for spores from four-spore viable tetrads. The total spore viability of the WT strain was 64.75%, compared to 61.62% in the Inverted-*URA3* strain, and 95.00% in the *TFP1/TFP1* strain (Table 3.2.5a). Scoring phenotypes in four-spore viable tetrads provided the opportunity to examine all chromatids following meiosis. The proportion of tetrads that had four viable spores in WT was 10.00%, compared to 7.00% in the Inverted-*URA3* strain, and 85.00% in the *TFP1/TFP1* strain (Table 3.2.5a). Therefore, while the *TFP1::VDE/TFP1* strains shared similar reduced spore viabilities, the *TFP1/TFP1* diploid was not compromised. This suggested that expression of VDE-endonuclease was the cause of reduced spore viability.

3.2.6 First and Second Deletion Product Formation Frequencies

Following tetrad dissection, the frequencies of Ade+ and Ura- spores were calculated (Table 3.2.6a). By considering VDE-chromatids from four-spore viable tetrads, three different spore phenotypes were expected (Section 2.13). The combination of adenine and uracil auxotrophies demonstrated that 40% of VDE-chromatid containing spores from the WT strain (dAG630) contained first deletion product (Table 3.2.6a, and Figure 3.2.6e). There were 15% of spores from the WT strain that contained second deletion product (Table 3.2.6a and Figure 3.2.6f). A surprisingly large amount of spores from the WT strain were Ura+ Ade- (45%), i.e. had maintained parental cassette DNA. There were 64.29% of spores from the Inverted-*URA3* strain that contained second deletion product (Table 3.2.6a and Figure 3.2.6f). The remaining 35.71% of spores were Ura- Ade-, indicating first

deletion product formation. From the *TFP1/TFP1* strain, all of the spores contained parental cassette DNA, (Table 3.2.6a and Figure 3.2.6b).

3.3 Southern Analysis of Cassette-Containing Diploids

The *ade2::arg4-VDE* assay was designed to report on VDE-DSB repair and on resection tract length, in a variety of mutants that were unable to generate viable spores. As this precluded meiotic genetic experimentation, southern analysis was used. The WT and Inverted-*URA* strains were assayed for VDE-DSB repair ability and resection tract length via southern analysis (Figure 3.3a shows example gels). The graphs in Figure 3.3b contain the quantified amounts of DNA repair intermediates, measured through meiosis, (as a proportion of VDE-chromatid DNA), at T=8hr.

3.3.1 Repair Ability and Resection Tract Length of the *ade2::arg4-VDE* allele

Figure 3.3.1a displays the proportions of VDE-chromatids that had suffered a VDE-DSB at T=8hr. Approximately 90% of the VDE-chromatids had been cleaved by VDE-endonuclease in the WT and Inverted-*Ura3* strains. Figure 3.3.1b displays the proportion of VDE-DSB repair of the *ade2::arg4-VDE* allele, normalised to the amount of VDE-chromatids that had suffered VDE-DSB, at T=8hr. Figure 3.3.1c contains the proportions of first and second deletion products formed in the strains at T=8hr. The WT strain generated 60.2% first deletion product and 16.7% second deletion product, while the Inverted-*URA3* cassette-containing strain formed 1.0% first deletion product and 90.8% second deletion product. To examine the WT regulation of DSB resectioning, it was appropriate to express the amount of second deletion product as a proportion of total deletion product (Repair

(a)

	Viability%	
	All Spores	Four-Spore
WT (dAG630)	64.75	10.00
Inverted-*URA3* (dAG649)	61.62	7.00
TFP1/TFP1 (dAG646)	95.00	85.00

(b) WT (*TFP1::VDE/TFP1*)

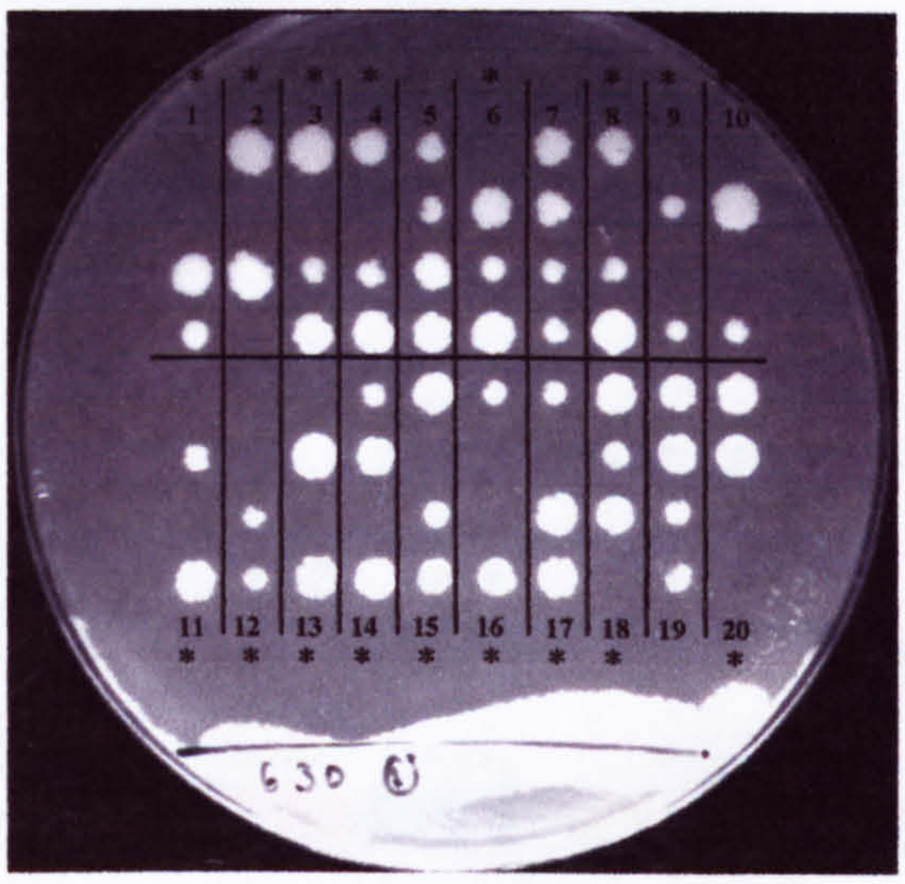

(c) *TFP1::VDE/TFP1::VDE*

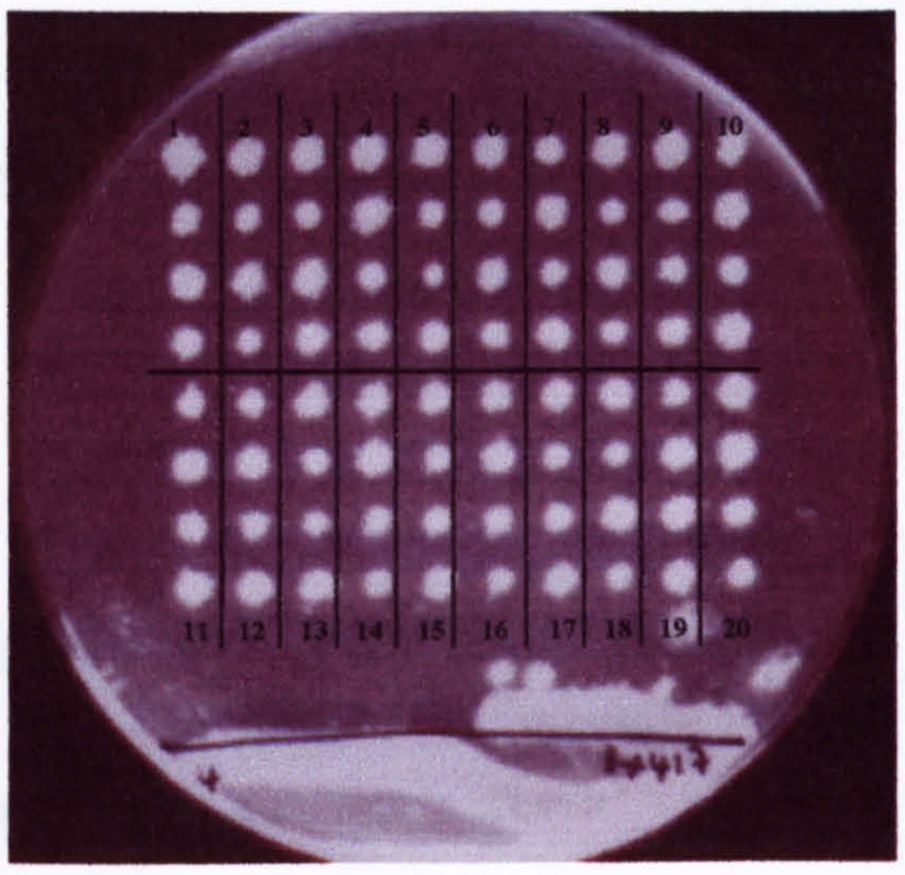

Figure 3.2.5: Spore Viability Table (a) contains the spore viabilities of the diploid strains dAG630, dAG649 and dAG646. (80 tetrads per strain spore-dissected). Viabilities calculated as proportion of viable spores or four spore viable tetrads, out of the total number plated. (b) An example dissection plate for the WT strain. Tetrads plated out in 2x10 grid. 17 out of 20 tetrads plated (85%) contain two or three viable spores (*). (c) A dissection plate of a *TFP1::VDE/TFP1::VDE* homozygous diploid strain (dAG720), average spore viability 97% (n=80 tetrads dissected).

Sporadic cleavage at the *TFP1* allele by VDE-endonuclease, without subsequent repair, may cause reduced spore viabilities in the WT and Inverted-*URA3* strains.

(a)

	First Deletion Product% Ura- Ade- spores	Second Deletion Product% Ura- Ade+ spores	Parental DNA% Ura+ Ade- spores
WT	40.00	15.00	45.00
Inverted-*URA3*	35.71	64.29	0.00
TFP1/TFP1	0.00	0.00	100.00

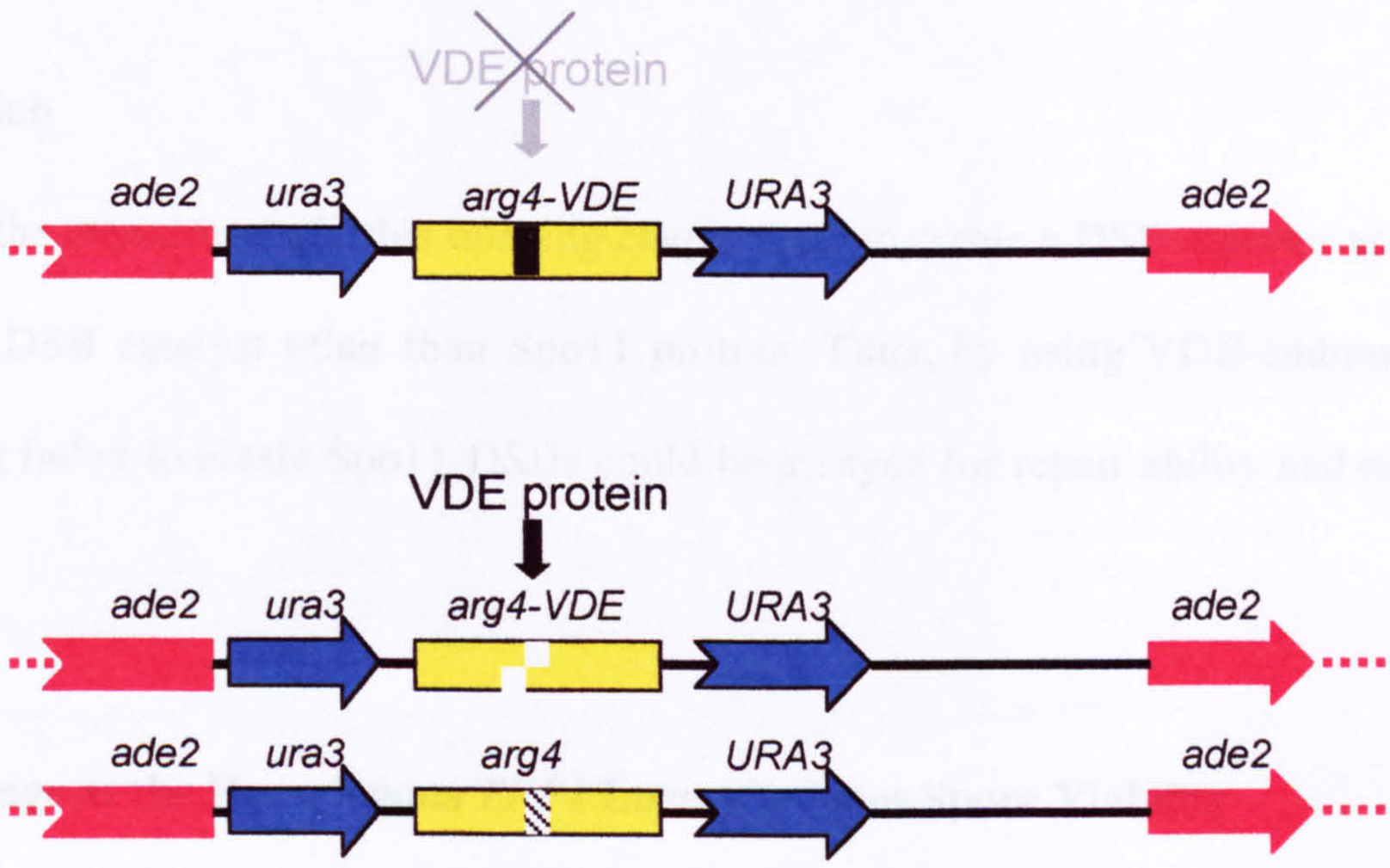

Figure 3.2.6: Genetic Analysis of DSB Repair of *arg4–VDE* allele. Table (a) The DSB repair outcomes at the *arg4-VDE* allele. Spores auxotrophic for adenine and uracil contained first deletion product. Spores prototrophic for adenine and auxotrophic for uracil contained second deletion product. Spores auxotrophic for adenine and prototrophic for uracil indicated Parental cassette DNA. (b-f): Repair outcomes of VDE-DSB repair of the *arg4-VDE* allele and the associated genotypes. (b) Parental cassette DNA, resulting from no VDE endonuclease cleavage, phenotype: Ura+ Ade-. (c) VDE-DSB cleavage of the *arg4-VDE* allele and (d) DSB repair via a non-homologous repair process (Diagonally-lined box denotes repair event, e.g. NHEJ): Ura+ Ade-. (e) First deletion product created after SSA repair of the *arg4-VDE* allele using the *URA3* repeated sequences: Ura- Ade-. (f) Second deletion product created after SSA repair of the *arg4-VDE* allele using the *ade2* repeated sequences: Ura- Ade+. (Data from n=3 experiments per strain)

product ratio = secondΔ/(firstΔ + secondΔ). This calculation revealed how many of the DSB resection tracts generated at the *arg4-VDE* allele, reached the distal repeated *ade2* homologous sequences, as a proportion of all resection tracts generated. The repair product ratio values are given in Figure 3.3.1d.

3.4 Discussion

The aim of the experiments in this opening chapter was to create a DSB reporter assay that relied on a DSB catalyst other than Spo11 protein. Thus, by using VDE-endonuclease, mutants that failed to create Spo11-DSBs could be assayed for repair ability and resection tract length.

VDE Cleavage at the Homologous *TFP1* Locus Reduces Spore Viability

Spore viabilities of the WT, Inverted-*URA3* and *TFP1/TFP1* strains were measured to look at the influence the reporter assay may have. Spores from the WT and Inverted-*URA3* diploids demonstrated reduced spore viabilities, while spores from the *TFP1/TFP1* strain displayed a similar viability to those reported for the SK1 background in *S. cerevisiae* (Table 3.2.5a), (Kane and Roth, 1974). This indicated that it was not the presence of the *ade2::arg4-VDE* cassette that compromised spore viability in the cassette-containing strains, but rather the *TFP1::VDE* allele. Previously, spores from *TFP1::VDE/TFP1* strains have been shown to have reduced viability (M.J.Neale, Unpub.). The most likely explanation is that VDE-endonuclease sometimes cleaves the homologous *TFP1* locus (Chromosome *IV*), to initiate intron homing. Without subsequent repair of the *TFP1* allele, the chromosome would be lost, resulting in spore death. The majority of tetrads from the WT and Inverted-*URA3* strains contained two or three viable spores, leading to overall

(a) Southern Analysis of DSB Repair of the *arg4-VDE* allele

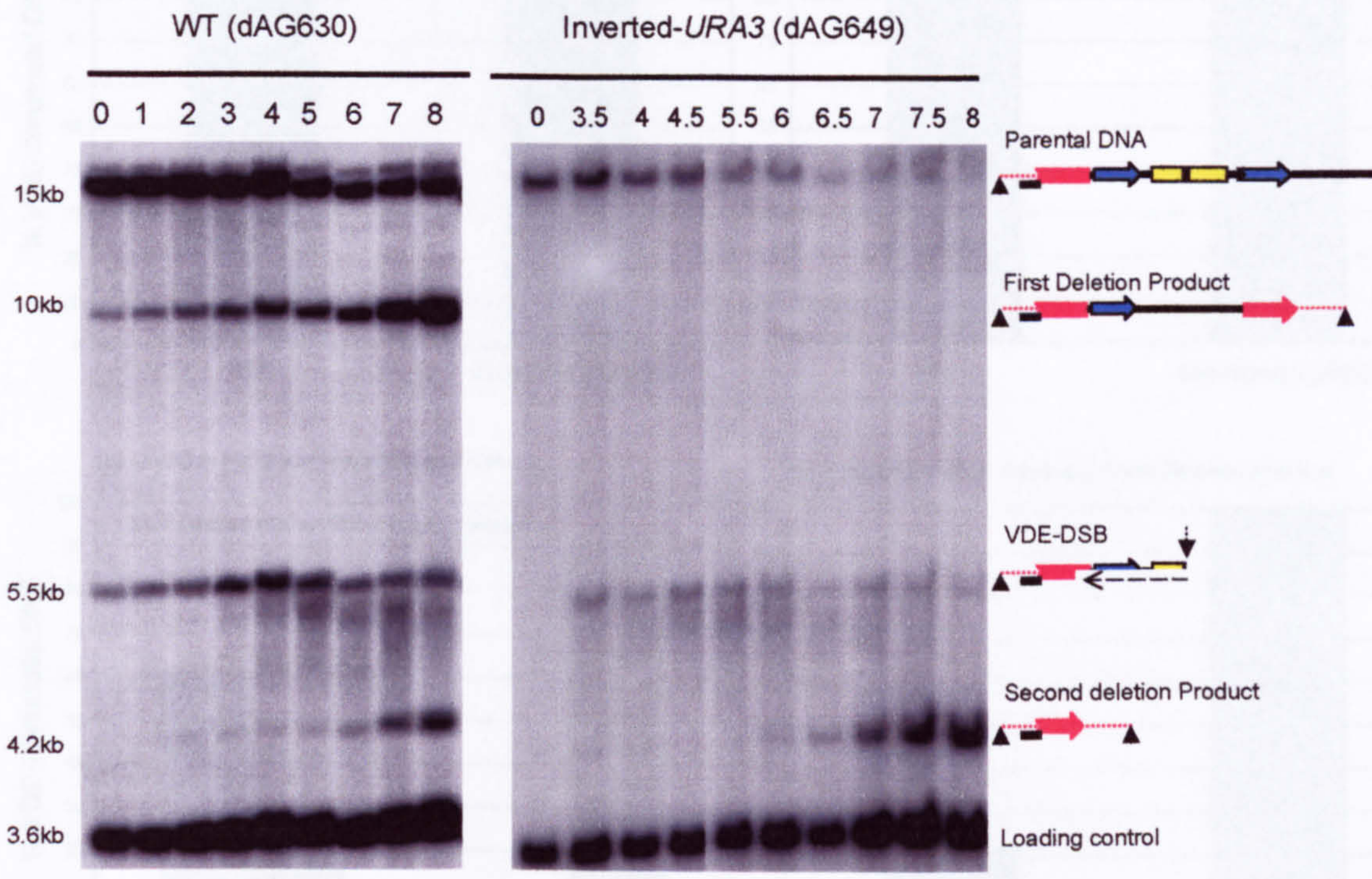

(b) Quantification of DSB Repair Intermediates of the *arg4-VDE* allele

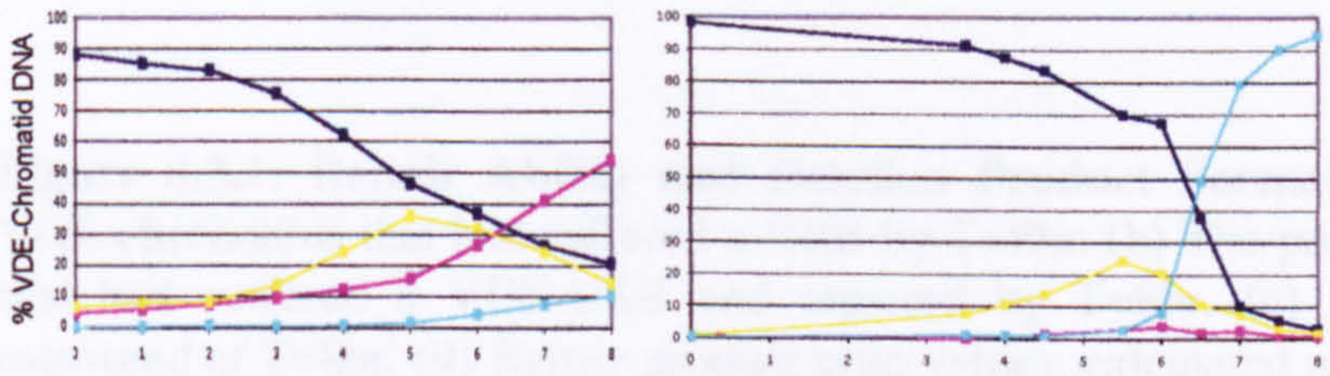

Figure 3.3: DNA Quantification of Cassette-Containing Strains. (a) DNA extracted from WT (dAG630) and Inverted-*URA3* (dAG649) synchronous meiotic cultures, digested with SpeI (arrow heads), and after fractionation and blotting, the DNA-membrane was hybridised with a probe specific to the upstream region of the *ADE2* locus (black box). (Time points shown above gel images). (b) DNA repair intermediates as a proportion of VDE-chromatid DNA: parental DNA (dark blue), VDE-DSB DNA (yellow), first deletion product (pink) and second deletion product (light blue). The most striking difference between these strains is the large accumulation of second deletion product in the Inverted-*URA3* strain. (Data from n=4 experiments per strain)

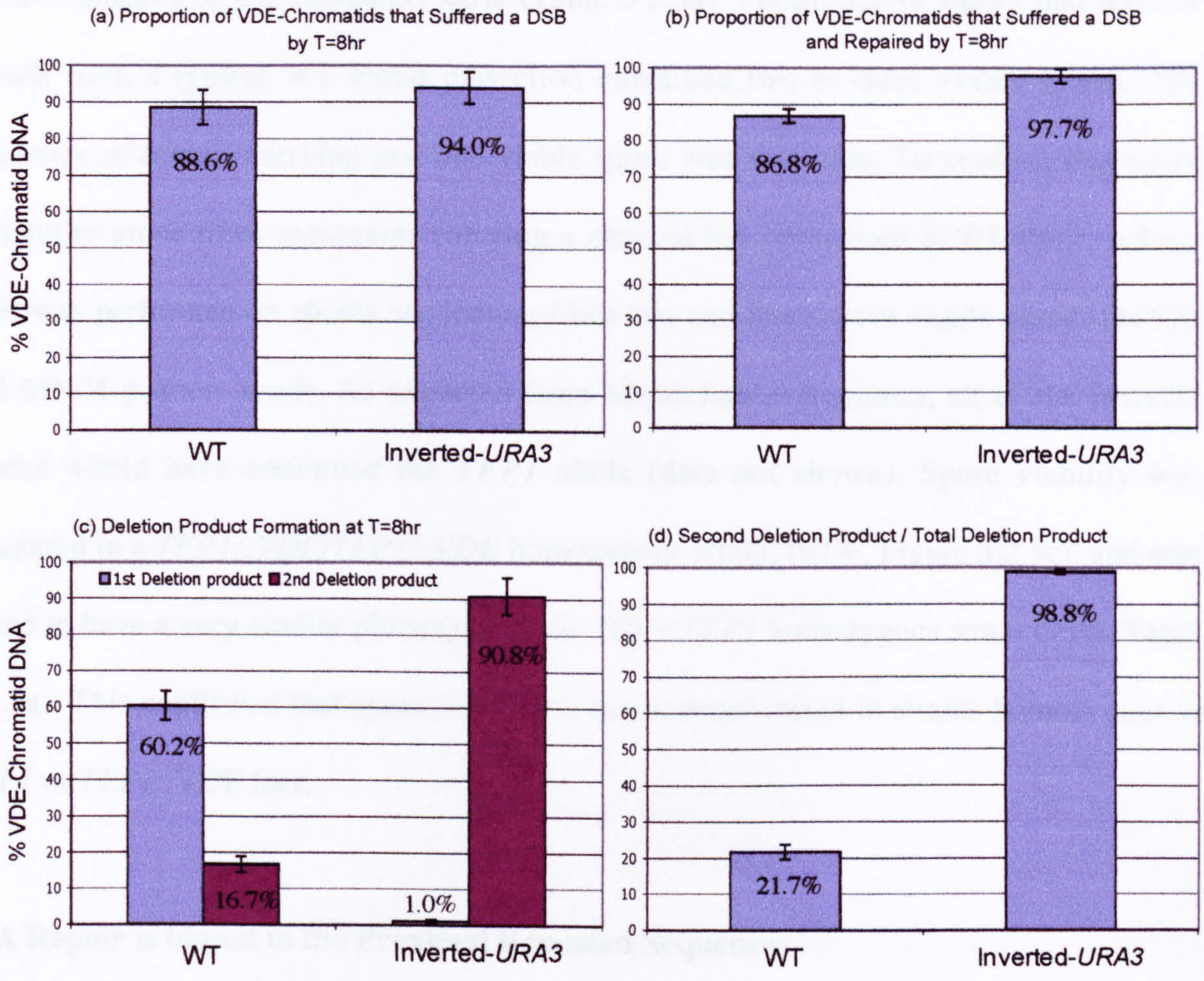

Figure 3.3.1: Repair Ability and Deletion Product Formation. (a) The proportion of VDE-chromatids that had suffered a DSB by T=8hr. (b) The proportion of VDE-chromatids that had suffered a VDE-DSB and repaired by T=8hr. (c) Deletion product formation measured at T=8hr. (d) Repair product ratio values, calculated as second deletion product as a proportion of total deletion product formation at T=8hr. (Error bars display standard deviation).
Inversion of the WT *URA3* allele (Inverted-*URA3* strain) biased SSA deletion repair to the distal *ade2* repeated sequences, resulting in an accumulation of second deletion product. (Data from n=4 experiments per strain)

spore viabilities of approximately 60% (Table 3.2.5a). Figure 3.2.5b shows that 85% of tetrads from a typical WT tetrad dissection contained two or three viable spores. The incidence of tetrads carrying just one viable spore was very rare. To confirm that spore inviability arose from segregants carrying a cleaved but unrepaired *TFP1* allele, colony PCR was performed on spores originating from two and three spore viable tetrads (MN03 and MN04 primers used). As expected from Mendelian segregation, all of the inviable spores would have contained the *TFP1* allele (data not shown). Spore viability was measured in a *TFP1::VDE/TFP1::VDE* homozygous strain, (97%, Figure 3.2.5c), and was found to have a very similar phenotype to the *TFP1/TFP1* homozygous strain (95%, Table 3.2.5a). This confirmed that spore viability was uncompromised in strains homozygous at *TFP1* or *TFP1*::VDE loci.

SSA Repair is biased to the Proximal Repeated Sequences

It was demonstrated that 40% of spores from the WT strain had repaired to first deletion product, and 15% to second deletion product (Table 3.2.6a). A greater proportion of repair using the proximal *URA3* repeated sequences was predicted from the reported bias of the SSA process for deletion repair using the closest set of available repeated sequences (Sugawara and Haber, 1992). Optimal SSA repair involves the minimum of DNA deletion from the genome, which is why the closest set of flanking repeated sequences to the DSB site are preferentially selected for repair.

Inversion of Proximal Repeated Sequences biased SSA Repair to Distal Repeats

The Inverted-*URA3* strain generated both first and second deletion product, although in different proportions to the WT strain (Table 3.2.6a). A greater proportion of spores from

the Inverted-*URA3* diploid were Ura- Ade+, indicating second deletion product formation (64.29%). This was evidence that inversion of the *URA3* sequence in this cassette had biased SSA repair of the DSB to the distal *ade2* homologies, as expected. However, Ura- Ade- spores from the Inverted-*URA3* strain were also created, at a frequency of 35.71%, implying the formation of first deletion product. It was predicted that SSA repair was not possible between indirect repeated *URA3* homologies. A model for homologous recombination between the indirect proximal repeated sequences is suggested in Figure 3.4. Briefly, it would involve contortion of the *ade2::arg4-VDE* cassette DNA, bringing the *URA3* and *ura3* repeated sequences into direct orientation. Alignment of the homologous regions in the *URA3* and *ura3* fragments would then permit DSB repair via homologous strand exchange (Figure 3.4).

All spores from the *TFP1/TFP1* diploid strain were Ura+ Ade-, and therefore contained parental DNA. Thus, DSB formation in the reporter assay was prevented in the absence of VDE protein expression, (Figure 3.2.6b).

Contribution of NHEJ

The large proportion of spores from the WT strain that displayed a parental DNA phenotype (Ura+ Ade-) was not predicted (45%, Table 3.2.6a). It was unlikely that cleavage had failed at *ade2::arg4-VDE* allele (Figure 3.2.6b), because VDE has been shown to cut with high efficiency (Bremer et al., 1992; Gimble and Thorner, 1993; Neale et al., 2002). A possible explanation is that VDE endonuclease had cleaved the DNA, but the DSB had repaired by a non-homologous repair method, (for example nonhomologous endjoining (NHEJ), Figure 3.2.6c and Figure 3.2.6d). On sustaining a lesion, DNA is

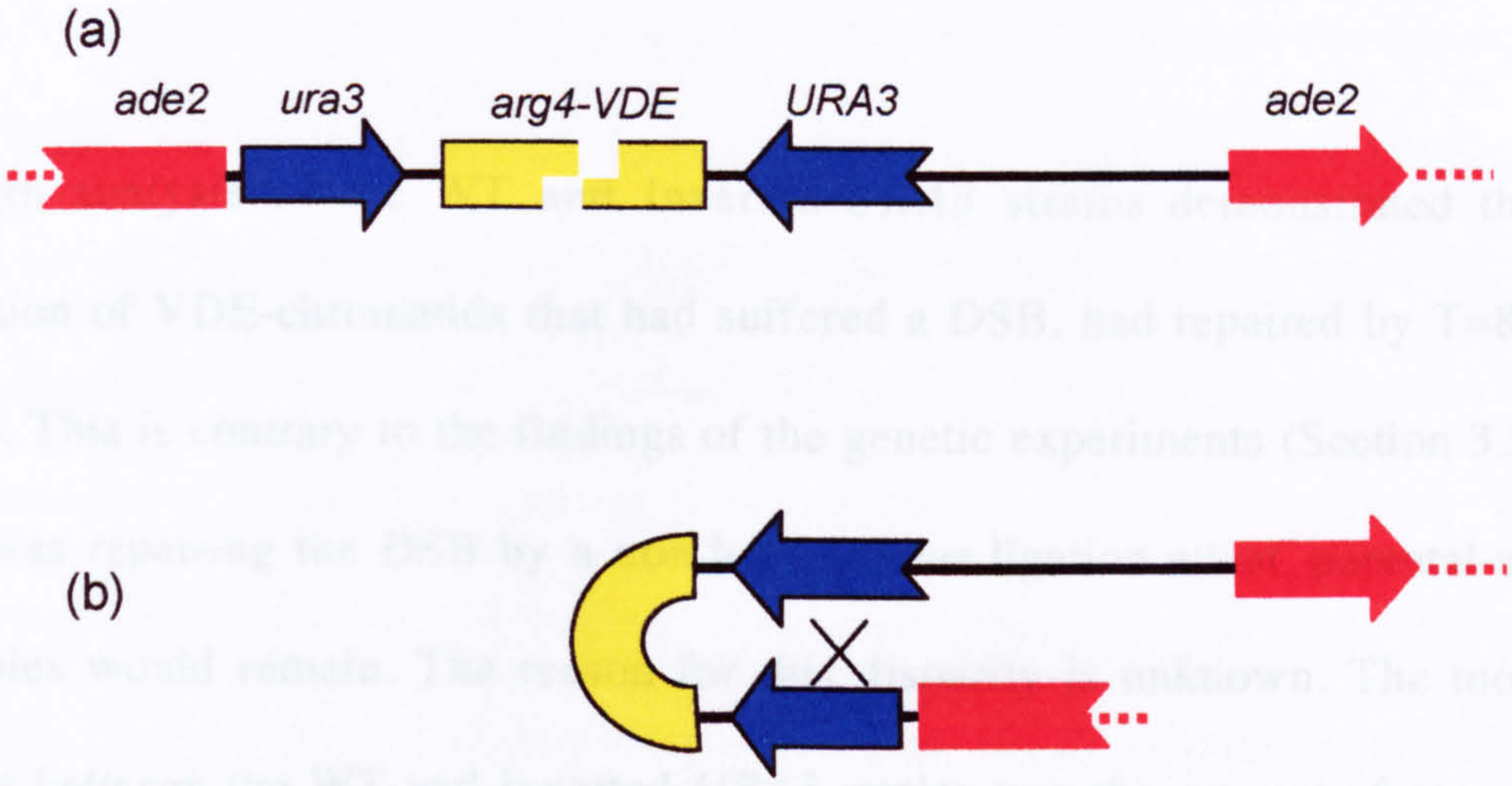

Figure 3.4: Proposed Model for Recombination between the Proximal *URA3* repeated sequences in the Inverted-*URA3* strain. The generation of Ura- Ade- spores from (a) the Inverted-*URA3* strain (dAG649), suggested the generation of first deletion product. This was not a predicted repair outcome, due to inversion of the *URA3* allele preventing homology alignment between the *URA3* and *ura3* alleles. (b) A model by which the *URA3* and *ura3* homologous regions could be brought into direct orientation through twisting of the cassette DNA.

capable of knitting back together, with the addition or loss of a limited number of DNA bases. NHEJ is not a common DSB repair method in *S. cerevisiae*, but it makes a large contribution to the repertoire of DNA repair systems in humans (reviewed in (Cromie et al., 2001)).

Southern analysis of the WT and Inverted-*URA3* strains demonstrated that a large proportion of VDE-chromatids that had suffered a DSB, had repaired by T=8hr (Figure 3.3.1b). This is contrary to the findings of the genetic experiments (Section 3.2.6). If the assay was repairing the DSB by a non-homologous ligation event, parental-sized DNA molecules would remain. The reason for this disparity is unknown. The most striking contrast between the WT and Inverted-*URA3* strains was the amount of second deletion product generated (Figure 3.3 and Figure 3.3.1c). Consequently, the repair product ratio value for the Inverted-*URA3* strain was much higher than for WT (Figure 3.3.1d). Very little first deletion product was generated in the Inverted-*URA3* strain (1.0%, Figure 3.3.1c), which is also disparate with the results of the genetic experiments. The reason for the discrepancies between genetic and DNA data are currently being investigated. However, it is reasonable to surmise that southern analysis of DSB repair provides a more detailed and accurate view of repair events at the *ade2::arg4-VDE* allele.

Chapter 4

Genetic Requirements for Intrachromosomal Repair of the *ade2::arg4-VDE* Allele

4.1 Introduction

The *ade2::arg4-VDE* repair assay used in this study was designed so that the double strand break (DSB) could only be repaired by single strand annealing (SSA), via the generation of first or second deletion product, (Figure 3.1). **5kb** of DSB resectioning of the VDE-DSB was required to uncover the proximal *URA3* repeated sequences, and **10.5kb** of resectioning was required to uncover the distal *ade2*Δ repeated sequences. The genetic requirements and influences over this type of repair were explored. The DSB was created by the meiosis-specific *VMA1*-derived endonuclease (VDE) (Bremer et al., 1992; Gimble and Thorner, 1993). SSA is an example of intrachromosomal DSB repair, which can occur in meiosis. Under normal circumstances the favoured DSB repair mechanism is interchromosomal repair that is, using the homologous chromosome as repair template. Intrachromosomal repair using the sister chromatid as repair template is also possible in meiosis, but occurs at a much lower frequency to interchromosomal repair, (Collins and Newlon, 1994; Schwacha and Kleckner, 1994; Schwacha and Kleckner, 1997). The assay developed in this study therefore provided the opportunity to study a meiosis-specific DSB, constrained to a distinctly 'unmeiotic' repair process. A brief explanation of the *S. cerevisiae* mutant strains studied in this chapter is given below.

The preferential direction of meiotic DSB repair towards the homologous chromosome, requires the meiosis-specific RecA homologue, **Dmc1** (Bishop et al., 1992). In this study, repair of the *ade2::arg4-VDE* allele using the homologue as a repair template was

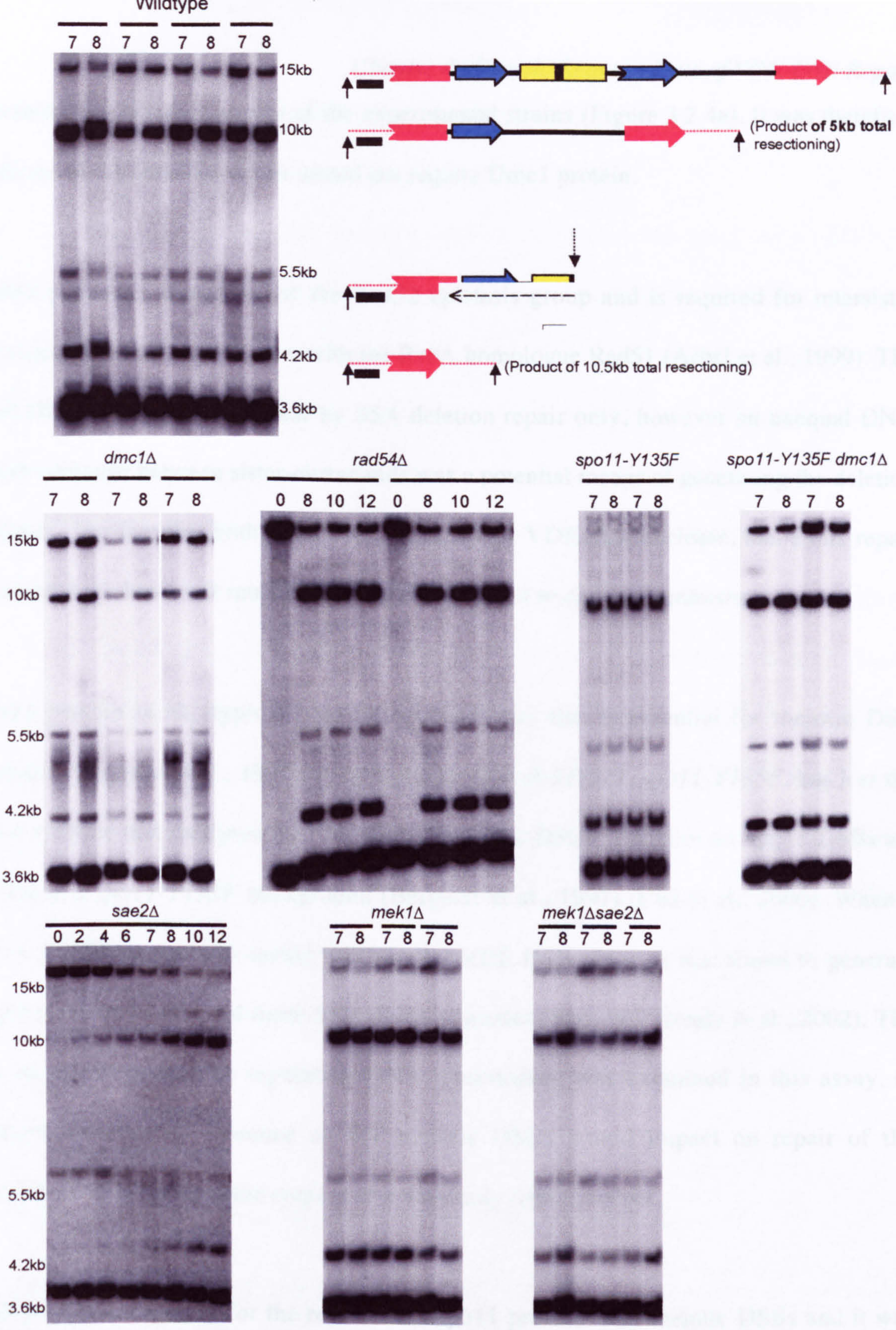

Figure 4.1: Southern Analysis of VDE-DSB Creation and Repair of the *arg4-VDE* allele: (Top panel): DNA extracted from WT (dAG630) synchronous meiotic cultures, digested with *SpeI* (black arrows), and after fractionation and blotting, the DNA-membrane was hybridised with a probe specific to the upstream region of *ADE2* (black box). (Timepoints shown above gel images). 15kb band: parental DNA, 10kb band: first deletion product, 5.5kb band(smeared): VDE-DSB, 4.2kb: second deletion product, 3.6kb: loading control. (Middle panel): Southern analysis of DNA from synchronous meiotic cultures of *dmc1*Δ (dAG1265), *rad54*Δ (dAG1236), *spo11-Y135F* (dAG759) and *spo11-Y135F dmc1*Δ (dAG1284). (Bottom panel): *sae2*Δ (dAG1200), *mek1*Δ (dAG732) and *mek1*Δ *sae2*Δ (dAG1215) mutant strains. Smearing of the VDE-DSB DNA was caused by ssDNA molecules of progressively shorter length, due to resectioning at the VDE-DSB (dashed arrows). (Data from n=3 experiments per strain)

prevented due to hemizygosity of the experimental strains (Figure 3.2.4a). It was therefore predicted that VDE-DSB repair would not require Dmc1 protein.

Rad54 protein is a member of the Rad52 epistasis group and is required for intersister chromatid repair, in conjunction with the RecA homologue Rad51 (Arbel et al., 1999). The VDE-DSB was expected to heal by SSA deletion repair only, however an unequal DNA strand exchange between sister-chromatids was a potential means of generating the deletion products. The fact that both sisters were cleaved by VDE-endonuclease, made this repair event unlikely, but a null mutation of *RAD54* was used to check for intersister repair.

Spo11 protein is an atypical type II topoisomerase that is essential for meiotic DSB formation (Keeney et al., 1997). A catalytic mutant of *SPO11*, *spo11-Y135F*, has lost the active tyrosine that catalyses the formation of meiotic DSBs, therefore no Spo11-DSBs are created in a *spo11-Y135F* background (Bergerat et al., 1997) (Cha et al., 2000). When a *spo11-Y135F* mutant was tested in a parallel VDE-DSB assay, it was found to generate longer resection tracts and more SSA deletion product than WT (Neale et al., 2002). The role of Spo11 protein in regulating DNA resectioning was examined in this assay, to examine whether the absence of WT meiotic DSBs would impact on repair of the *ade2::arg4-VDE* allele in the context of a SSA-only repair process.

Sae2 protein is required for the removal of Spo11 protein from meiotic DSBs and it was first isolated and characterised in a screen for mutants blocked at intermediate stages of meiotic prophase (McKee and Kleckner, 1997; Prinz et al., 1997). Loss of Sae2 protein function causes Spo11 protein to remain covalently bound to meiotic DSBs, creating an

accumulation of unresected breaks.

A contributory mechanism for ensuring that crossovers in meiosis occur between homologous chromosomes has been identified. This involves three meiosis-specific chromosomal core proteins, **Mek1**, Red1 and Hop1 (Wan et al., 2004). Activation of the Mek1 kinase, (which coincides with the formation of Spo11-DSBs), is thought to mediate inhibition of the components required for intersister repair, e.g. Rad54 protein (Wan et al., 2004) (Niu et al., 2005). Thus, during Spo11-DSB processing, Mek1 protein would effectively create a barrier to sister chromatid repair, and through this action, bias repair towards the homologous chromosome (Wan et al., 2004). The argument that the Mek1 protein complex is required for the meiotic cells' drive towards interchromosomal repair is a robust one, however the proposed mode of action, that is, specific inhibition of intrachromosomal repair is worth exploring. To test this idea, a *mek1*Δ mutant was examined in this study, where assay design prevented DSB repair of the *ade2::arg4-VDE* allele via an interhomologue exchange. Particular emphasis was placed on VDE-DSB resection tract length in the *mek1*Δ mutant, with the aim of elucidating the mechanism by which Mek1 protein exerts its influence over partner choice.

4.2 The impact of Candidate Mutations on Repair of the VDE-DSB

The reporter assay was used to determine whether any of the genes outlined in Section 4.1, were required for repair of the *ade2::arg4-VDE* allele. The experimental diploids consisted of homozygous deletion mutants: *dmc1*Δ (dAG1265), *rad54*Δ (dAG1236), *spo11-Y135F* (dAG759), *sae2*Δ (dAG1200), *spo11-Y135F dmc1*Δ (dAG1284), *mek1*Δ (dAG732) and

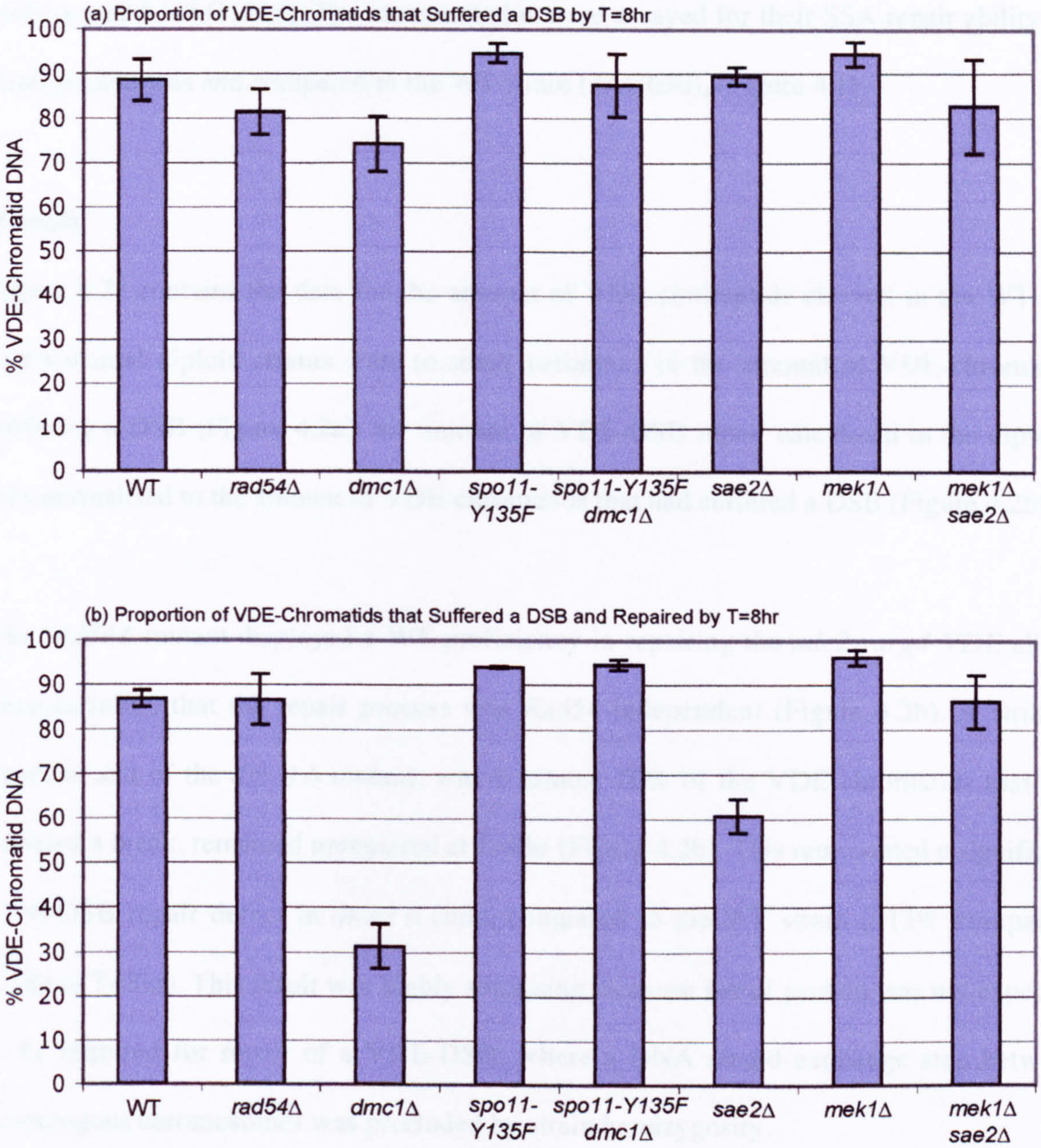

Figure 4.2: Amount of SSA repair of the *arg4-VDE* allele. (a) Amount of VDE-chromatids that had suffered a VDE-DSB ('broken') at T=8hr in WT and mutant strains. Calculated as (total VDE-chromatid DNA)-(parental DNA). (b) Amount of repair of the VDE-DSB, as a proportion of broken VDE-chromatids. Calculated as (total deletion repair product)/(broken VDE-chromatids). All values expressed as percentage of total VDE-chromatid DNA. See Figure 4.1 for strain information. (Error bars display standard deviation). (Data from n=3 experiments per strain)

*mek1*Δ *sae2*Δ (dAG1215). The mutant strains were assayed for their SSA repair ability via southern analysis and compared to the WT strain (dAG630), (Figure 4.1).

Results

Figure 4.2a contains the data for the amount of VDE-chromatids cleaved in the WT and experimental diploid strains. Due to small variations in the amount of VDE-chromatids suffering a DSB (Figure 4.2a), the amount of VDE-DSB repair calculated in the diploids was normalised to the amount of VDE-chromatids that had suffered a DSB (Figure 4.2b).

The *rad54*Δ mutant displayed a WT proficiency in repairing the *ade2::arg4-VDE* allele, demonstrating that the repair process was Rad54-independent (Figure 4.2b). A striking result is that of the *dmc1*Δ mutant, where almost 70% of the VDE-chromatids that had suffered a break, remained unrepaired at T=8hr (Figure 4.2b). This represented a significant VDE-DSB repair defect in *dmc1*Δ cells, compared to the WT strain (~13% unrepaired DSBs at T=8hr). This result was highly surprising, because Dmc1 protein was not expected to be required for repair of a VDE-DSB, where a DNA strand exchange step between homologous chromosomes was precluded by strain hemizygosity.

The *spo11-Y135F* mutant strain repaired the *ade2::arg4-VDE* allele to approximately WT levels (Figure 4.2b), demonstrating that the absence of meiotic DSBs did not hinder repair of the single *ade2::arg4-VDE* allele. As Dmc1 protein was found to be required for repair of the VDE-DSB, a *spo11-Y135F dmc1*Δ double mutation was used to test this dependency. The *spo11-Y135F* mutation rescued the repair defect of *dmc1*Δ, 94.5% of broken DNA was repaired in the *spo11-Y135F dmc1*Δ double mutant, compared to 31.4% in the *dmc1*Δ

single mutant (Figure 4.2b). This result matched the findings of the parallel study, that VDE-DSB repair was Dmc1-independent in cells lacking functional Spo11 protein (M.J.N and A.S.H.G, Unpub.).

Interestingly, the *sae2*Δ mutation conveyed a defect in DSB repair of the *ade2::arg4-VDE* allele: 60.7% of VDE-chromatids that had suffered a VDE-DSB had repaired at T=8hr in *sae2*Δ, compared to 86.8% in WT (Figure 4.2b).

The *mek1*Δ and *mek1*Δ *sae2*Δ mutants were also found to repair the *ade2::arg4-VDE* allele to WT levels (Figure 4.2b).

4.3 An Assay to Compare Deletion Product Formation

The reporter assay was used to indicate whether any of the candidate genes influenced the regulation of VDE-DSB resectioning, by considering first and second deletion product formation. Cells that had repaired the *ade2::arg4-VDE* allele by generating DSB resection tracts spanning a distance of **5kb** would preferentially use the proximal *URA3* direct repeated sequences, thus creating first deletion product (Figure 3.1b). While cells that repaired the VDE-DSB by generating resection tracts spanning a distance of **10.5kb**, would preferentially use the distal *ade2* repeated sequences, to create second deletion product (Figure 3.1c). The repair product ratio values for the experimental diploids were determined via southern analysis (Figure 4.1). The amount of second deletion product, as a proportion of total deletion product formation at T=8hr, was calculated for each strain (Repair product ratio = secondΔ/(firstΔ + secondΔ). Consequently, an altered ratio value (compared to the WT strain, dAG630) indicated that the balance between 5kb and 10kb DSB resection tract formation had been disturbed, signalling irregularity in the critical regulation of DSB

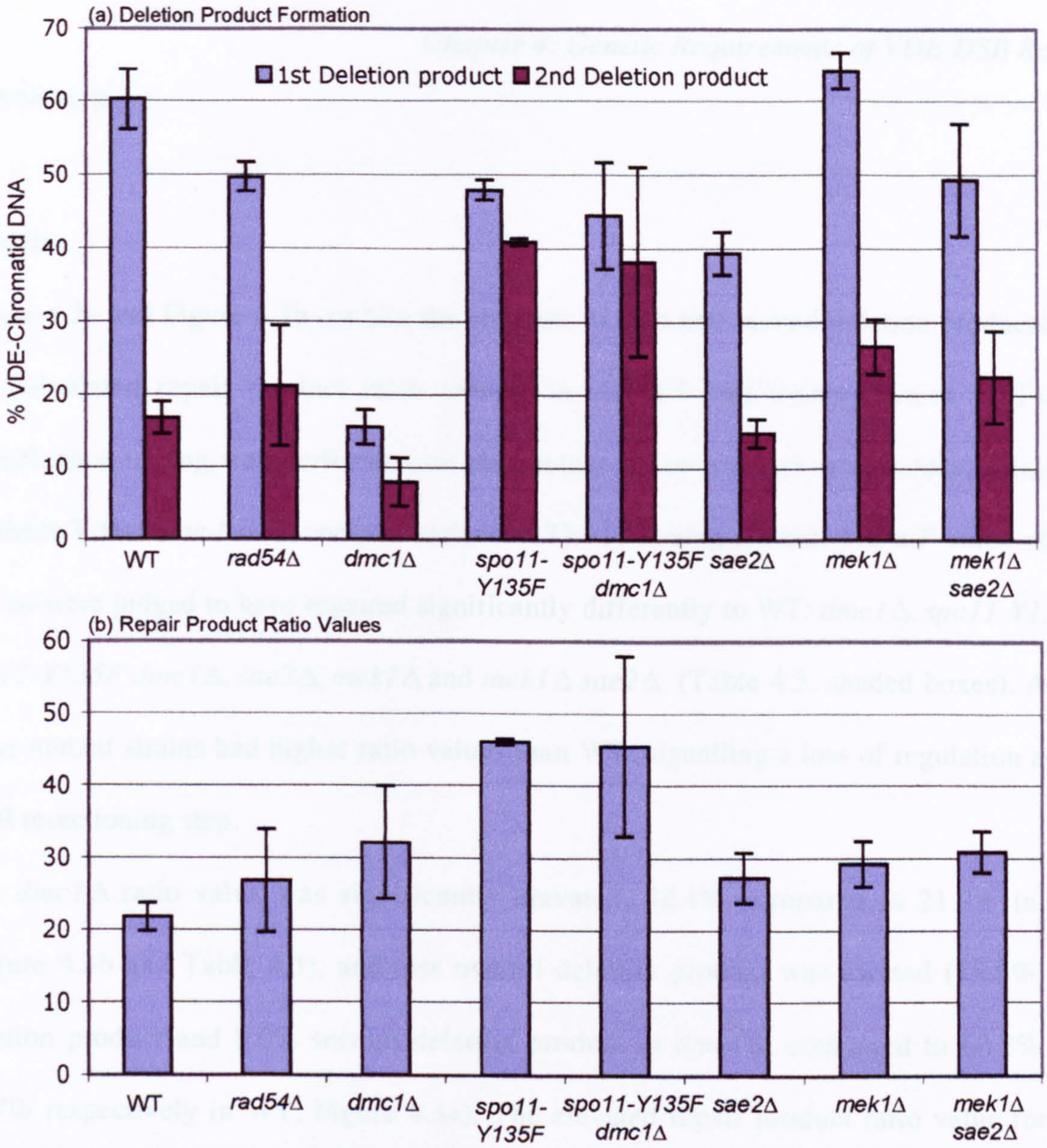

Table 4.3: Repair Product Ratio Values and their Associated Significances

	Repair Product Ratio(%)	*P* value (*P* <0.05)
wildtype	21.7	-
rad54Δ	26.8	0.08
dmc1Δ	32.1	3.33E-03
spo11-Y135F	46.1	3.13E-05
spo11-Y135F dmc1Δ	45.5	0.02
sae2Δ	27.3	0.02
mek1Δ	29.2	4.99E-03
mek1Δ sae2Δ	30.9	1.27E-03

Figure 4.3: Deletion Product Formation and Repair Product Ratio Values in the *arg4-VDE* assay at T=8hr (a) Amounts of first and second deletion product formation in WT and mutant strains, (expressed as a percentage of total VDE-chromatid DNA). (Error bars display standard deviation). (b) Repair product ratio values, calculated as second deletion product as a proportion of total deletion product formation. Table 4.3 contains tabulated data from (b), and the associated *P* values (calculated using the Students T-test, Section 2.11). (Mutant ratio values significantly different to WT ($P<0.05$), shaded boxes). See Figure 4.1 for strain information. (Data from n=3 experiments per strain)

resectioning.

Results

Figure 4.3a and Figure 4.3b contain the amounts of first and second deletion products and the calculated repair product ratio values, in the WT and mutant strains at T=8hr. Significance testing was performed on the mutant repair product ratio values, using the Students T-test (one-tailed, unequal variance). The following mutants had a *P* value <0.05, and so were judged to have repaired significantly differently to WT: *dmc1*Δ, *spo11-Y135F*, *spo11-Y135F dmc1*Δ, *sae2*Δ, *mek1*Δ and *mek1*Δ *sae2*Δ (Table 4.3, shaded boxes). All of these mutant strains had higher ratio values than WT, signalling a loss of regulation at the DSB resectioning step.

The *dmc1*Δ ratio value was significantly elevated, 32.1% compared to 21.7% in WT (Figure 4.3b and Table 4.3), and less overall deletion product was formed (15.5% first deletion product and 8.0% second deletion product in *dmc1*Δ, compared to 60.2% and 16.7% respectively in WT, Figure 4.3a). The elevated repair product ratio value for the *spo11-Y135F* mutant (Figure 4.3b and Table 4.3), was a result of an increased formation of second deletion product, 40.9%, compared to 16.7% in WT, (Figure 4.3a). Therefore, the *spo11-Y135F* mutant generated a larger number of very long resection tracts when repairing the VDE-DSB, and as expected, this was also true of the *spo11-Y135F dmc1*Δ double mutant, which generated 38.2% second deletion product (Figure 4.3a). In the *sae2*Δ mutant (dAG1200), the observed increase in repair product ratio was caused by a proportional reduction in the generation of first deletion product, 39.4%, compared to 60.2% in WT. This suggested that *sae2*Δ cells were defective in creating resection tracts that spanned 10.5kb. Both the *mek1*Δ and *mek1*Δ *sae2*Δ mutants created increased amounts of second

deletion product (26.6% in *mek1*Δ and 22.5% in *mek1*Δ*sae2*Δ, compared to 16.7% in WT), while the amount of first deletion product remained similar to WT (Figure 4.3a).

4.4 Discussion

The genetic requirements for repairing a meiotic DSB, and the regulation of DNA resectioning were examined in the *ade2::arg4-VDE* DSB assay in this chapter.

Influence of Dmc1 Protein

Repair of the VDE-DSB was found to be independent of Rad54 protein, (Figure 4.2b), which supported the view that repair was only occurring via SSA. In light of this result, it was surprising to discover that repair of the VDE-DSB was affected by a *dmc1*Δ mutation (Figure 4.2b). The *dmc1*Δ mutation blocked repair in almost 70% of VDE-chromatids that had suffered a DSB by T=8hr, resulting in a large reduction in deletion product formation (Figure 4.3a). There is no previous evidence to suggest a role for Dmc1 protein in any homologous recombination repair process other than that involving a strand exchange step. The idea that Dmc1 protein impacted on repair of the *ade2::arg4-VDE* allele was reinforced by the fact that a *spo11-Y135F* mutation relieved the dependency on Dmc1 protein in meiotic cells (Figure 4.2b and Figure 4.3a). It has previously been demonstrated that Spo11, along with Sae2 and Mek1 proteins are required to establish Dmc1-dependent DSB repair in meiotic cells (M.J.N and A.S.H.G, Unpub.). It was assumed that this was to allow DSB repair to be directed towards the homologous chromosome as repair template, fulfilling both the mechanical and evolutionary requirements of meiotic recombination. However, the assay used in this study reported exclusively on SSA repair, a route that does not provide the fundamental requirements of meiosis, that is, promoting the accurate

segregation of homologues at MI. The fact that a *spo11-Y135F* mutation relieved the SSA repair defect observed in Dmc1-deficient cells, supported the idea that DSB repair at a VDE-DSB site allele can be influenced by events at Spo11-DSB sites (Neale et al., 2002), (Figure 4.4*i* and Table 4.4*i*).

Protein Sequestration in *dmc1*Δ

An explanation for the observed repair defect in the *dmc1*Δ mutant is that the single VDE-DSB site has to compete for the components of DSB repair, and may be affected by protein sequestration at multiple Spo11-DSBs sites, (previously suggested in (Neale et al., 2002). At the same time that VDE endonuclease cleaves the DNA, more than 200 Spo11-DSBs are created in the *S. cerevisiae* genome to induce meiotic recombination (Gimble and Thorner, 1992) (Cao et al., 1990). The Spo11-DSBs are then resected, ready for interhomologue recombinational repair. The turnover of resected DNA at Spo11-DSB sites generates transient levels of (single-stranded) ssDNA molecules, which become coated with the proteins required for homologous recombination, including the ssDNA-binding protein, RPA and Rad52 (reviewed in (Symington, 2002)). As these proteins are required for recombination between direct DNA repeated sequences (Davis and Symington, 2001) (Shinohara et al., 1998), their availability at the *ade2::arg4-VDE* allele may be reduced, particularly if they are derived from a limited pool. In a *dmc1*Δ mutant a defect in the conversion of Spo11-DSBs into the recombination intermediates required for interhomologue repair, causes an accumulation of meiotic DSBs (Bishop et al., 1992). The broken DNA termini undergo 5′-3′ resectioning, which generates large amounts of ssDNA. The accumulated ssDNA within *dmc1*Δ cells may sequester the Rad52 and RPA proteins, preventing their recruitment to the VDE-DSB site. This inhibition to the VDE-DSB repair

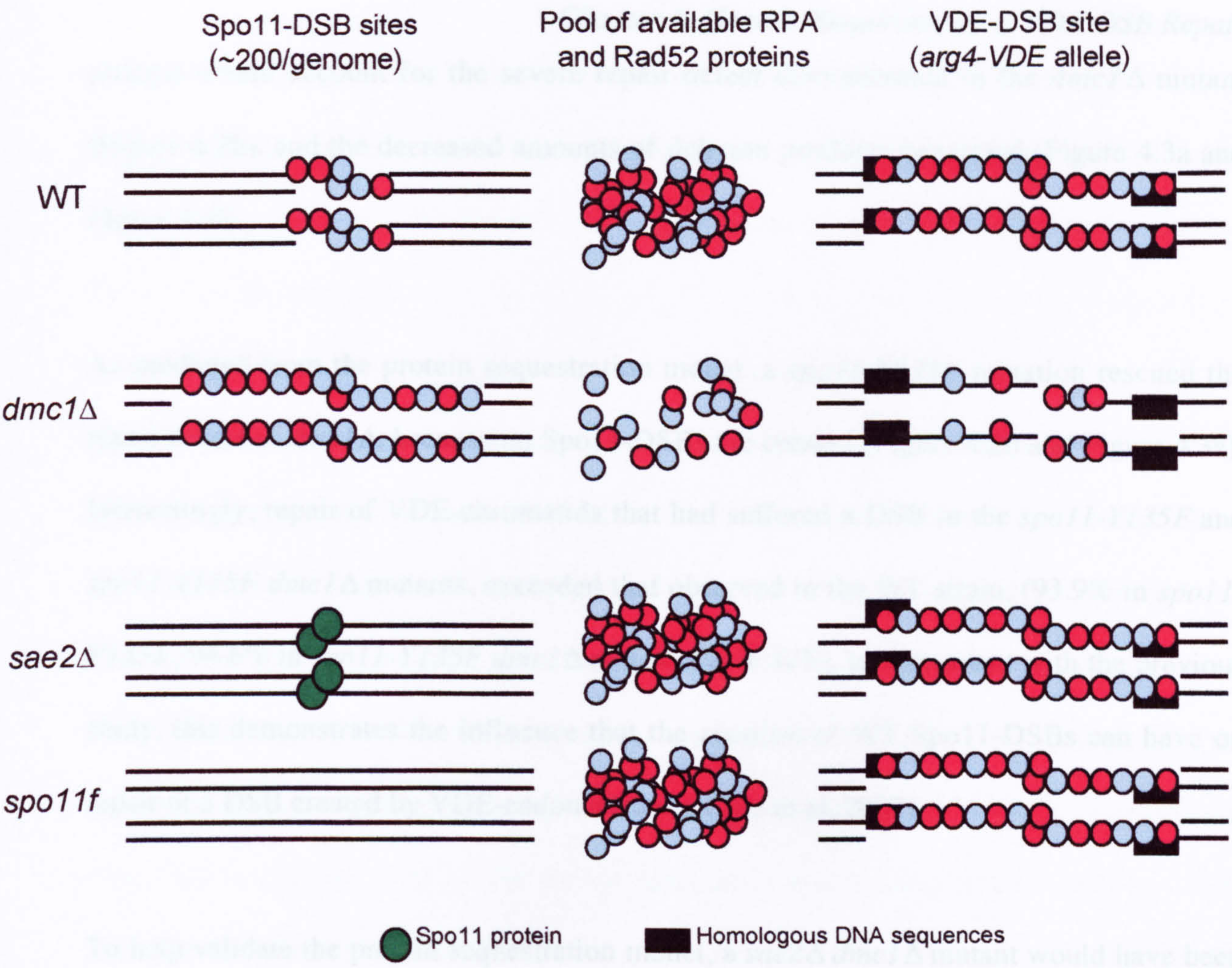

Table 4.4*i*

	Spo11-DSBs ssDNA	Spo11-DSBs Sequestration	VDE-DSB Repair
WT	+	+	++
dmc1Δ	+++	+++	+
sae2Δ	-	-	++
spo11	-	-	++

Figure 4.4*i*: Protein Sequestration at Sites of Excess ssDNA. A schematic representation of the events at multiple Spo11-break sites and the singular VDE-DSB site during meiotic DSB repair. Transient ssDNA formation at Spo11-DSBs in WT, is not sufficient to sequester the SSA proteins away from the VDE-DSB site. In *sae2*Δ and *spo11f* mutants, (also *spo11f dmc1*Δ, not shown), the absolute lack of ssDNA at Spo11-DSB sites frees up all of the available RPA/Rad52 protein for coating the ssDNA at the *arg4-VDE* allele, allowing optimal repair. In *dmc1*Δ cells, hyperresectioning of the accumulating Spo11-DSBs generates sufficient ssDNA to sequester the SSA-required proteins away from the VDE-DSB, therefore impairing SSA repair of the *arg4-VDE* allele. Table 4.4*i* summarizes the predictions for protein sequestration and the associated VDE-DSB repair data, based on the results from Section 4.2.

process would account for the severe repair defect demonstrated in the *dmc1*Δ mutant (Figure 4.2b), and the decreased amounts of deletion products generated (Figure 4.3a and Figure 4.4*i*).

As predicted from the protein sequestration model, a *spo11-Y135F* mutation rescued the repair defect of *dmc1*Δ, because no Spo11-DSBs are created (Figure 4.2b and Figure 4.3a). Interestingly, repair of VDE-chromatids that had suffered a DSB in the *spo11-Y135F* and *spo11-Y135F dmc1*Δ mutants, exceeded that observed in the WT strain, (93.9% in *spo11-Y135F*, 94.6% in *spo11-Y135F dmc1*Δ and 86.8% in WT). In agreement with the previous study, this demonstrates the influence that the creation of WT Spo11-DSBs can have on repair of a DSB created by VDE-endonuclease (Neale et al, 2002).

To help validate the protein sequestration model, a *sae2*Δ *dmc1*Δ mutant would have been very useful. In a *sae2*Δ *dmc1*Δ mutant background, a WT number of Spo11-DSBs are created, but the removal of Spo11 protein from the break sites is prevented (McKee and Kleckner 1997; Prinz, Amon et al. 1997). As Spo11 protein effectively blocks the DNA termini, the ends are rendered inaccessible to the resectioning machinery, and there is an absolute lack of ssDNA. Unfortunately, due to technical difficulties, a *sae2*Δ *dmc1*Δ mutant was unavailable for this study.

Preliminary chromatin immunoprecipitation (ChIP) experiments using anti-RPA1 antibody directed to a Spo11-DSB hot spot, have demonstrated an enrichment of hot spot DNA in a *dmc1*Δ mutant, as compared to WT (S.H and A.S.H.G, Unpub.). Corresponding to this, at an equivalent VDE-DSB hotspot, there was an enrichment of VDE-DSB DNA in WT,

compared to *dmc1*Δ. These preliminary findings support the idea that VDE-DSB repair is subject to inhibition by sequestration of RPA protein, at Spo11-DSB sites in *dmc1*Δ cells (Figure 4.4i and Table 4.4i). Further ChIP experiments are currently underway to examine how robust this model is.

The idea that protein sequestration could inhibit SSA repair at the VDE-DSB is compatible with the proposal that optimal SSA repair of a DSB occurs between the closest set of flanking repeated sequences (Sugawara and Haber, 1992). Minimising genome deletion reduces the risk of loss of heterozygosity, however, the generation of ssDNA repair intermediates generated in SSA may also be important. VDE-DSB repair using the proximal *URA3* homologous sequences requires a minimum of 5kb of resectioning, compared to a minimum of 10.5kb for the distal *ade2* repeated sequences. Therefore VDE-DSB repair using the closest set of available repeated sequences would minimise the burden on the ssDNA-binding proteins, especially if they were limiting factors.

Absence of Spo11-DSBs Affect VDE-DSB Resection Tract Length

As expected of a mutant that has previously been demonstrated to generate longer resection tracts, (Neale et al., 2002), the *spo11-Y135F* mutant created more second deletion product than WT in this study, confirming that this mutant created a greater number of 10.5kb resection tracts (Figure 4.3a). As a consequence, the *spo11-Y135F* mutant had a significantly greater repair product ratio value than WT (Figure 4.3b). It is likely that the *spo11-Y135F* mutant phenotype of creating longer resection tracts was accompanied by a faster turnover of broken DNA, evidenced by the discrete *Nature* of the VDE-DSB band (Figure 4.1).

Sae2 Protein is required for First Deletion Product Formation

The proportion of *ade2::arg4-VDE* chromatids that suffered a DSB and then repaired by T=8hr, was lower in the *sae2*Δ mutant, 60.7%, compared to 86.8% in WT (Figure 4.2b). Less first deletion product was also generated in *sae2*Δ, 39.4%, compared to 60.2% in WT (Figure 4.3a). As similar proportions of second deletion product were formed, 14.8% in *sae2*Δ and 16.7% in WT, this suggests that impairment of VDE-DSB repair in the *sae2*Δ mutant was due to a failure of some cells to resect the DSB-DNA as far as the proximal *URA3* repeated sequences. However, cells that were able to resect this far, displayed no defect in resecting out to the distal *ade2*Δ repeated sequences.

In the *ade2::arg4-VDE* repair assay, resectioning of the VDE-DSB can be considered as three distinct steps. An initial resectioning step of a limited number of DNA bases, involving the generation of 'short' resection tracts. A second resectioning step, involving the generation of 'long' resection tracts, required for deletion repair of the *ade2::arg4-VDE* allele utilising the proximal *URA3* repeated sequences (5kb resectioning required). The third resectioning step would involve the generation of 'very long' resection tracts, required for deletion repair using the distal *ade2* repeated sequences (10.5kb DNA resectioning required). It is possible that Sae2 protein is required for the initial resectioning step in the VDE-DSB assay, because of its essential function in Spo11 protein removal from the sites of meiotic DSBs (Prinz et al., 1997; McKee and Kleckner, 1997). It has recently been reported that Spo11 protein is released from the DSB site, via endonucleolytic cleavage (Neale et al., 2005). It can be surmised that helicase activity is also required to unwind the

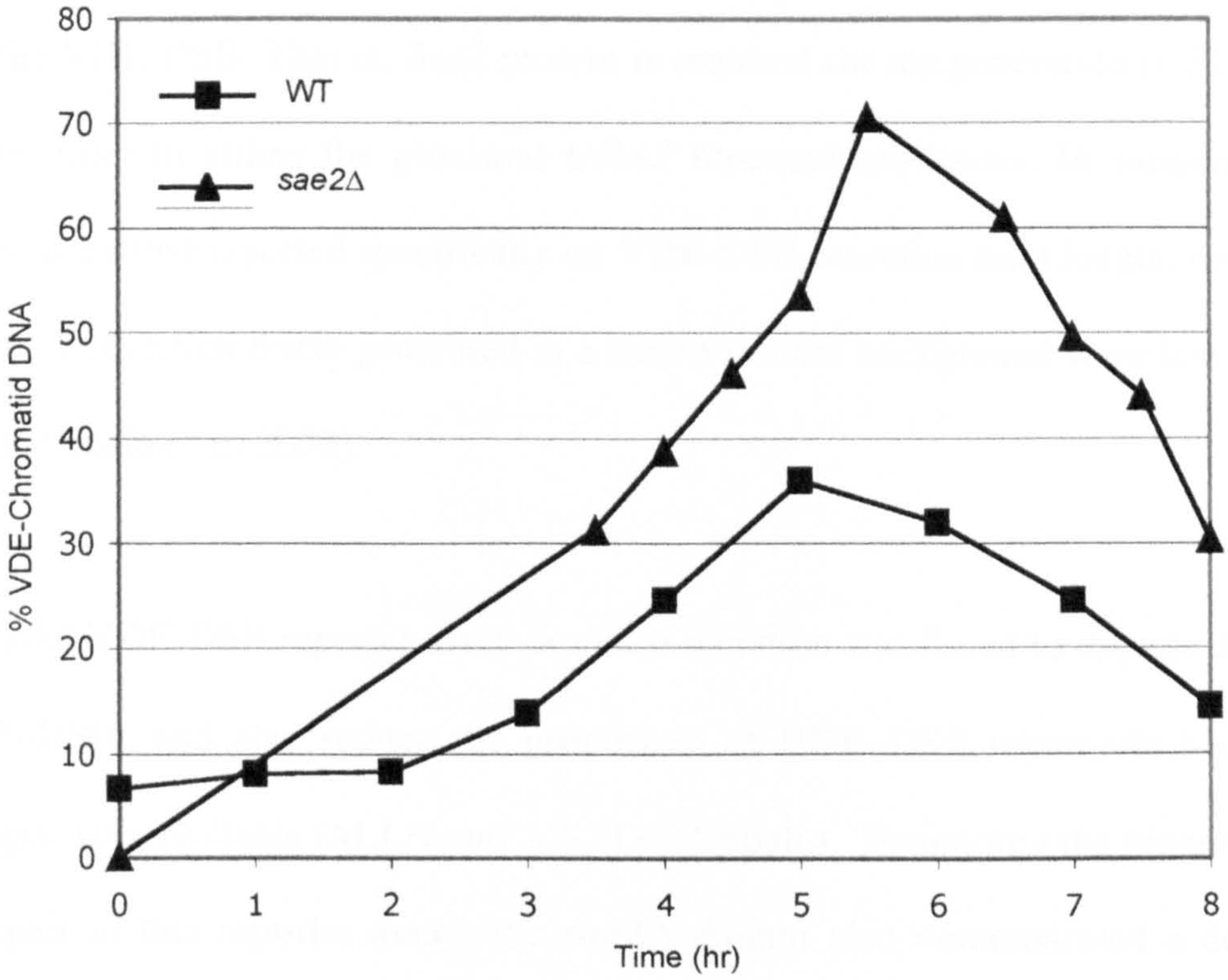

Figure 4.4*ii*: Quantification of VDE-DSB Turnover in *sae2*Δ. DNA extracted from WT (dAG630) and *sae2*Δ (dAG1200) strains and southern analysis performed (see Figure 4.1). Turnover of VDE-DSB is delayed in *sae2*Δ . (Turnover expressed as a proportion of VDE-chromatid DNA). (Data from n=4 experiments per strain)

double-stranded (ds)DNA, before a ssDNA endonuclease, such as Mre11 snips off the terminal bases, coated with Spo11 protein. The MRX complex is known to be involved in this initial resectioning step ((Moreau et al., 1999)), and Sae2 protein is also required. In the *ade2::arg4-VDE* assay, the *sae2*Δ mutant was defective in creating resection tracts that spanned 5kb, which resulted in the reduction of first deletion product formation. It is therefore plausible that Sae2 protein is also required for the (so-called) second resectioning step at the VDE-DSB. That is, Sae2 protein is required for the generation of 5kb resection tracts, in order to utilise the proximal *URA3* repeated sequences. In support of this, a previous assay that reported specifically on VDE-DSB resection tract length, demonstrated that 80% of resection tracts generated in a *sae2*Δ mutant background were less than 1.8kb in length. (Neale et al, 2002).

In a parallel VDE-DSB reporter assay, a *sae2*Δ mutation was found to impede the turnover of VDE–DSBs and also reduce the proportion of VDE–DSB repair via SSA, when a homologue was available (M.J.N and A.S.H.G, Unpub.). Examining the kinetics of VDE-DSB repair in this reporter assay, the *sae2*Δ mutant also demonstrated a delay in the turnover of VDE-DSBs, as compared to WT (Figure 4.4*ii*). This further supports the suggestion that Sae2 protein may have an additional role downstream of Spo11 protein removal from DSB sites. This function in early resectioning may help to influence repair template choice. When no homologous chromosome is available, like in this SSA assay, further progression of resection is indistinguishable from WT; hence similar amounts of second deletion product are formed. Recently, Sae2 protein has been examined in a mitotic SSA assay, where it was found to slow down HO-DSB induced resectioning (Clerici et al., 2005).

Mek1 Protein Negatively Regulates VDE-DSB Resectioning

The *mek1*Δ mutant conveyed no defect in repair of the VDE-DSB, as compared to WT (Figure 4.2b). However, when considering resection tract length at the VDE-DSB, the *mek1*Δ mutant was markedly different (Figures 4.3a and 4.3b). While similar amounts of 5kb resection tracts were created (first deletion product: 60.2% in WT and 64.2% in *mek1*Δ), the *mek1*Δ mutant created more 10.5kb resection tracts than WT, (second deletion product: 26.6% and 16.7%, respectively). This suggests that the Mek1-dependent push towards DSB-repair, using the homologue as partner, may be mediated by resection tract length. That is, the Mek1 protein negatively regulates the resectioning of VDE-DSB DNA, and by limiting resection tract length, both minimises the possibility of uncovering flanking homologies and improves the probability of a homologous chromosome becoming captured as repair template. As the *ade2::arg4-VDE* reporter assay reports on resection tract length during SSA repair only, the previously proposed mode of action of Mek1 protein (that is, promoting interchromosomal DSB repair through blocking the sister-chromatid) is not discounted.

The VDE-DSB resectioning demonstrated in the *mek1*Δ *sae2*Δ mutant was very similar to the *mek1*Δ single mutant, and consequently both the single and double *mek1*Δ mutations conveyed significantly increased repair product ratio values (Figure 4.3b). The fact that *MEK1* was epistatic to *SAE2* was not expected, and suggests that Mek1 protein is a major regulator of VDE-DSB repair upstream of Sae2.

Chapter 5

Repair of a VDE-DSB in Mutants that Prevent Spo11-DSB Formation and Processing

5.1 Introduction

The data presented in Chapter 4, along with those from a parallel VDE-assay, have demonstrated that repair of a VDE-DSB is influenced by events at Spo11-DSB sites (Neale et al., 2002; This Study). The *arg4-VDE* repair assay was also used to examine VDE-DSB repair in mutants of genes specifically involved in the formation and processing of Spo11-DSBs, that is *MRE11*, *RAD50* and *XRS2* (MRX) (reviewed (Krogh and Symington, 2004)). The protein products of these genes form a stable complex, which is involved in a myriad of cellular functions in yeast and human cells. Pertinent to this study, the MRX protein complex plays an integral role in meiotic recombination events, that is, in the creation and processing of meiotic DSBs. The ability to study DSB repair at a VDE-DSB, provides a unique opportunity to examine the MRX complex, because a null mutation in any of these genes prevents the formation of Spo11-DSBs. The MRX complex is required for the critical step of regulating DSB resectioning. In the *arg4-VDE* reporter assay, cells have the opportunity to repair the VDE-DSB by using proximal *URA3* repeated sequences, or distal *ade2* repeated sequences. This choice of deletion repair is dependant on DSB resection tract length. It was demonstrated in Section 3.3.1 that the WT strain (dAG630) preferentially created first deletion product when repairing the *arg4-VDE* allele. Null and functional mutants of the MRX complex, along with *EXO1*, were examined for their ability to repair the VDE-DSB and their influence over the regulation of DSB resectioning. A brief explanation of the mutant alleles is given below.

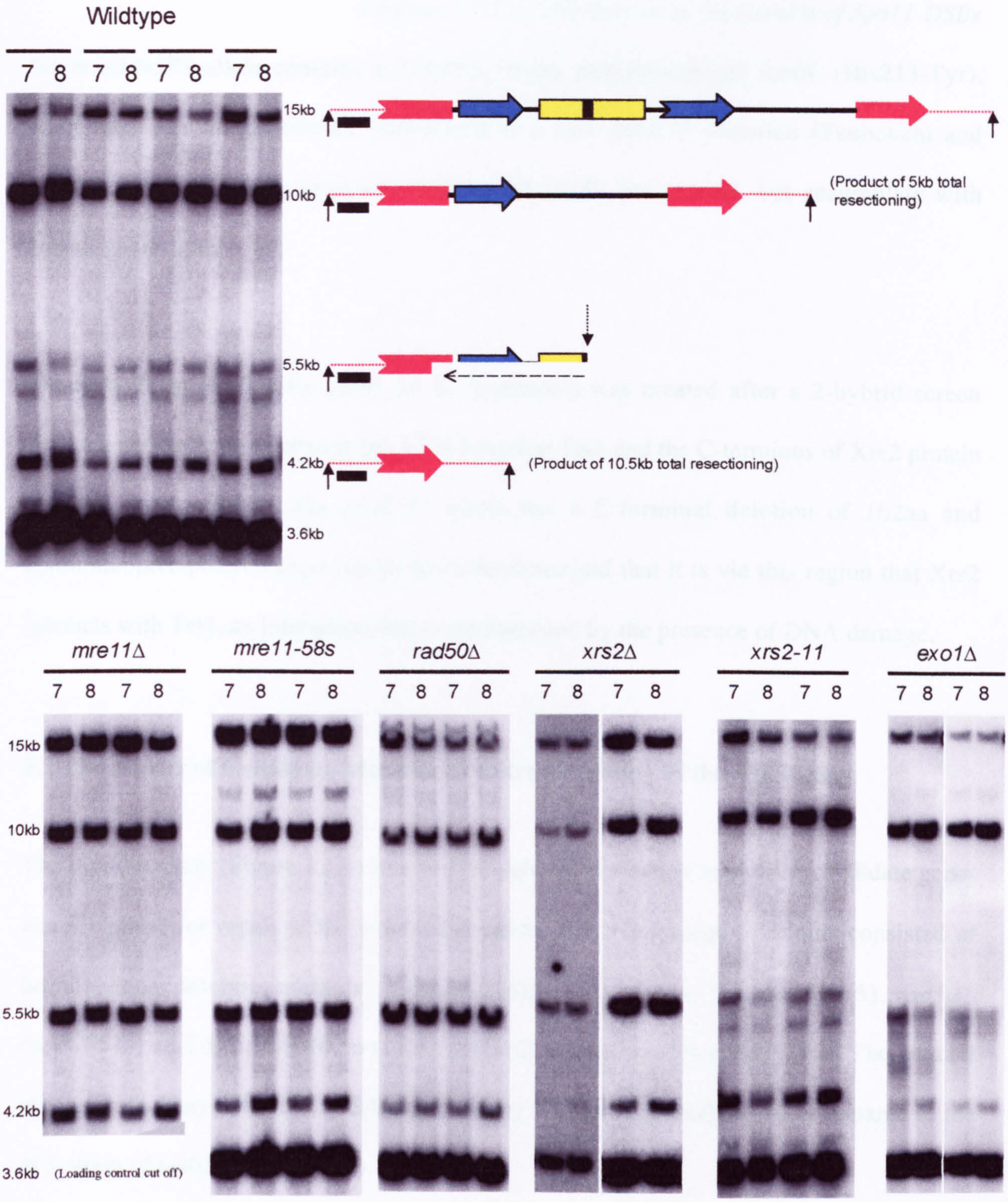

Figure 5.1: Southern Analysis of VDE-DSB Creation and Repair at the *arg4-VDE* allele: (Top panel): DNA extracted from WT *arg4-VDE TFP1::VDE* (dAG630) synchronous meiotic cultures, digested with *SpeI* (black arrows), and after fractionation and blotting, the DNA-membrane was hybridised with a probe specific to the upstream region of ADE2 (black box). (T=7 and 8hr of 4 WT meioses shown). 15kb band: uncut parental DNA, 10kb band: first deletion product, 5.5kb band(smeared): VDE-DSB, 4.2kb band: second deletion product, 3.6kb: homologous copy of *ade2*, (loading control). Smearing of the VDE-DSB DNA was caused by ssDNA molecules of progressively shorter length, due to resectioning at the VDE-DSB (dashed arrows). (Bottom panel): Southern analysis of DNA from synchronous meiotic cultures of *mre11Δ (*dAG1010), *mre11-58s (*dAG975), *rad50Δ* (dAG951), *xrs2Δ* (dAG946), *xrs2-11* (dAG1271) and *exo1Δ* (dAG1305) mutant strains. (Timepoints shown above gel images, data from n=3 experiments per strain).

An ***mre11-58S*** allele contains a mutation in the phosphoesterase motif, (His213-Tyr), which conveys similar mitotic phenotypes to a null *MRE11* mutation (Tsubouchi and Ogawa, 1998). Crucially in *mre11-58S*, Spo11-DSBs are created, but accumulate with unresected termini.

The ***xrs2-11*** allele (kindly gifted by K. Sugimoto) was created after a 2-hybrid screen detected an interaction between the ATM homolog Tel1 and the C-terminus of Xrs2 protein (Nakada et al., 2003). The *xrs2-11* allele has a C-terminal deletion of 162aa and coimmunoprecipitation experiments have demonstrated that it is via this region that Xrs2 interacts with Tel1, an interaction that is strengthened by the presence of DNA damage.

5.2 The impact of Candidate Mutations on Repair Ability of the VDE-DSB

The reporter assay (Figure 3.1.1) was used to determine whether any of the candidate genes were required for repair of the *arg4-VDE* allele. The experimental diploids consisted of homozygous deletion mutants: *mre11*Δ (dAG1010), *mre11-58s* (dAG975), *rad50*Δ (dAG951), *xrs2*Δ (dAG946), *xrs2-11* (dAG1271) and *exo1*Δ (dAG1305), The mutant strains were assayed for their SSA repair ability via southern analysis and compared to the WT strain (dAG630) (Figure 5.1).

Results

Figure 5.2a and Table 5.2 contain the data for the amount of VDE-chromatids cleaved in the WT and experimental diploid strains. As there was some variation in the amount of VDE-chromatid cleavage (Figure 5.2a), the amount of VDE-DSB repair calculated in the

experimental diploids was normalised to the amount of VDE-chromatids that had suffered a DSB (Figure 5.2b and Table 5.2). All of the candidate mutant strains exhibited a statistically significant defect in DSB repair of the VDE-DSB, with the exception of the *xrs2-11* strain (dAG1271).

5.3 An Assay to Compare Deletion Product Formation

The reporter assay was used to indicate whether any of the candidate genes influenced the regulation of VDE-DSB resectioning, by considering first and second deletion product formation. Cells that repaired the *arg4-VDE* allele by generating resection tracts that spanned 5kb would preferentially use the proximal *URA3* direct repeated sequences, thus creating first deletion product. While cells that repaired the VDE-DSB by generating 10.5kb resection tracts would preferentially use the distal *ade2* repeated sequences, thus creating second deletion product. The repair product ratio values for the experimental strains were determined via southern analysis (Figure 5.1). The ratio values were calculated as the amount of second deletion product, as a proportion of total deletion product formation at T=8hr, (Repair product ratio = secondΔ/(firstΔ + secondΔ). Consequently, the repair product ratio value was sensitive to changes in the proportions of 5kb and 10kb resection tract formation. An elevated ratio value, compared to the WT strain, would indicate a proportional increase in the amount of 10.5kb resection tracts.

Results

Figure 5.3a contains the amounts of first and second deletion products formed in WT and the mutant strains, as a proportion of VDE-chromatid DNA. It was then informative to calculate the repair product ratio values, (Figure 5.3b and Table 5.3). Significance testing

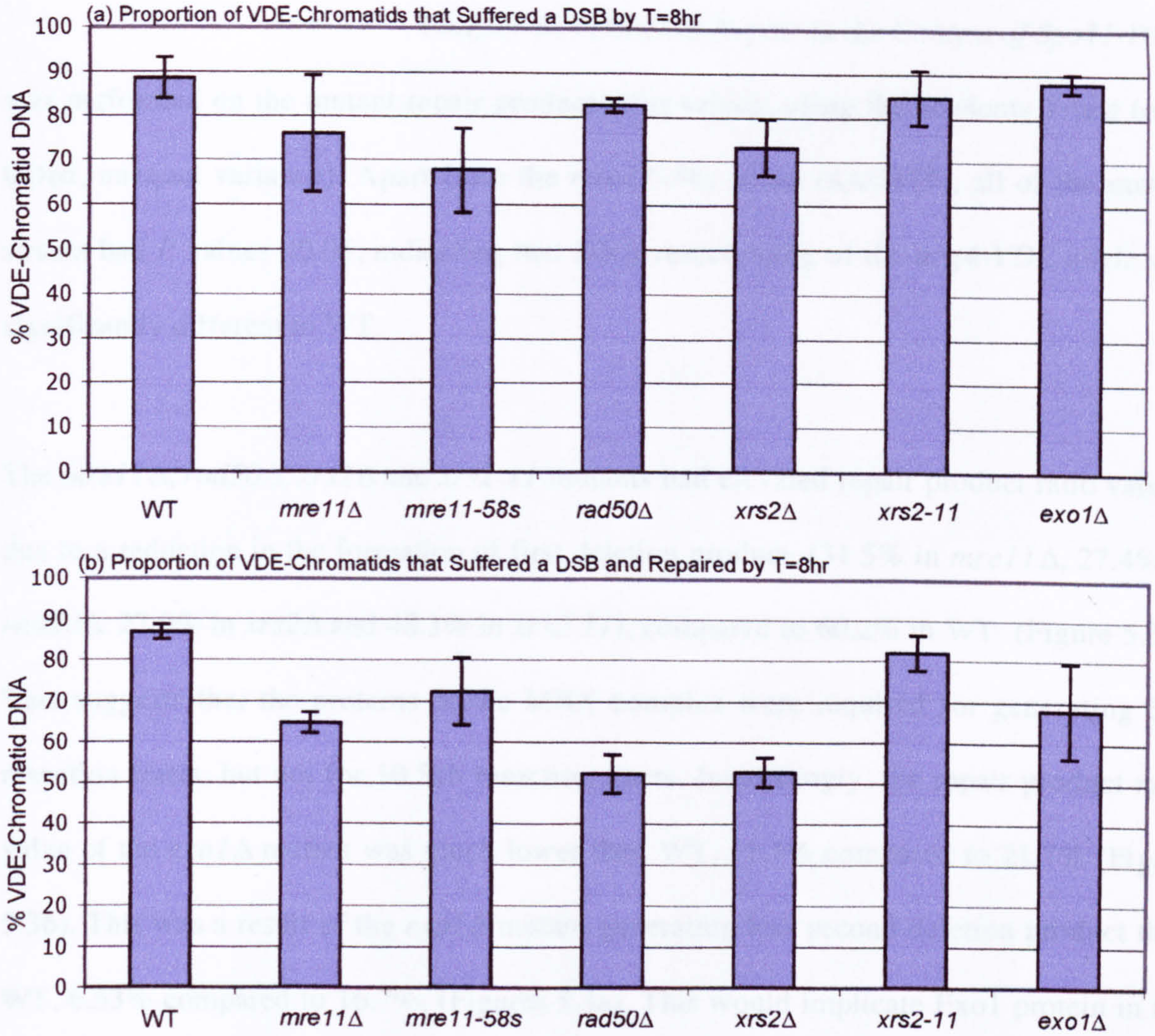

Table 5.2

	Broken VDE-Chromatids%	Repaired/Broken DNA%
WT	88.6	86.8
mre11Δ	76.0	64.7 (7.85E-06)
mre11-58s	67.8	72.3 (0.02)
rad50Δ	82.7	52.3 (0.02)
xrs2Δ	73.2	52.7 (1.25E-05)
xrs2-11	84.8	82.0 (0.06)
exo1Δ	88.0	68.0 (0.02)

Figure 5.2: Amount of SSA Repair at the *arg4-VDE* Allele. (a) Amount of VDE-chromatids that had suffered a DSB ('broken') at T=8hr in WT and mutant strains (See Figure 5.1 for strain information). Calculated as (total VDE-chromatid DNA)-(parental DNA). (b) Amount of repair at the *arg4-VDE* allele, as a proportion of broken VDE-chromatids. Calculated as (total deletion repair product)/(broken VDE-chromatids). All values expressed as percentage of total VDE-chromatid DNA. (Error bars display standard deviation). Table 5.2 contains tabulated data from (a) and (b). Numbers in parentheses are the associated *P* values, calculated using the Students T-test, (Section 2.11). The mutant values that differ significantly from WT, ($p<0.05$), are shaded. (Data from n=3 experiments per strain)

was performed on the mutant repair product ratio values, using the Students T-test (one-tailed, unequal variance). Apart from the *mre11-58s* strain (dAG975), all of the mutant strains had *P* values <0.05, indicating that DNA resectioning of the *arg4-VDE* allele was significantly different to WT.

The *mre11*Δ, *rad50*Δ, *xrs2*Δ and *xrs2-11* mutants had elevated repair product ratio values, due to a reduction in the formation of first deletion product, (31.5% in *mre11*Δ, 27.4% in *rad50*Δ, 27.0% in *xrs2*Δ and 48.3% in *xrs2-11*), compared to 60.2% in WT (Figure 5.3a). This suggests that the proteins of the MRX complex were required for generating 5kb resection tracts, but not for 10.5kb resection tracts. Interestingly, the repair product ratio value of the *exo1*Δ mutant was much lower than WT, 11.1% compared to 21.7% (Figure 5.3b). This was a result of the *exo1*Δ mutant generating less second deletion product than WT, 6.53% compared to 16.7%, (Figures 5.3a). This would implicate Exo1 protein in the generation of 10.5kb DSB resection tracts in the *ade2::arg4-VDE* assay.

5.4 Discussion

The influence of Spo11-DSB formation and processing on VDE-DSB repair and resection tract length were examined in this chapter.

Strains containing null mutations of the *MRE11*, *RAD50* and *XRS2* genes, were all compromised for VDE-DSB repair of the *arg4-VDE* allele, with each mutation conveying a significant reduction in the proportion of repaired VDE-chromatids at T=8hr (Figure 5.2b). The *mre11-58S* allele conveyed a less profound VDE-DSB repair defect, 72.3% of broken VDE-chromatids repaired in *mre11-58s*, compared to 64.7% in *mre11*Δ, and 86.8% in WT

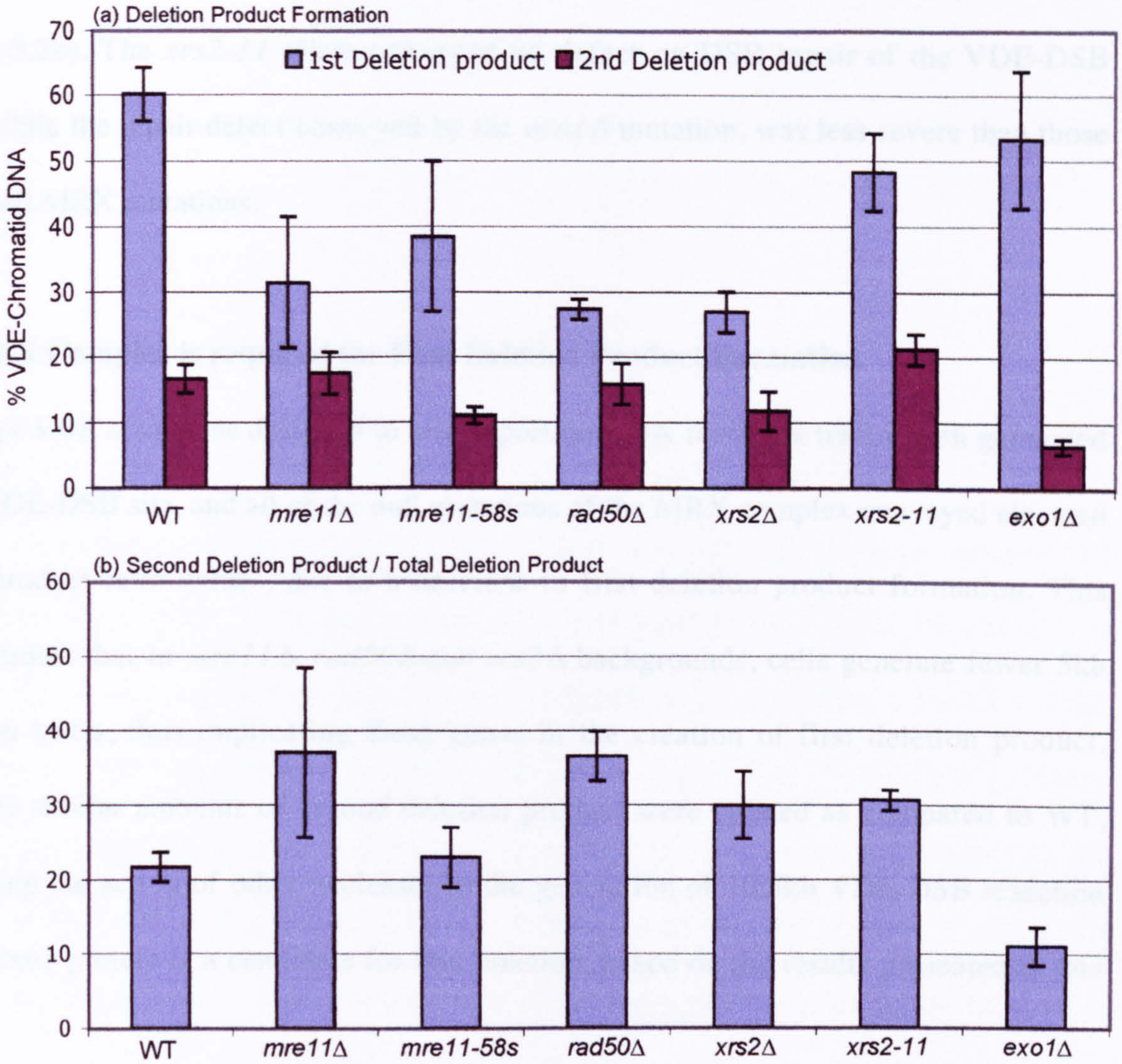

Table 5.3: Repair Product Ratio Values and their Associated Significances

	Repair Product Ratio(%)	P value (p<0.05)
wildtype	21.7	-
mre11Δ	37.1	0.04
mre11-58s	23.0	0.30
rad50Δ	36.6	0.03
xrs2Δ	30.0	0.01
xrs2-11	30.7	2.61E-04
exo1Δ	11.1	4.14E-04

Figure 5.3: Deletion Product Formation and Repair Product Ratio values in *arg4-VDE* assay at T=8hr (a) Amounts of first and second deletion product formation in WT and mutant strains, (expressed as a percentage of total VDE-chromatid DNA). (see Figure 5.1 for strain information). (b) Repair product ratio values, calculated as second deletion product as a proportion of total deletion product formation. (Error bars display standard deviation). Table 5.3 contains tabulated data from (b), and the associated *P* values (calculated using the Students T-test, Section 2.11). (Mutant ratio values significantly different to WT ($p<0.05$), shaded). (Data from n=3 experiments per strain)

(Figure 5.2b). The *xrs2-11* allele conveyed no defect on DSB repair of the VDE-DSB allele, while the repair defect conveyed by the *exo1*Δ mutation, was less severe than those of the null MRX mutations.

The MRX Complex is required for First Deletion Product Formation

The *arg4-VDE* assay was designed to also report on DNA resection tract length generated at the VDE-DSB site, and all of the null mutations of the MRX complex conveyed elevated repair product ratio values, due to a decrease in first deletion product formation. This demonstrates that in *mre11*Δ, *rad50*Δ and *xrs2*Δ backgrounds, cells generate fewer 5kb resection tracts, thus implicating these genes in the creation of first deletion product. However similar amounts of second deletion product were created as compared to WT, suggesting the action of other nucleases in the generation of 10.5kb VDE-DSB resection tracts. Exo1 protein is a candidate for this function, based on the results presented in this work.

Exo1 protein is required for the Formation of Second Deletion Product

Uniquely, the *exo1*Δ mutant generated less second deletion product than WT, a manifestation of reduced levels of 10.5kb resection tracts, (6.5% in *exo1*Δ and 16.7% in WT, Figure 5.3a). However, the *exo1*Δ mutant generated similar amounts of 5kb resection tracts to WT, demonstrating that Exo1 resectioning function was constrained to 10.5kb VDE-DSB resection tracts only. The demonstration that an *exo1*Δ mutation caused a defect in the generation of 10.5kb resection tracts at the *arg4-VDE* allele is in accord with a previous study on *EXO1*. In that HO-DSB mitotic assay, an *exo1*Δ mutation demonstrated a fourfold decrease in an ssDNA intermediate, resultant from extensive DNA resectioning

(5kb), at the *MAT* locus (Llorente and Symington, 2004). Like in this meiotic assay, similar amounts of shorter resection tracts were created, and a small delay in resectioning was reported in *exo1*Δ.

Exo1 and the Rate of VDE-DSB Resectioning

To expand on the *exo1*Δ results, DNA from full WT (dAG630) and *exo1*Δ (dAG1305) meiotic time courses was compared (Figure 5.4i(a)). By studying complete meioses, the kinetics of *arg4-VDE* allele repair and resection tract length could be examined. Graphically, it was demonstrated that the *exo1*Δ mutant accumulated far more VDE-DSB DNA than the WT strain, peaking at T=5hr, with 75.3% in *exo1*Δ and 35.9% in WT (Figure 5.4*ii*, yellow plot). The amount of DNA present in the VDE-DSB band is dependent on the amount of parental DNA that has suffered a VDE-DSB and on the amount of repair. To account for the effects of different VDE-DSB formation rate the amounts of VDE-DSB DNA created in *exo1*Δ and WT, were expressed as a proportion of residual parental DNA (Figure 5.4i(b)). The *exo1*Δ mutant accumulated four times more VDE-DSB DNA than WT at T=5hr. The idea that an *exo1*Δ mutation caused an accumulation of DSB-DNA, and a decrease in the formation of 10.5kb resection tracts, leads to the proposal that when Exo1 protein is involved in resection of the VDE-DSB, it creates long resection tracts. Further evidence to support this is the high visibility of the VDE-DSB band in the *exo1*Δ strain, caused by smearing (Figure 5.4aii). Smearing of the VDE-DSB band is due to the 5′-3′ DNA resectioning process, generating increasingly longer single stranded (ss)DNA molecules. Figure 5.4ii displays the signal intensities running through the WT and *exo1*Δ VDE-DSB bands at T=4hr, (normalised to the maximum signal). The wider span of the

(a) Southern Analysis of DSB Repair at the *arg4-VDE* allele

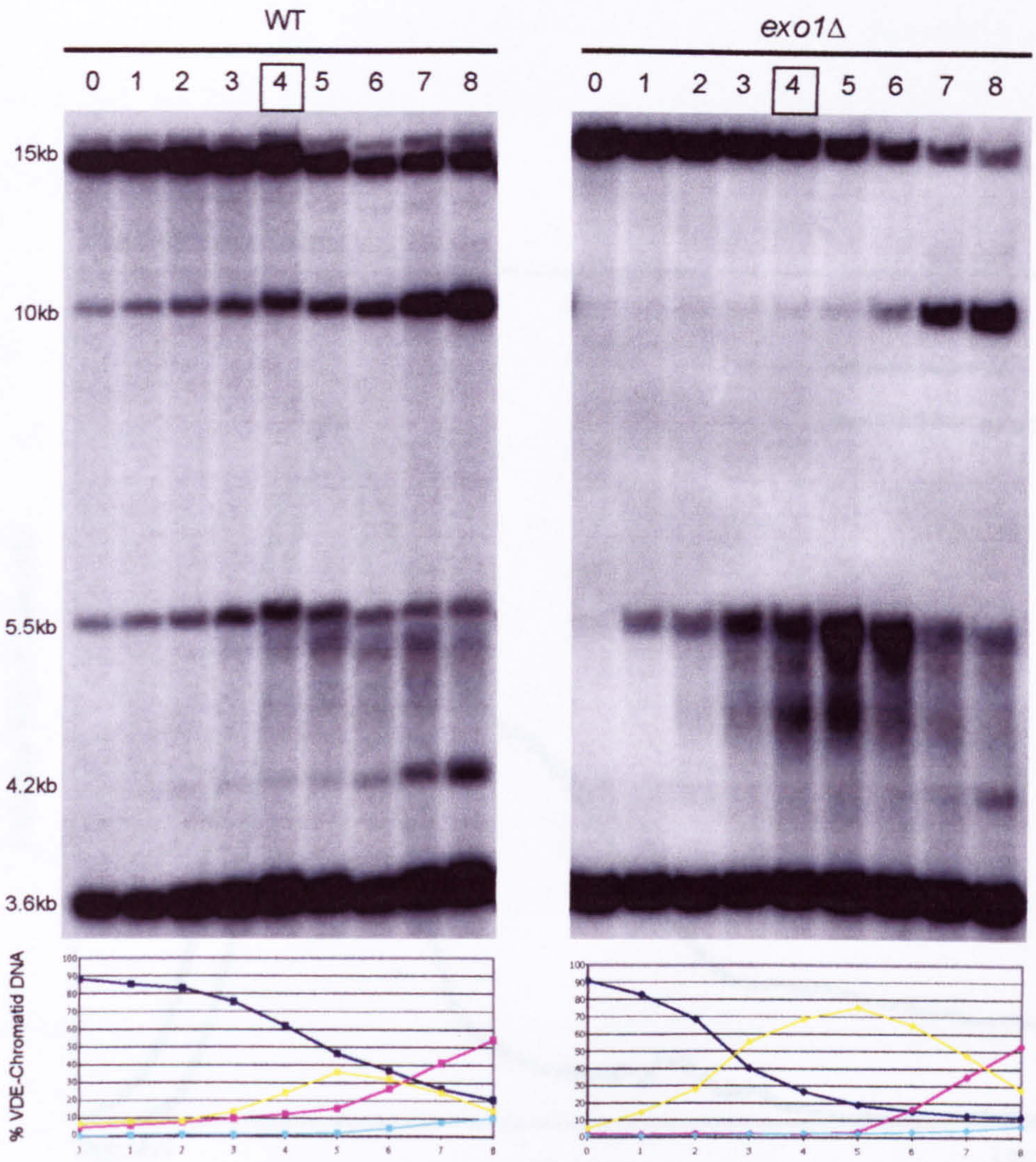

(b) VDE-DSB DNA as a Proportion of Residual Parental DNA

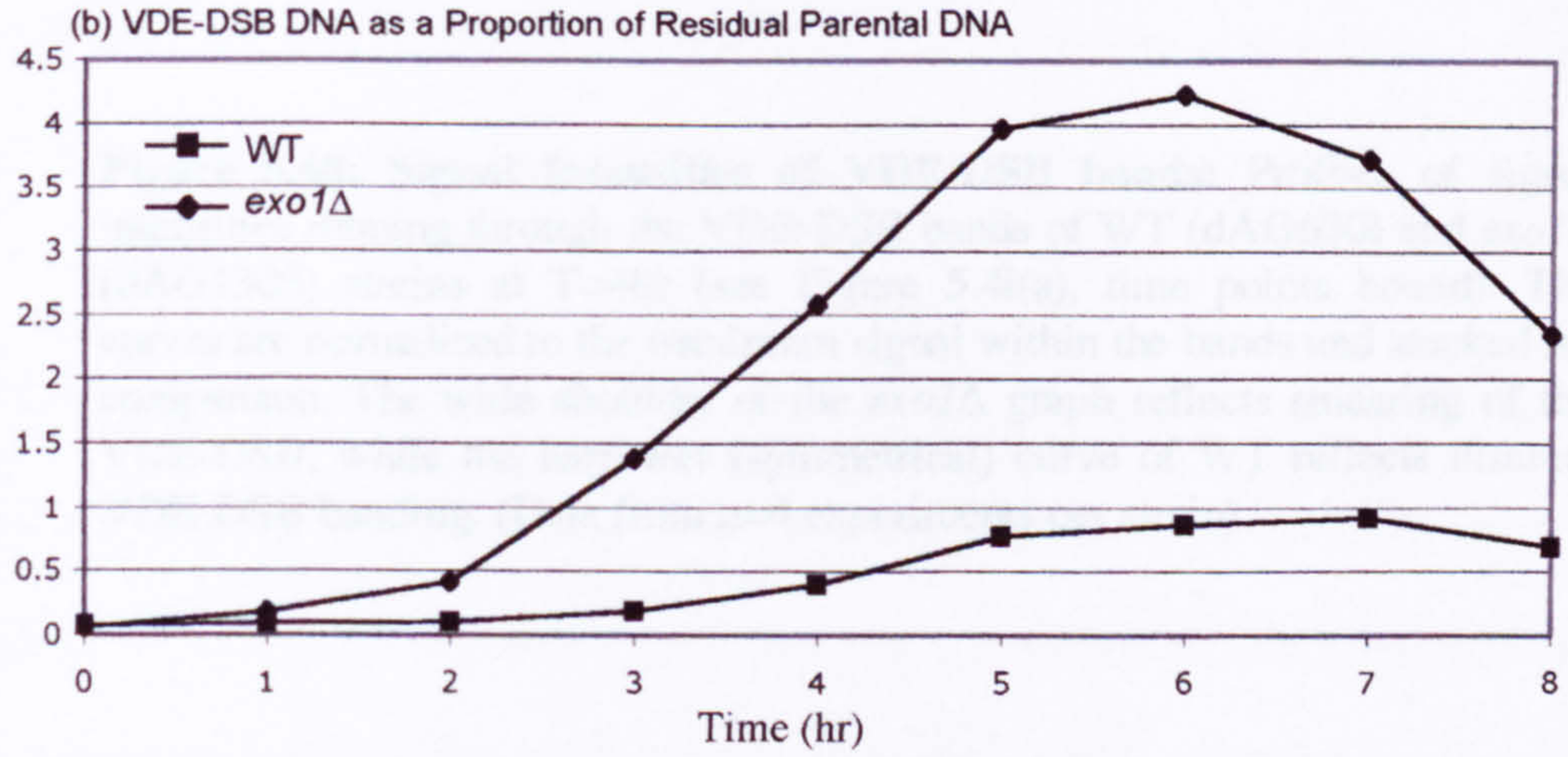

Figure 5.4i: Physical Analysis of DNA Repair Events at the *arg4–VDE* Allele (a) DNA extracted from WT (dAG630) and *exo1*Δ (dAG1305) strains and southern analysis performed (see Figure 5.1 for strain information). (Time points shown above gel images). Graphs below gels display DNA repair intermediates as a proportion of VDE-chromatid DNA: parental DNA (15kb band on gel, blue plot on graph), VDE-DSB DNA (5.5kb band, yellow plot), first deletion product (10kb band, pink plot) and second deletion product (4.2kb band, turquoise plot). (b) Accumulation of VDE-DSB DNA in WT and *exo1*Δ strains, (normalised to amount of residual parental DNA). (Data from n=3 experiments per strain)

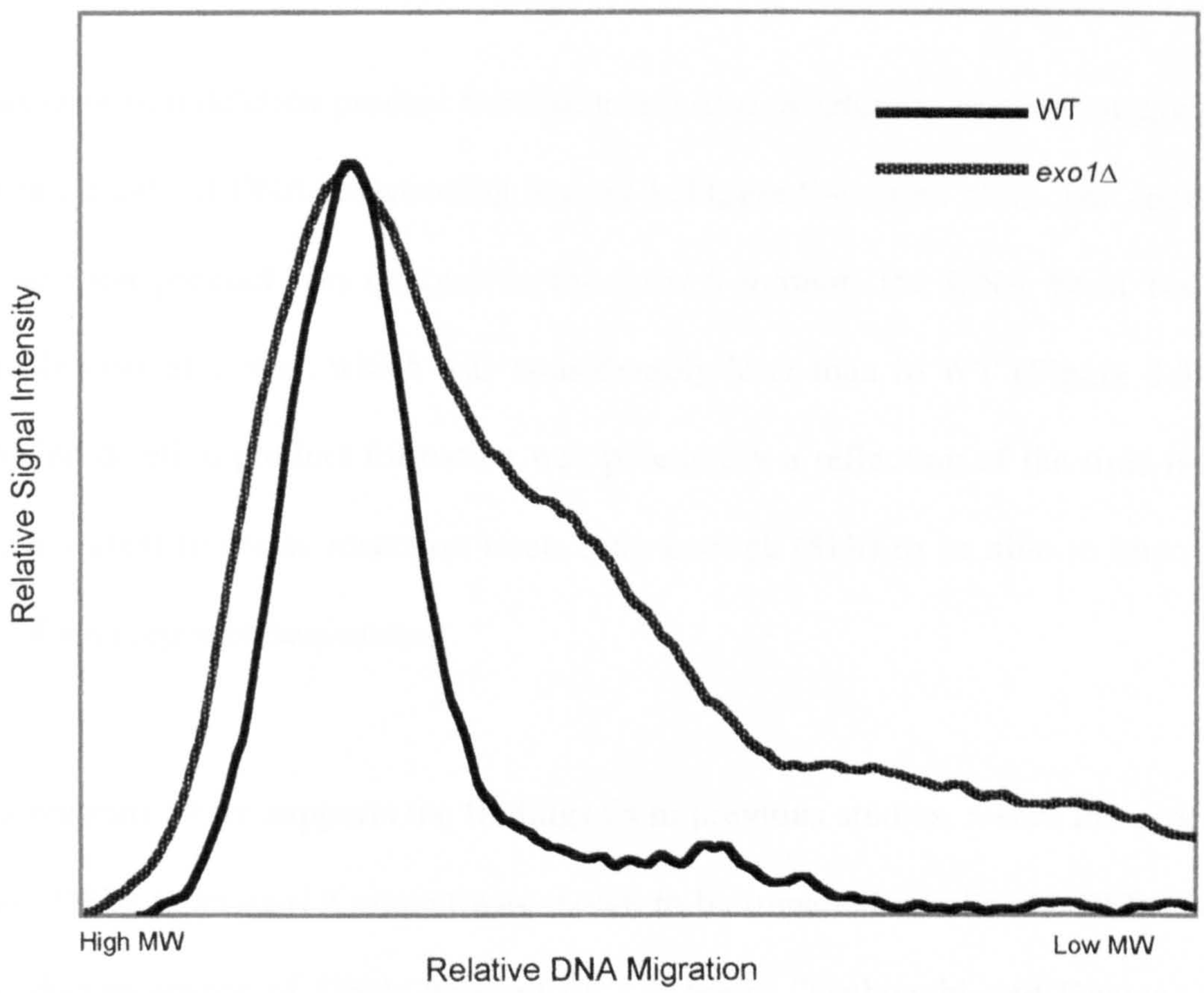

Figure 5.4ii: Signal Intensities of VDE-DSB bands: Profiles of signal intensities running through the VDE-DSB bands of WT (dAG630) and *exo1*Δ (dAG1305) strains at T=4hr (see Figure 5.4i(a), time points boxed). The curves are normalised to the maximum signal within the bands and stacked for comparison. The wide shoulder of the *exo1*Δ graph reflects smearing of the VDE-DSB, while the narrower (symmetrical) curve of WT reflects discrete VDE-DSB banding. (Data from n=4 experiments per strain)

*exo1*Δ curve reflects DSB smearing, while the more narrow WT curve results from a more discrete DSB band.

The kinetics of first deletion product formation was also of interest, as it was suggestive of a defect in the rate of DNA resectioning in *exo1*Δ (Figure 5.4*i*, pink plot). The appearance of first deletion product was delayed in the *exo1*Δ mutant, the DNA band becoming quantifiable only at T=6hr, which was considerably later than in WT (Figure 5.4*i*). The delay in first deletion product formation was potentially a reflection of the time taken by the *exo1*Δ mutant to create resection tracts long enough (5kb) to be able to uncover the proximal *URA3* repeated sequences.

The data presented here supports the findings from previous studies, where the processing of meiotic DSBs in an *exo1*Δ mutant was shown to be impaired at a Spo11-DSB hot spot, with the disappearance of DSBs delayed by 1-2 hours (Tsubouchi and Ogawa, 1998). Furthermore in a *dmc1*Δ mutant background, an *exo1*Δ mutation reduced the amount of excessive DNA resectioning, characteristic of these breaks(Bishop 1994)..

The *exo1*Δ mutation conveyed a weaker defect in VDE-DSB repair compared to the MRXΔ mutations, confirming that the Exo1 protein is not an essential exonuclease for DSB resectioning, but rather contributes to the process (probably in conjunction with other nucleases, for example Mre11/Rad27/Fen1)(Moreau, Morgan et al. 2001). Interestingly, the idea that Exo1 protein is required for the generation of 10.5kb resection tracts, fits in with the demonstration that in null mutations of the MRX complex, these resection tracts were still created.

The C-terminal of Xrs2 Protein is required for VDE-DSB Resectioning

There was a phenotypic difference in the amount of VDE-DSB repair in the truncated and null mutant alleles of *XRS2* (Figure 5.2b and Table 5.2). In *xrs2*Δ, the amount of VDE-DSB chromatids that had suffered and then repaired a VDE-DSB, was significantly reduced at T=8hr, (52.7%) while repair in the *xrs2-11* mutant was very similar to WT, (82.0% and 86.8%, respectively). As the C-terminal deletion of *XRS2* did not convey a defect in VDE-DSB repair, it is likely that this region of the protein is non-essential for SSA repair of a VDE-DSB. This result correlates with a previous study of an *xrs2-11* mutation, where it was demonstrated that the mutant allele did not convey sensitivity to DNA damaging agents in mitosis (Nakada et al., 2003). Furthermore, a recent meiotic study that examined the effects of a larger truncation at the C-terminal of Xrs2 protein (Δ190aa, *xrs2-664*) did not convey a defect in either DSB formation or recombination (Shima et al., 2005).

When the VDE-DSB reporter assay was used to examine DNA resection tract length, the *xrs2-11* mutant strain displayed the same phenotype as *xrs2*Δ. While there was more overall deletion repair in *xrs2-11* than in the null mutant (Figure 5.3a), both mutants had repair product ratio values of approximately 30%, which was significantly different from the WT value of 21.7% (Figure 5.3b and Table 5.3). This indicates that the C-terminal region of Xrs2 protein does influence VDE-DSB resectioning.

This idea contrasts with the previous findings of an *xrs2-11* study, where the mutant demonstrated WT levels of DNA resectioning, although that was in mitosis (Nakada et al., 2003). This implies that the C-terminal region of Xrs2 protein may function specifically in VDE-DSB resectioning in meiosis. One explanation could be that it is the Xrs2-Tel1

protein-protein interaction that influences resection tract length at VDE-DSBs. Therefore, it is predicted that the *xrs2-664* mutant allele (Shima et al., 2005), would share the same DSB resectioning phenotype as *xrs2-11*, as Tel1 interaction would likewise be prevented. (See Chapter 7 for discussion on Tel1 and xrs2-11 proteins).

Chapter 6

A Genetic Screen for Mutations that Affect Regulation of DSB Resectioning

6.1 Introduction

A qualitative genetic screen was developed in order to identify novel mutations that compromise VDE-DSB repair in *S. cerevisiae* (Section 2.12.2 and Figure 2.12.2). Through this screening process, and with the availability of new equipment, a quantitative genetic screen was then developed (Section 2.12.3). The ability of the *arg4-VDE* assay to report on resection tract length was used to assess the critical process of regulation of DNA resectioning. Solid and liquid media were used to report on adenine prototrophy created at the *ade2::arg4-VDE* allele, as conveyed by randomly mutagenised plasmid-borne *XRS2* alleles. The rationale for comparing adenine prototrophy in wildtype (WT) and mutant strains following VDE-DSB formation and repair was that this permitted the measurement of resection tracts of approximately 10.5kb (total length). Consequently, mutants that were found to generate significantly higher amounts of 10.5kb resection tracts were considered to be deficient in the regulation of DSB resectioning. This loss of regulation could be a result of a failure to recognise the proximal *URA3* sequences as being homologous, and/or by a failure to regulate the rate or degree of DNA resectioning, beyond the minimum 5kb required. Whichever the cause, these mutants would be compromised for DSB repair, increasing their risk of genomic instability and loss of heterozygosity. Initially, three candidate genes were considered for the genetic screen; *MRE11*, *RAD50* and *XRS2* (MRX). Most progress was made on mutagenising *XRS2*, therefore most of the data presented here are from these experiments. Null mutants of *MRE11*, *RAD50* and *XRS2* do not form Spo11-

DSBs, therefore are sporulation deficient. The MRX complex has been specifically implicated in the regulation of resectioning at Spo11-DSBs.

6.2 Rescue of *xrs2*Δ and *rad50*Δ Mutants by Plasmid-Borne *XRS2* and *RAD50*

Expression plasmids containing *XRS2* (pAG73, *p.XRS2::hph*MX*)* and *RAD50* (pAG75, *p.RAD50::nat*MX) alleles, were episomally transformed into *xrs2*Δ and *rad50*Δ diploid strains, (dAG946 and dAG951, respectively). Transformant growth was shifted to K-Ac medium and meiosis-competency was assessed by tetrad dissection. The *xrs2*Δ strain transformed with *p.XRS2::hph*MX had an average spore viability of 82.5%, while the *rad50*Δ strain transformed with *p.RAD50::nat*MX had a spore viability of 85.5%. Therefore, plasmid-borne *XRS2* and *RAD50* alleles were able to rescue the non-sporulation phenotype of *xrs2*Δ and *rad50*Δ mutants. The dissection plates were replica plated to selective media, and there was 14% plasmid loss in the *p.XRS2::hph*MX containing spores and 4.5% in the *p.RAD50::nat*MX containing spores.

6.3 Expression of Plasmid-Borne Drug Resistance in *E.coli*

The genetic screen involved the amplification of plasmid DNA rescued from *S. cerevisiae* transformants, Therefore plasmid selection had to be maintained through bacterial growth. Bacterial transformations with pAG73 (*p.XRS2::hph*MX) yielded cells that were growth competent on 2TY plus hygromycin B medium, while transformation with pAG75 (*p.RAD50::nat*MX) yielded cells growth competent on 2TY plus nourseothricin. Therefore the drug resistance marker genes of *p.XRS2::hph*MX and *p.RAD50::nat*MX plasmids were expressed in *E.coli* cells.

6.4 Transformant Screening

An approximately equal number of *xrs2Δ/xrs2Δ NDT80/NDT80* (dAG946) and *xrs2Δ/xrs2Δ ndt80/ndt80* (dAG1093) strains were episomally transformed with mutagenised *p.xrs2::hphMX* plasmids. In total, approximately 1,500 *XRS2* transformants were tested via the solid medium screen, and 8,500 transformants tested via the liquid medium screen. From the solid medium screen, one transformant emerged from the retesting process as being of possible interest, and five transformants from the liquid medium screen.

6.4.1 Plasmid Sequencing and Retransformation

The plasmids recovered from the six transformants, plus WT (pAG73) were sequenced, (sequencing primers in Table 2.4). The WT *p.XRS2::hphMX* plasmid was found to contain a number of point mutations in the *XRS2* open reading frame (ORF), and the sequences from the recovered plasmids were not useful. Meanwhile the six transformants from the solid and liquid media screens were tetrad dissected for adenine prototrophy, and for every transformant examined, approximately 100% of the VDE-chromatid containing spores were Ade+. Plasmids recovered from these strains and retransformed into *xrs2Δ* strains did not however yield the same phenotype. The original transformants were re-examined and found to be Ade+ prior to meiosis. The screen was stopped here.

6.6 Discussion

Two genetic screens for novel mutants that are defective in the regulation of VDE-DSB repair were established in this chapter.

Discovering that the*XRS2* ORF of expression plasmid *p.XRS2::hphMX* (pAG73) contained a number of mutations, and having screened 10,000 transformants, with no interesting transformants identified, the genetic screen was abandoned. In order to screen for novel mutations in a gene, the original ORF must contain the consensus sequence for that gene. However, the version of *XRS2* contained on the expression plasmid *p.XRS2::hphMX*, was able to rescue the sporulation deficiency of an *xrs2*Δ mutant (82.5%).

Chapter 7

General Discussion

Meiosis is an essential process for sexual reproduction, and it comprises of one round of DNA synthesis followed by two successive nuclear divisions. The first meiotic division (MI) is a reductional segregation of nonsister chromatids (homologous chromosomes), and the second division is an equational segregation of sister chromatids. Recombination between homologous chromosomes is initiated at high levels by DNA double strand breaks (DSBs), created by Spo11 protein, and repair of these breaks is essential for the production of interhomologue connections (chiasmata; observed genetically as crossovers). These connections serve as a platform for genetic recombination and to promote accurate homologue disjunction at MI. Specific mechanisms are in place to ensure that meiotic DSB repair is directed towards the homologue as repair template, and the components of these mechanisms were examined in a DSB assay where interhomologue repair was precluded. In meiosis, the regulation of resectioning is critical to repair outcome, and this assay was designed to measure two deletion products arising from DSB resectioning repair.

In Chapter 3, a meiotic repair assay was created that did not require Spo11 protein as a DSB catalyst, and was designed to repair using homologous sequences that flanked the DSB site. In Chapters 4 and 5, candidate genes were examined for their influences over single-stranded annealing (SSA) repair and resection tract length. Finally, in Chapter 6 a genetic screen was performed to search for novel mutations that affect the regulation of resectioning.

Modifications to Flanking Sequences Affects Resection Tract Length

SSA repair preferentially utilises the nearest set of available repeated homologies to the DSB site (Sugawara and Haber 1992), and this was confirmed in Chapter 3. When the proximal flanking sequences became inverted, a majority of repair was switched to the distal repeated sequences (Table 3.2.6a and Figure 3.3.1c). However, there was some disparity between the genetic and southern analysis data, particularly in terms of the amount of residual parental DNA in the genetic experiments. One explanation was that VDE-endonuclease was failing to cut 100% of the *arg4::VDE* chromatids, or alternatively, a proportion of the VDE-DSBs created were repaired by nonhomologous endjoining (NHEJ). In order to discount NHEJ as a potential repair pathway, null mutants of *KU70* and *KU80* could be utilised in the assay.

Sites of Excess single-stranded (ss)DNA May Sequester Repair Proteins

The genetic requirements for SSA repair of the *ade2::arg4::VDE* allele was examined in Chapter 4, and it was discovered that SSA annealing repair was profoundly affected in a *dmc1*Δ background. One explanation is that the accumulation of resected Spo11-DSBs, characteristic of *dmc1*Δ cells, sequesters the proteins required for homologous recombination between direct flanking homologies, limiting their availability at the single VDE-DSB site (Figure 4.4*i*). This is an idea previously suggested by Neale *et al*, (2002).

A Role in Repair Template Choice for Sae2 Protein

Cells mutated for *SAE2* were found to be defective in VDE-DSB repair (Figure 4.2b), created fewer resection tracts that spanned 5kb (Figure 4.3a), and were delayed for VDE-DSB turnover (Figure 4.4*ii*). These results indicate that Sae2 protein is required early in the

DSB resectioning process, which suggests a possible role in the promotion of interchromosomal repair. This would be an additional role for Sae2 protein, downstream of Spo11 protein removal at meiotic DSB sites. In this reporter assay, where no homologue was available for interchromosomal repair, the delay in resectioning was resolved, followed by wildtype (WT) levels of resectioning (Figure 4.3a, second deletion product). In a parallel VDE-DSB assay, where both interchromosomal and intrachromosomal repair were possible, the turnover of VDE-DSBs was also impeded and less deletion repair occurred in a *sae2*Δ background (M.J.N and A.S.H.G, Unpub.).

Mek1 Protein Negatively Regulates VDE-DSB Resectioning to Influence Repair Partner Choice

Recent studies of Mek1 protein have implicated it in the push towards interhomologue repair, by creating a block to intersister repair (Wan, de los Santos et al. 2004; Niu, Wan et al. 2005). In Chapter 4, the influence of resection tract length on repair template choice was examined and interestingly, a *mek1*Δ mutation caused an increase in the number of resection tracts that spanned 10.5kb (Figure 4.3a). This lead to the suggestion that Mek1 protein negatively regulates VDE-DSB resectioning, and it is this action that both minimises the possibility of exposing flanking homologies, and improves the chances of a homologue being used as a repair template in meiosis. Deletion of *MEK1* has been demonstrated to reduce the steady state levels of Spo11-DSBs, (Leem and Ogawa 1992; Xu, Weiner et al. 1997)(this study, data not shown), which may indeed be a reflection of increased resectioning in a *mek1*Δ background. As outlined in Chapter 4, this proposed mode of action does not preclude a role for Mek1 in blocking intersister repair, however both mechanisms may contribute in the push towards interhomologue repair.

The fact that *MEK1* was epistatic to *SAE2*, in the repair assay (Figure 4.2b), places Mek1 protein at an early stage of regulation of VDE-DSB repair.

In Chapter 5, genes known to be involved in the formation and processing of Spo11-DSBs were studied. As expected, null mutations of *MRE11*, *RAD50* and *XRS2* (MRX) were demonstrated to reduce repair of the VDE-DSB (Figure 5.2b), and were also impaired for resectioning that spanned 5kb (Figure 5.3a, first deletion product).

Exo1 Protein is required to Create Longer Resection Tracts

A null mutation of *EXO1* was found to cause a decrease in second deletion product formation (Figure 5.3a), implicating Exo1 protein in the generation of 10.5kb resection tracts. Indeed, Exo1 protein may be the redundant nuclease that creates these longer resection tracts in the absence of components of the MRX complex. Furthermore, the rate of resectioning in an *exo1*Δ background appeared to be retarded (Figure 5.4*i* and Figure 5.4*ii*). The next logical experiment would be to examine VDE-DSB repair in a double *mre11*Δ *exo1*Δ mutant, where it would be predicted that little/no deletion repair would occur.

Requirement of Tel1-Xrs2 Protein Interaction for DSB Repair Response

Chapter 5 examined VDE-DSB repair in a truncated allele of *XRS2*, (*xrs2-11*, C-terminal Δ162aa), and it is via this region that Xrs2 protein interacts with the ATM homologue, Tel1 (Morrow, Tagle et al. 1995; Mallory and Petes 2000; Nakada, Matsumoto et al. 2003). Therefore, the *xrs2-11* mutant was used to test a hypothesis about Tel1 protein that has emerged from preliminary experiments in the laboratory. Initial studies have demonstrated

(a) Southern Analysis of DSB Repair at the *arg4-VDE* allele

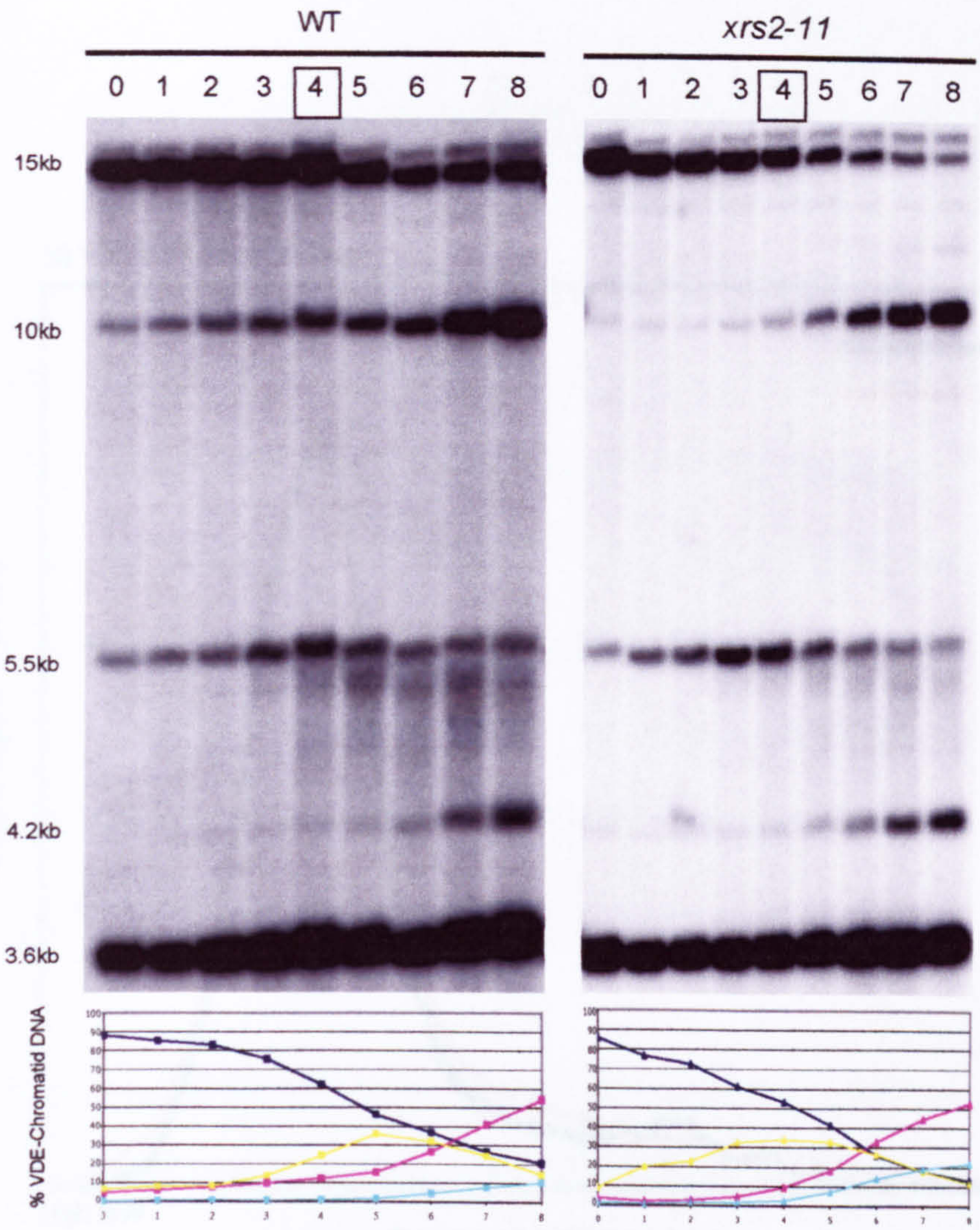

(b) VDE-DSB DNA as a Proportion of Residual Parental DNA

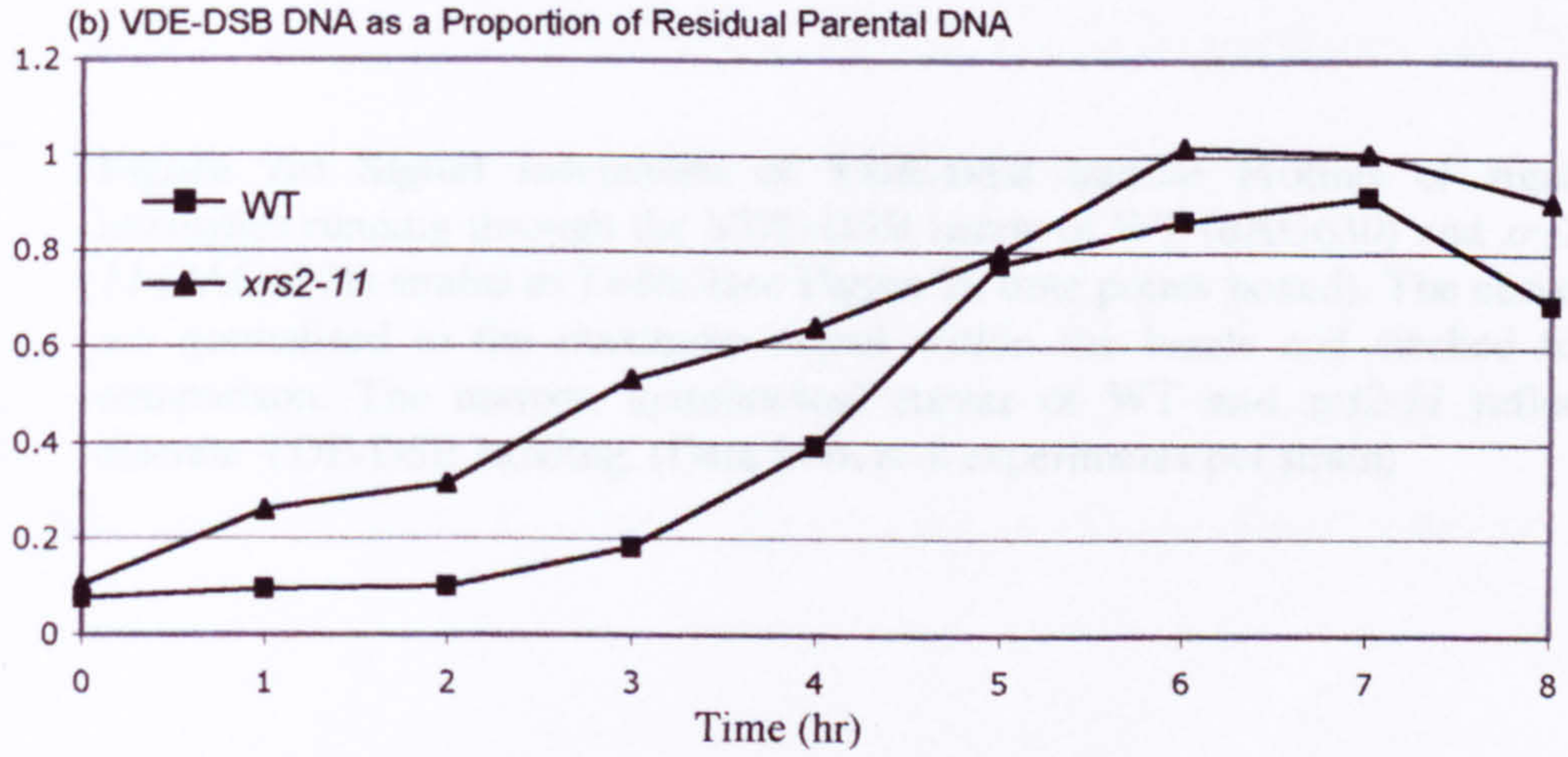

Figure 7*i*: Physical analysis of DNA repair events at the *arg4–VDE* allele (a) DNA extracted from WT (dAG630) and *xrs2-11* (dAG1271) strains and southern analysis performed (see Figure 5.1). (Time points shown above gel images). Graphs below gels, display DNA repair intermediates as a proportion of VDE-chromatid DNA: parental DNA (15kb band on gel, blue plot on graph), VDE-DSB DNA (5.5kb band, yellow plot), first deletion product (10kb band, pink plot) and second deletion product (4.2kb band, turquoise plot). (b) Accumulation of VDE-DSB DNA in WT and *xrs2-11* strains, (normalised to amount of residual parental DNA). (Data from n=4 experiments per strain)

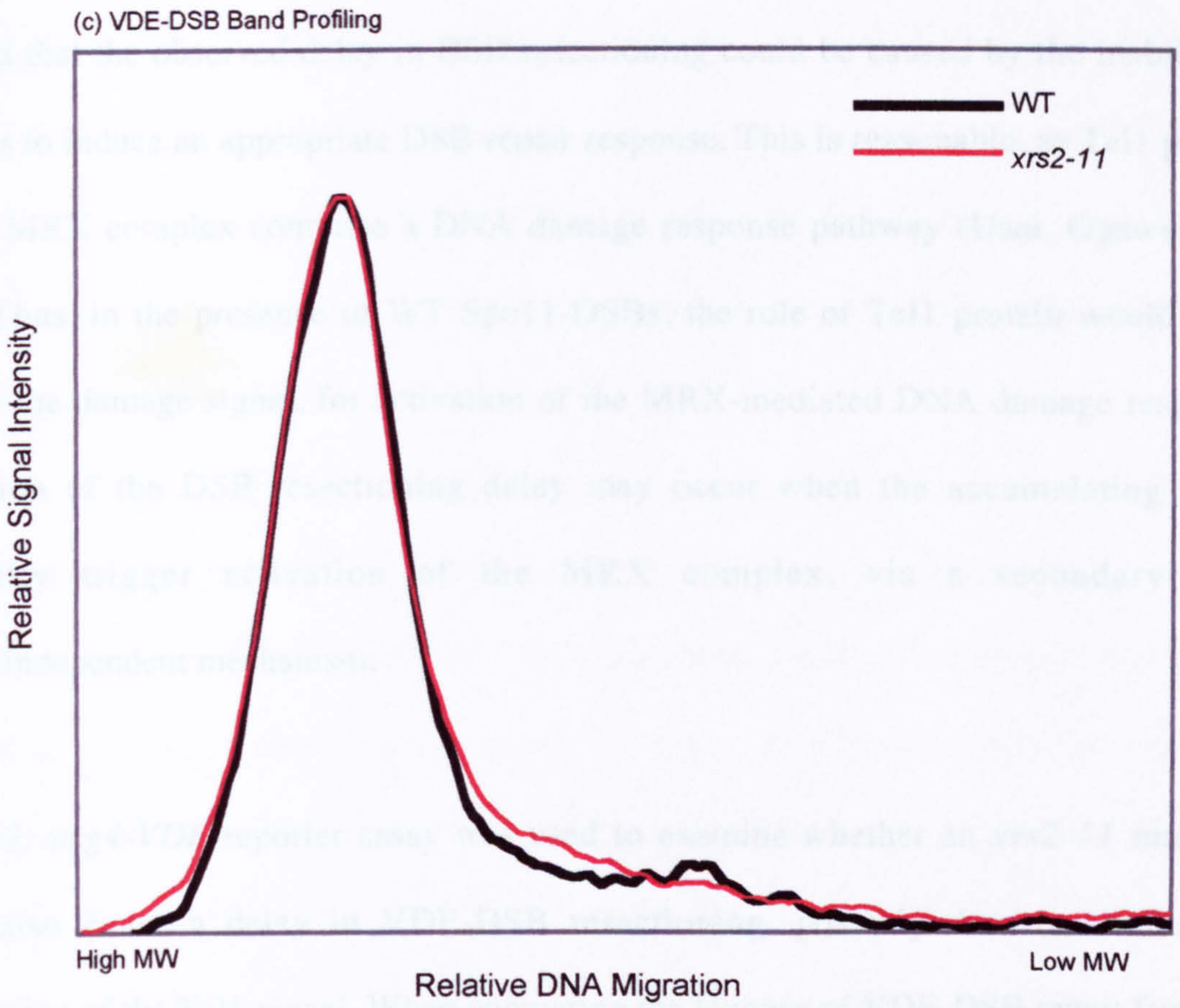

Figure 7*ii*: Signal Intensities of VDE-DSB bands: Profiles of signal intensities running through the VDE-DSB bands of WT (dAG630) and *xrs2-11* (dAG1271) strains at T=4hr (see Figure 7*i*, time points boxed). The curves are normalised to the maximum signal within the bands and stacked for comparison. The narrow, symmetrical curves of WT and *xrs2-11* reflect discrete VDE-DSB banding. (Data from n=4 experiments per strain)

that a partial deletion of *TEL1* causes a delay in DSB resectioning at both Spo11- and VDE-induced DSBs, prior to WT levels of repair (M.J.N and A.S.H.G Unpub.). It was surmised that the observed delay in DSB resectioning could be caused by the inability of *tel1* cells to induce an appropriate DSB repair response. This is reasonable, as Tel1 protein and the MRX complex comprise a DNA damage response pathway (Usui, Ogawa et al. 2001). Thus, in the presence of WT Spo11-DSBs, the role of Tel1 protein would be to transmit the damage signal, for activation of the MRX-mediated DNA damage response. Resolution of the DSB resectioning delay may occur when the accumulating DSBs eventually trigger activation of the MRX complex, via a secondary Tel1 protein–independent mechanism.

The *ade2::arg4-VDE* reporter assay was used to examine whether an *xrs2-11* mutation would also cause a delay in VDE-DSB resectioning, possibly due to a failure of transmission of the Tel1-signal. When comparing the kinetics of VDE-DSB repair from full WT and *xrs2-11* meiotic time courses, there was a transient accumulation of VDE-DSB DNA in the *xrs2-11* mutant, up to T=5hr (Figure 7*i*(a), yellow plot). When normalised to the amount of residual parental DNA, there was a greater than two-fold increase in VDE-DSB DNA in *xrs2-11* compared to WT, at T=3hr (Figure 7*i*(b)). Figure 5.2b demonstrates that by T=8hr, repair of the VDE-DSB in the *xrs2-11* mutant has been restored to a WT level.

The phenotype observed in *xrs2-11* suggests a delay in DSB resectioning at the VDE-DSB site, which concurs with the previous *tel1* study (M.J.N and A.S.H.G Unpub.). This suggests that it is not the presence of Tel1 protein at the VDE-DSB site *per se*, that

generates the DNA damage response, but rather the specific protein interaction between Tel1 and Xrs2. It is expected that DSB resectioning at Spo11-DSB sites would be similarly delayed in an *xrs2-11* mutant, due to the mutual requirements of Spo11- and VDE-DSBs on the Tel1-Xrs2 interaction for the DNA damage response. (Figure 7*ii* displays the signal intensities running through the WT and *xrs2-11* VDE-DSB bands at T=4hr, (normalised to the maximum signal). Despite the delay in VDE-DSB resectioning in *xrs2-11*, the banding profile remains almost identical to WT).

When *XRS2* was examined in a genetic screen for mutations that affect the regulation of resectioning, (Chapter 6), no novel mutants were identified. The human (h)*NBS1* gene is mutated in the human chromosomal instability disorder, Nijmegen breakage syndrome (NBS), however no resectioning phenotypes pertaining to a loss of regulation of DSB repair were identified in random *xrs2* mutants. NBS is caused by a truncated allele, and one possibility is that the method of mutagenesis used in this study did not provide a wide enough spectrum of mutations in *XRS2* (base transitions). Therefore, a different method of mutagenesis could be employed if this screen was to be repeated, for example library mutagenesis by PCR (reviewed in (Ling and Robinson 1997)).

Bibliography

Alani, E., Padmore, R., and Kleckner, N. (1990). Analysis of wild-type and *rad50* mutants of yeast suggests an intimate relationship between meiotic chromosome synapsis and recombination. *Cell 61*, 419-436.

Allers, T., and Lichten, M. (2000). A method for preparing genomic DNA that restrains branch migration of Holliday junctions. *Nucleic Acids Res 28*.

Allers, T., and Lichten, M. (2001). Differential timing and control of noncrossover and crossover recombination during meiosis. *Cell 106*, 47-57.

Arbel, A., Zenvirth, D., and Simchen, G. (1999). Sister chromatid-based DNA repair is mediated by *RAD54*, not by *DMC1* or *TID1*. *Embo J 18*, 2648-2658.

Baudat, F., and Nicolas, A. (1997). Clustering of meiotic double-strand breaks on yeast chromosome III. *Proc Natl Acad Sci U S A 94*, 5213-5218.

Bergerat, A., de Massy, B., Gadelle, D., Varoutas, P. C., Nicolas, A., and Forterre, P. (1997). An atypical topoisomerase II from *Archaea* with implications for meiotic recombination. *Nature 386*, 414-417.

Bishop, D. K., Park, D., Xu, L., and Kleckner, N. (1992). *DMC1*: a meiosis-specific yeast homolog of *E. coli RecA* required for recombination, synaptonemal complex formation, and cell cycle progression. *Cell 69*, 439-456.

Bishop, D. K. (1994). "RecA homologs Dmc1 and Rad51 interact to form multiple nuclear complexes prior to meiotic chromosome synapsis." *Cell 79*(6): 1081-92.

Bremer, M. C., Gimble, F. S., Thorner, J., and Smith, C. L. (1992). VDE endonuclease cleaves *Saccharomyces cerevisiae* genomic DNA at a single site: physical mapping of the *VMA1* gene. *Nucleic Acids Res 20*, 5484.

Bressan, D. A., Baxter, B. K., and Petrini, J. H. (1999). The Mre11-Rad50-Xrs2 protein complex facilitates homologous recombination-based double-strand break repair in *Saccharomyces cerevisiae*. *Molecular and Cellular Biology 19*, 7681-7687.

Busby, S., Irani, M., and Crombrugghe, B. (1982). Isolation of mutant promoters in the *Escherichia coli* galactose operon using local mutagenesis on cloned DNA fragments. *J Mol Biol 154*, 197-209.

Cao, L., Alani, E., and Kleckner, N. (1990). A pathway for generation and processing of double-strand breaks during meiotic recombination in *S. cerevisiae*. *Cell 61*, 1089-1101.

Cha, R. S., Weiner, B. M., Keeney, S., Dekker, J., and Kleckner, N. (2000). Progression of meiotic DNA replication is modulated by interchromosomal interaction proteins, negatively by Spo11p and positively by Rec8p. *Genes Dev 14*, 493-503.

Clerici, M., Mantiero, D., Lucchini, G., and Longhese, M. P. (2005). The *Saccharomyces cerevisiae* Sae2 protein promotes resection and bridging of double strand break ends. *J Biol Chem 280*, 38631-38638.

Collins, I., and Newlon, C. S. (1994). Meiosis-specific formation of joint DNA molecules containing sequences from homologous chromosomes. *Cell 76*, 65-75.

Cromie, G. A., Connelly, J. C., and Leach, D. R. (2001). Recombination at double-strand breaks and DNA ends: conserved mechanisms from phage to humans. *Mol Cell 8*, 1163-1174.

D'Amours, D., and Jackson, S. P. (2002). The Mre11 complex: at the crossroads of DNA repair and checkpoint signalling. *Nat Rev Mol Cell Biol 3*, 317-327.

Davis, A. P., and Symington, L. S. (2001). The yeast recombinational repair protein Rad59 interacts with Rad52 and stimulates single-strand annealing. *Genetics 159*, 515-525.

Fan, Q., Xu, F., and Petes, T. D. (1995). Meiosis-specific double-strand DNA breaks at the *HIS4* recombination hot spot in the yeast *Saccharomyces cerevisiae*: control in *cis* and *trans*. *Mol Cell Biol 15*, 1679-1688.

Fogel, S., and Hurst, D. D. (1967). Meiotic gene conversion in yeast tetrads and the theory of recombination. *Genetics 57*, 455-481.

Fukuda, T., Nogami, S., and Ohya, Y. (2003). VDE-initiated intein homing in *Saccharomyces cerevisiae* proceeds in a meiotic recombination-like manner. *Genes Cells 8*, 587-602.

Furuse, M., Nagase, Y., Tsubouchi, H., Murakami-Murofushi, K., Shibata, T., and Ohta, K. (1998). Distinct roles of two separable *in vitro* activities of yeast Mre11 in mitotic and meiotic recombination. *Embo J 17*, 6412-6425.

Gietz, R. D., Schiestl, R. H., Willems, A. R., and Woods, R. A. (1995). Studies on the transformation of intact yeast cells by the LiAc/SS-DNA/PEG procedure. *Yeast 11*, 355-360.

Gilbertson, L. A., and Stahl, F. W. (1996). A test of the double-strand break repair model for meiotic recombination in *Saccharomyces cerevisiae*. *Genetics 144*, 27-41.

Gimble, F. S., and Thorner, J. (1992). Homing of a DNA endonuclease gene by meiotic gene conversion in *Saccharomyces cerevisiae*. *Nature 357*, 301-306.

Gimble, F. S., and Thorner, J. (1993). Purification and characterization of VDE, a site-specific endonuclease from the yeast *Saccharomyces cerevisiae*. *J Biol Chem 268*, 21844-21853.

Goldstein, A. L., and McCusker, J. H. (1999). Three new dominant drug resistance cassettes for gene disruption in *Saccharomyces cerevisiae*. *Yeast 15*, 1541-1553.

Goyon, C., and Lichten, M. (1993). Timing of molecular events in meiosis in *Saccharomyces cerevisiae*: stable heteroduplex DNA is formed late in meiotic prophase. *Mol Cell Biol 13*, 373-382.

Haber, J. E. (1998). The many interfaces of Mre11. *Cell 95*, 583-586.

Haber, J. E. (2000). Lucky breaks: analysis of recombination in *Saccharomyces*. *Mutation Research 451*, 53-69.

Heyting, C. (1996). Synaptonemal complexes: structure and function. *Curr Opin Cell Biol 8*, 389-396.

Hopfner, K. P., Craig, L., Moncalian, G., Zinkel, R. A., Usui, T., Owen, B. A., Karcher, A., Henderson, B., Bodmer, J. L., McMurray, C. T., *et al.* (2002). The Rad50 zinc-hook is a structure joining Mre11 complexes in DNA recombination and repair. *Nature 418*, 562-566.

Ivanov, E. L., Korolev, V. G., and Fabre, F. (1992). *XRS2*, a DNA repair gene of *Saccharomyces cerevisiae*, is needed for meiotic recombination. *Genetics 132*, 651-664.

Ivanov, E. L., Sugawara, N., White, C. I., Fabre, F., and Haber, J. E. (1994). Mutations in *XRS2* and *RAD50* delay but do not prevent mating-type switching in *Saccharomyces cerevisiae*. *Mol Cell Biol 14*, 3414-3425.

Jinks-Robertson, S., and Petes, T. D. (1986). Chromosomal translocations generated by high-frequency meiotic recombination between repeated yeast genes. *Genetics 114*, 731-752.

Johzuka, K., and Ogawa, H. (1995). Interaction of Mre11 and Rad50: two proteins required for DNA repair and meiosis-specific double-strand break formation in *Saccharomyces cerevisiae*. *Genetics 139*, 1521-1532.

Kadyk, L. C., and Hartwell, L. H. (1992). Sister chromatids are preferred over homologs as substrates for recombinational repair in *Saccharomyces cerevisiae*. *Genetics 132*, 387-402.

Kane, S. M., and Roth, R. (1974). Carbohydrate metabolism during ascospore development in yeast. *J Bacteriol 118*, 8-14.

Keeney, S., Giroux, C. N., and Kleckner, N. (1997). Meiosis-specific DNA double-strand breaks are catalyzed by Spo11, a member of a widely conserved protein family. *Cell 88*, 375-384.

Keeney, S., and Kleckner, N. (1995). Covalent protein-DNA complexes at the 5' strand termini of meiosis-specific double-strand breaks in yeast. *Proc Natl Acad Sci U S A 92*, 11274-11278.

Khazanehdari, K. A., and Borts, R. H. (2000). *EXO1* and *MSH4* differentially affect crossing-over and segregation. *Chromosoma 109*, 94-102.

Kirkpatrick, D. T., Ferguson, J. R., Petes, T. D., and Symington, L. S. (2000). Decreased meiotic intergenic recombination and increased meiosis I nondisjunction in *exo1* mutants of *Saccharomyces cerevisiae*. *Genetics 156*, 1549-1557.

Klein, F., Mahr, P., Galova, M., Buonomo, S. B., Michaelis, C., Nairz, K., and Nasmyth, K. (1999). A central role for cohesins in sister chromatid cohesion, formation of axial elements, and recombination during yeast meiosis. *Cell 98*, 91-103.

Klein, S. (1994). Choose your partner: chromosome pairing in yeast meiosis. *Bioessays 16*, 869-871.

Kolodkin, A. L., Klar, A. J., and Stahl, F. W. (1986). Double-strand breaks can initiate meiotic recombination in *S. cerevisiae*. *Cell 46*, 733-740.

Krogh, B. O., and Symington, L. S. (2004). Recombination proteins in yeast. *Annu Rev Genet 38*, 233-271.

Leem, S. H. and H. Ogawa (1992). "The *MRE4* gene encodes a novel protein kinase homologue required for meiotic recombination in *Saccharomyces cerevisiae*." *Nucleic Acids Res* 20(3): 449-57.

Lewis, L. K., Karthikeyan, G., Westmoreland, J. W., and Resnick, M. A. (2002). Differential suppression of DNA repair deficiencies of yeast *rad50*, *mre11* and *xrs2* mutants by *EXO1* and *TLC1* (the RNA component of telomerase). *Genetics 160*, 49-62.

Ling, M. M. and B. H. Robinson (1997). "Approaches to DNA mutagenesis: an overview." *Anal Biochem* 254(2): 157-78.

Liu, J., Wu, T. C., and Lichten, M. (1995). The location and structure of double-strand DNA breaks induced during yeast meiosis: evidence for a covalently linked DNA-protein intermediate. *Embo J 14*, 4599-4608.

Llorente, B., and Symington, L. S. (2004). The Mre11 nuclease is not required for 5' to 3' resection at multiple HO-induced double-strand breaks. *Mol Cell Biol 24*, 9682-9694.

Loidl, J., Klein, F., and Scherthan, H. (1994). Homologous pairing is reduced but not abolished in asynaptic mutants of yeast. *J Cell Biol 125*, 1191-1200.

Malkova, A., Ross, L., Dawson, D., Hoekstra, M. F., and Haber, J. E. (1996). Meiotic recombination initiated by a double-strand break in *rad50*Δ yeast cells otherwise unable to initiate meiotic recombination. *Genetics 143*, 741-754.

Mallory, J. C. and T. D. Petes (2000). "Protein kinase activity of Tel1p and Mec1p, two *Saccharomyces cerevisiae* proteins related to the human ATM protein kinase." *Proc Natl Acad Sci U S A* 97(25): 13749-54.

McKee, A. H., and Kleckner, N. (1997). A general method for identifying recessive diploid-specific mutations in *Saccharomyces cerevisiae*, its application to the isolation of mutants blocked at intermediate stages of meiotic prophase and characterization of a new gene *SAE2*. *Genetics 146*, 797-816.

Moreau, S., Ferguson, J. R., and Symington, L. S. (1999). The nuclease activity of Mre11 is required for meiosis but not for mating type switching, end joining, or telomere maintenance. *Molecular and Cellular Biology 19*, 556-566.
Moreau, S., E. A. Morgan, et al. (2001). "Overlapping functions of the *Saccharomyces cerevisiae* Mre11, Exo1 and Rad27 nucleases in DNA metabolism." *Genetics 159*(4): 1423-33.

Morrow, D. M., D. A. Tagle, et al. (1995). "*TEL1*, an *S. cerevisiae* homolog of the human gene mutated in ataxia telangiectasia, is functionally related to the yeast checkpoint gene *MEC1*." *Cell* 82(5): 831-40.

Nakada, D., Matsumoto, K., and Sugimoto, K. (2003). ATM-related Tel1 associates with double-strand breaks through an Xrs2-dependent mechanism. *Genes Dev 17*, 1957-1962.

Nasmyth, K., Peters, J. M., and Uhlmann, F. (2000). Splitting the chromosome: cutting the ties that bind sister chromatids. *Science 288*, 1379-1385.

Neale, M. J., Pan, J., and Keeney, S. (2005). Endonucleolytic processing of covalent protein-linked DNA double-strand breaks. *Nature 436*, 1053-1057.

Neale, M. J., Ramachandran, M., Trelles-Sticken, E., Scherthan, H., and Goldman, A. S. H. (2002). Wild-Type levels of Spo11-induced DSBs are required for normal single-strand resection during meiosis. *Mol Cell 9*, 835-846.

Nicolas, A., Treco, D., Schultes, N. P., and Szostak, J. W. (1989). An initiation site for meiotic gene conversion in the yeast *Saccharomyces cerevisiae*. *Nature 338*, 35-39.

Niu, H., Wan, L., Baumgartner, B., Schaefer, D., Loidl, J., and Hollingsworth, N. M. (2005). Partner choice during meiosis is regulated by Hop1-promoted dimerization of Mek1. *Mol Biol Cell 16*, 5804-5818.

Orr-Weaver, T. L., and Szostak, J. W. (1985). Fungal recombination. *Microbiol Rev 49*, 33-58.

Padmore, R., Cao, L., and Kleckner, N. (1991). Temporal comparison of recombination and synaptonemal complex formation during meiosis in *S. cerevisiae*. *Cell 66*, 1239-1256.

Paques, F., and Haber, J. E. (1999). Multiple pathways of recombination induced by double-strand breaks in *Saccharomyces cerevisiae*. *Microbiol Mol Biol Rev 63*, 349-404.

Pastink, A., Eeken, J. C., and Lohman, P. H. (2001). Genomic integrity and the repair of double-strand DNA breaks. *Mutat Res 480-481*, 37-50.

Paull, T. T., and Gellert, M. (1998). The 3' to 5' exonuclease activity of Mre 11 facilitates repair of DNA double-strand breaks. *Mol Cell 1*, 969-979.

Pawlowski, W. P., and Cande, W. Z. (2005). Coordinating the events of the meiotic prophase. *Trends Cell Biol 15*, 674-681.

Petrini, J. H. (1999). The mammalian Mre11-Rad50-Nbs1 protein complex: integration of functions in the cellular DNA-damage response. *Am J Hum Genet 64*, 1264-1269.

Prinz, S., Amon, A., and Klein, F. (1997). Isolation of *COM1*, a new gene required to complete meiotic double-strand break-induced recombination in *Saccharomyces cerevisiae*. *Genetics 146*, 781-795.

Rockmill, B., Sym, M., Scherthan, H., and Roeder, G. S. (1995). Roles for two RecA homologs in promoting meiotic chromosome synapsis. *Genes Dev 9*, 2684-2695.

Roeder, G. S., and Bailis, J. M. (2000). The pachytene checkpoint. *Trends Genet 16*, 395-403.

Scherthan, H., Bahler, J., and Kohli, J. (1994). Dynamics of chromosome organization and pairing during meiotic prophase in fission yeast. *J Cell Biol 127*, 273-285.

Schwacha, A., and Kleckner, N. (1994). Identification of joint molecules that form frequently between homologs but rarely between sister chromatids during yeast meiosis. *Cell 76*, 51-63.

Schwacha, A., and Kleckner, N. (1997). Interhomolog bias during meiotic recombination: meiotic functions promote a highly differentiated interhomolog-only pathway. *Cell 90*, 1123-1135.

Sharples, G. J., and Leach, D. R. (1995). Structural and functional similarities between the SbcCD proteins of *Escherichia coli* and the Rad50 and Mre11 (Rad32) recombination and repair proteins of yeast. *Mol Microbiol 17*, 1215-1217.

Shima, H., Suzuki, M., and Shinohara, M. (2005). Isolation and characterization of novel *xrs2* mutations in *Saccharomyces cerevisiae*. *Genetics 170*, 71-85.

Shinohara, A., Shinohara, M., Ohta, T., Matsuda, S., and Ogawa, T. (1998). Rad52 forms ring structures and co-operates with RPA in single-strand DNA annealing. *Genes Cells 3*, 145-156.

Stewart, G. S., Maser, R. S., Stankovic, T., Bressan, D. A., Kaplan, M. I., Jaspers, N. G., Raams, A., Byrd, P. J., Petrini, J. H., and Taylor, A. M. (1999). The DNA double-strand break repair gene h*MRE11* is mutated in individuals with an ataxia-telangiectasia-like disorder. *Cell 99*, 577-587.

Sugawara, N., and Haber, J. E. (1992). Characterization of double-strand break-induced recombination: homology requirements and single-stranded DNA formation. *Mol Cell Biol 12*, 563-575.

Sugawara, N., Ira, G., and Haber, J. E. (2000). DNA length dependence of the single-strand annealing pathway and the role of *Saccharomyces cerevisiae RAD59* in double-strand break repair. *Mol Cell Biol 20*, 5300-5309.

Symington, L. S. (2002). Role of *RAD52* epistasis group genes in homologous recombination and double-strand break repair. *Microbiol Mol Biol Rev 66*, 630-670.

Szankasi, P., and Smith, G. R. (1992). A DNA exonuclease induced during meiosis of *Schizosaccharomyces pombe*. *J Biol Chem 267*, 3014-3023.

Tauchi, H., Kobayashi, J., Morishima, K., van Gent, D. C., Shiraishi, T., Verkaik, N. S., vanHeems, D., Ito, E., Nakamura, A., Sonoda, E., *et al.* (2002). Nbs1 is essential for DNA repair by homologous recombination in higher vertebrate cells. *Nature 420*, 93-98.

Tran, P. T., Erdeniz, N., Symington, L. S., and Liskay, R. M. (2004). *EXO1*-A multi-tasking eukaryotic nuclease. *DNA Repair 3*, 1549-1559.

Trujillo, K. M., Yuan, S. S., Lee, E. Y., and Sung, P. (1998). Nuclease activities in a complex of human recombination and DNA repair factors Rad50, Mre11, and p95. *J Biol Chem 273*, 21447-21450.

Tsubouchi, H., and Ogawa, H. (1998). A novel *mre11* mutation impairs processing of double-strand breaks of DNA during both mitosis and meiosis. *Mol Cell Biol 18*, 260-268.

Tsubouchi, H., and Ogawa, H. (2000). Exo1 roles for repair of DNA double-strand breaks and meiotic crossing over in *Saccharomyces cerevisiae*. Mol Biol *Cell 11*, 2221-2233.

Tsubouchi, H., and Roeder, G. S. (2003). The importance of genetic recombination for fidelity of chromosome pairing in meiosis. *Dev Cell 5*, 915-925.

Usui, T., Ogawa, H., and Petrini, J. H. (2001). A DNA damage response pathway controlled by Tel1 and the Mre11 complex. *Mol Cell 7*, 1255-1266.

Usui, T., Ohta, T., Oshiumi, H., Tomizawa, J., Ogawa, H., and Ogawa, T. (1998). Complex formation and functional versatility of Mre11 of budding yeast in recombination. *Cell 95*, 705-716.

van den Bosch, M., Lohman, P. H., and Pastink, A. (2002). DNA double-strand break repair by homologous recombination. *Biol Chem 383*, 873-892.

Varon, R., Vissinga, C., Platzer, M., Cerosaletti, K. M., Chrzanowska, K. H., Saar, K., Beckmann, G., Seemanova, E., Cooper, P. R., Nowak, N. J., *et al.* (1998). Nibrin, a novel DNA double-strand break repair protein, is mutated in Nijmegen breakage syndrome. *Cell 93*, 467-476.

Villeneuve, A. M., and Hillers, K. J. (2001). Whence meiosis? *Cell 106*, 647-650.

Wan, L., de los Santos, T., Zhang, C., Shokat, K., and Hollingsworth, N. M. (2004). Mek1 kinase activity functions downstream of *RED1* in the regulation of meiotic double strand break repair in budding yeast. *Mol Biol Cell 15*, 11-23.

Weiner, B. M., and Kleckner, N. (1994). Chromosome pairing via multiple interstitial interactions before and during meiosis in yeast. *Cell 77*, 977-991.

Wu, T. C., and Lichten, M. (1994). Meiosis-induced double-strand break sites determined by yeast chromatin structure. *Science 263*, 515-518.

Wu, T. C., and Lichten, M. (1995). Factors that affect the location and frequency of meiosis-induced double-strand breaks in *Saccharomyces cerevisiae*. *Genetics 140*, 55-66.

Xu, L., B. M. Weiner, et al. (1997). "Meiotic cells monitor the status of the interhomolog recombination complex." *Genes Dev 11*(1): 106-18.

Zickler, D., and Kleckner, N. (1998). The leptotene-zygotene transition of meiosis. *Annu Rev Genet 32*, 619-697

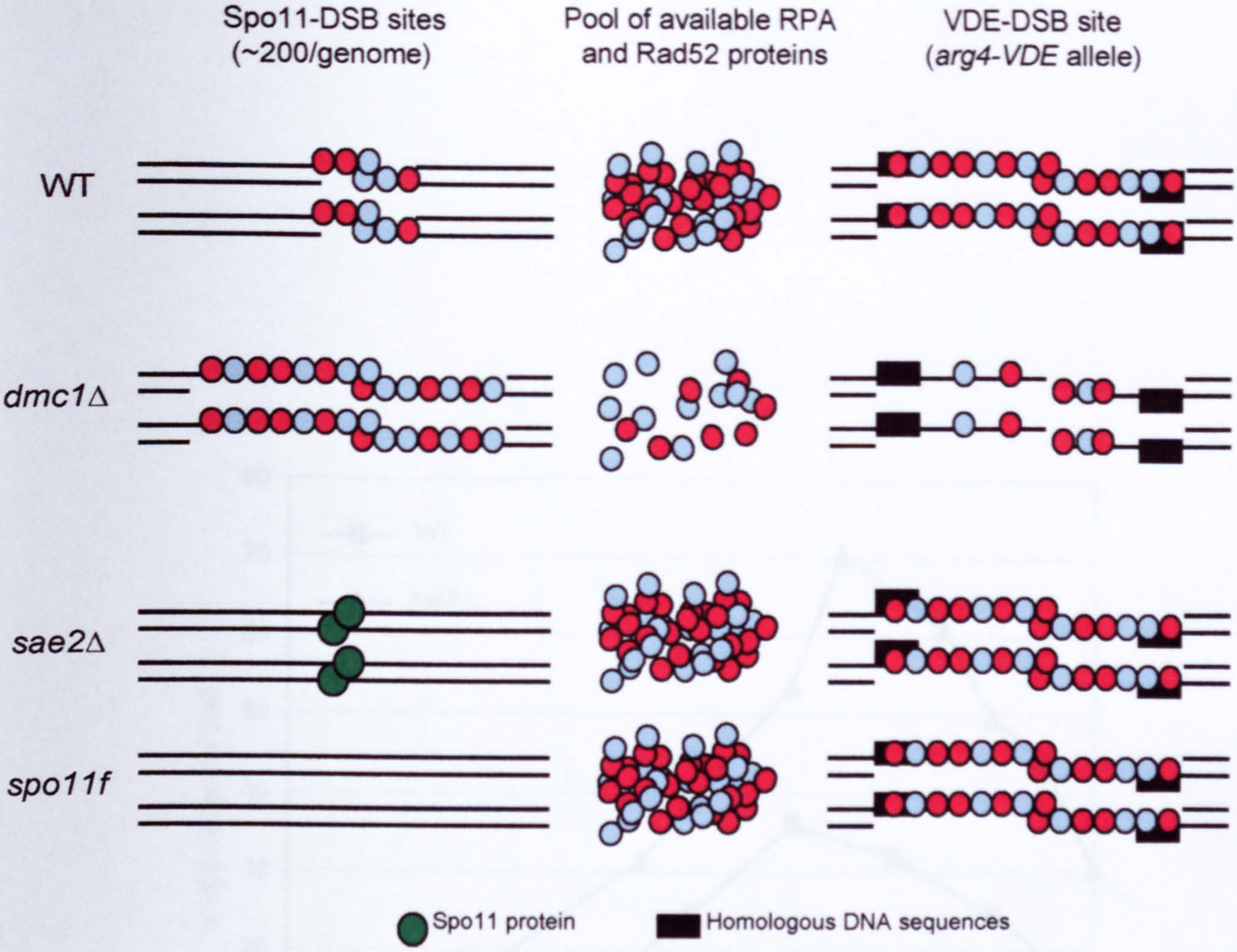

Table 4.4*i*

	Spo11-DSBs		VDE-DSB
	ssDNA	Sequestration	Repair
WT	+	+	++
dmc1Δ	+++	+++	+
sae2Δ	-	-	++
spo11	-	-	++

Figure 4.4*i*: Protein Sequestration at Sites of Excess ssDNA. A schematic representation of the events at multiple Spo11-break sites and the singular VDE-DSB site during meiotic DSB repair. Transient ssDNA formation at Spo11-DSBs in WT, is not sufficient to sequester the SSA proteins away from the VDE-DSB site. In *sae2*Δ and *spo11f* mutants, (also *spo11f dmc1*Δ, not shown), the absolute lack of ssDNA at Spo11-DSB sites frees up all of the available RPA/Rad52 protein for coating the ssDNA at the *arg4-VDE* allele, allowing optimal repair. In *dmc1*Δ cells, hyperresectioning of the accumulating Spo11-DSBs generates sufficient ssDNA to sequester the SSA-required proteins away from the VDE-DSB, therefore impairing SSA repair of the *arg4-VDE* allele. Table 4.4*i* summarizes the predictions for protein sequestration and the associated VDE-DSB repair data, based on the results from Section 4.2.

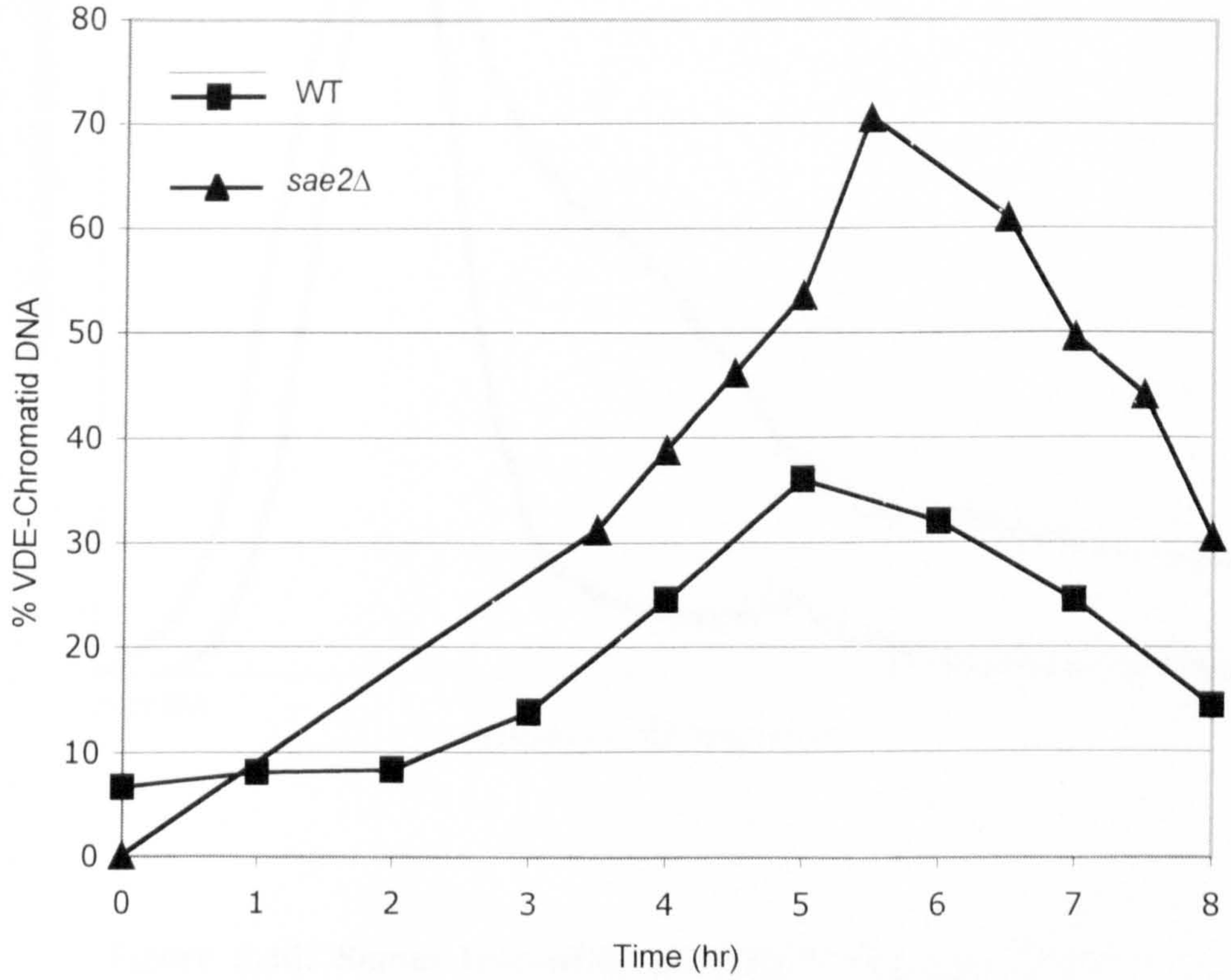

Figure 4.4*ii*: Quantification of VDE-DSB Turnover in *sae2*Δ. DNA extracted from WT (dAG630) and *sae2*Δ (dAG1200) strains and southern analysis performed (see Figure 4.1). Turnover of VDE-DSB is delayed in *sae2*Δ . (Turnover expressed as a proportion of VDE-chromatid DNA). (Data from n=4 experiments per strain)

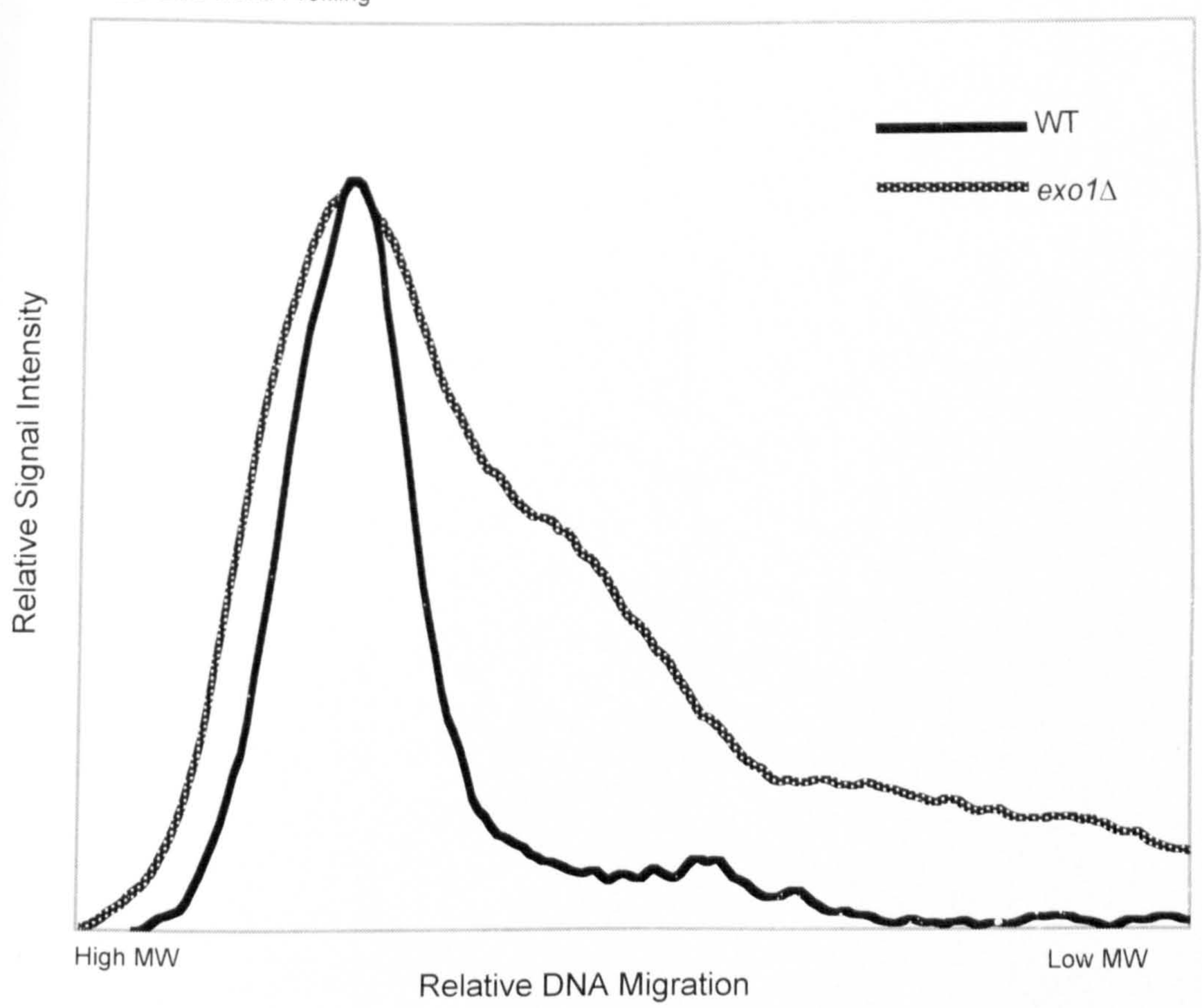

Figure 5.4ii: Signal Intensities of VDE-DSB bands: Profiles of signal intensities running through the VDE-DSB bands of WT (dAG630) and *exo1*Δ (dAG1305) strains at T=4hr (see Figure 5.4i(a), time points boxed). The curves are normalised to the maximum signal within the bands and stacked for comparison. The wide shoulder of the *exo1*Δ graph reflects smearing of the VDE-DSB, while the narrower (symmetrical) curve of WT reflects discrete VDE-DSB banding. (Data from n=4 experiments per strain)